An Intelligent Energy Measurement System

Denis Bonavia

Department of Industrial Electrical Power Conversion

Faculty of Engineering

University of Malta

A Dissertation submitted to the Faculty of Engineering in partial fulfillment of the requirements for the research-based degree of Master of Science in Engineering

December 2013

No portion of the work referred to in the dissertation has been submitted in support of an application for another degree or qualification of this or any other university or other institute of learning.

COPYRIGHT NOTICE

1. Copyright in text of this dissertation rests with the Author. Copies (by any process) either in full or of extracts may be made **only** in accordance with regulations held by the Library of the University of Malta. Details may be obtained from the Librarian. This page must form part of any such copies made. Further copies (by any process) of copies made in accordance with such instructions may not be made without the permission (in writing) of the Author.

2. Ownership of the right over any original intellectual property which may be contained in, or derived from, this dissertation is vested in the University of Malta and may not be made available for use by third parties without the written permission of the University, which will prescribe the terms and conditions of any such agreement.

An Intelligent Energy Measurement System

By Denis Bonavia

Supervised by Prof. Joseph Cilia and Dr. Saviour Zammit

Abstract

Energy efficient buildings are becoming popular nowadays thanks to the increase of energy costs and to the ongoing awareness on the subject. In this research, a system which measures the steady state heat loss coefficient of a residential building was built. Part of this research involved the development of three energy performance protocols, each of which was tested against a benchmark formed from real data. The best protocol, on average, deviated by 6% from the actual energy use. The worst deviation, in this case, was 10% of the actual energy used. For this study a room in a typical Maltese building was used. It had its internal temperature as well as its relative humidity monitored for one complete year. The outcome of this investigation is also discussed in this dissertation.

The developed system is designed in such a way that it reduces human intervention. It integrates a weather station and a number of nodes with sensors. The communication among the sensor nodes is performed through a wireless channel. Each sensor node consists of up to eight temperature sensors, a humidity sensor and a temperature control. The data is collected and stored in a PC. The design of the system permits easy adaptation of the system for other energy performance protocols or building analysis.

ACKNOWLEDGEMENTS

I would like to thank my tutors Prof. Joseph Cilia and Dr. Saviour Zammit for their invaluable support and help in this project. This work would not have been complete without their esteemed guidance.

Contents

List of Figures

Chapter 5: Thermal Model for Building Performance Analysis

Chapter 6: Implementation of the Hardware and the Software

Chapter 7: Energy Performance Protocols

Chapter 8: Results

Chapter 9: Conclusion and Future Work

List of Tables

Glossary of Symbols

V	Volume
T	Temperature
m	Mass
q_c	Convection heat flow rate
C_{th}	Thermal mass
C_p	Specific heat capacitance
t/T	Time
ρ_{ws}	partial pressure at saturation
R	Resistance or Thermal Resistance
P	Power
Q	Heat Energy
L	Length or thickness
A	Area
k	Thermal conductivity
U	heat transfer coefficient
ρ	density

I dedicate this work to my girlfriend Daniella and to both

our families for their continuous support.

1. Introduction

1.1 Overview

With the energy prices going up, energy efficient buildings are becoming more and more popular than they were a few years ago. Energy efficient buildings come with a cost and people are ready to pay for them as long as they can enjoy their benefits. As a consequence, authorities introduced Building Energy Rating Certificate Schemes which rate the buildings according to their efficiency. These schemes are based on audit visits and calculations which are subject to model errors and human errors.

Such errors undermine the whole system and discourage people from buying more efficient buildings. Having a system which is able to measure the actual energy efficiency of a building will be of great benefit.

1.2 Research Objective

The main objective of this research is to develop a system which measures the energy efficiency of a residential building. This involves the development of a the necessary hardware and software which makes the implementation of an energy performance protocol easy and with the least human intervention. This involves also the development of an energy performance protocol which is feasible to perform on regular basis.

The development of the energy performance protocol involves the monitoring of a room in a typical Maltese building for one complete year. Several experiments were carried out in this room. These experiments are used to validate the methods to be used. The outcome from the experiments was that of three different energy performance protocols. These protocols were tested with actual data and their results were compared.

1.3 Dissertation Layout

The dissertation is made up of the following chapters:

Chapter 1: Introduction

This chapter gives an overview of the background problem and discusses briefly the objectives and the outcome of this research.

Chapter 2: Energy Performance of a Building.

An overview of the historical developments is given here. This chapter describes a typical building energy rating scheme which uses a calculation method. It also gives an overview of the theory involved to calculate the energy efficiency of a building along with the problems faced. This chapter concludes with the objective of this research.

Chapter 3: Literature Review

The literature review covers different protocols and other methods which measure the energy performance of a building. It also covers equivalent thermal networks which are used.

Chapter 4: Analysis of Humidity, Temperature and Solar Irradiance

In this chapter, the analysis is done on the behavior of humidity, temperature and solar irradiance, both inside the test room and outside in the external environment. It also investigates how the external humidity and temperature affect the internal ones.

Chapter 5: Thermal model for a building performance analysis

The thermal model adopted for the energy performance protocol is described in this chapter. It discusses a number of methods used to determine the effective heat loss coefficient and also explains another method used to estimate the thermal mass.

Chapter 6: Implementation of the Hardware and the Software

This chapter gives a description of the hardware and the software developed to implement the proposed energy performance protocols.

Chapter 7: Energy Performance Protocols

Three different energy performance protocols are described here. This chapter explains in detail how to calculate the energy requirements using the measured Effective U-Value by any of the three protocols. Furthermore, it explains the methodology to evaluate the three energy performance protocols. It also describes how to perform the same measurements in multi-room buildings.

Chapter 8: Results

This chapter discusses the results obtained from the three energy performance protocols and compares the results. It also identifies the external conditions which influence the correctness of the measured Effective U-Value and explains how to avoid them.

Chapter 9: Conclusion and Future Work

This chapter gives a brief description of the work done and the results obtained. It concludes with possible future work.

2. Energy Performance of Buildings

2.1 Introduction

This chapter begins by providing a historical development which leads to the implementation of Building Energy Rating Certificate Schemes around the world. Then, the chapter goes through some selected theories related to the measurement of energy usage for heating and cooling in a building and concludes by defining the objective of this research.

2.2 Historical Developments

The building energy rating of residential buildings was first introduced in Sweden following the energy crisis of 1973. In countries where the temperature goes down below -30 ^{o}C in winter, heating is not an option but a necessity. Moreover, the heat losses from a building are more or less directly proportional to the difference between the external and the internal temperatures. As a consequence, cold countries such as Sweden suffered the increase in oil prices more dearly than the warm countries. In 1974, the Swedish government decided to reduce the gross annual heating consumption in residential buildings. As a consequence, a number of financial initiatives for energy saving measures were introduced. Eventually, the Swedish government wanted to identify the effectiveness of these initiatives. Consequently, energy performance ratings were introduced.

Another development which led to the implementation of the Building Energy Rating Certificate Scheme around the world was the Global Warming. Global Warming caused a lot of problems around the world and the problems are expected to get worst if the proper actions are not taken. Global warming is caused by excessive release of green house gases in the atmosphere. More than 80% of the primary energy sources are fossil fuels. Unfortunately, fossil fuels release Carbon dioxide which is one of the Green House Gases. Luckily, governments around the world started to take some actions. One of the actions taken was the Kyoto protocol where in 1997 it was agreed

to reduce the emission of the green house gases by 5.2% from the 1990 levels. The European Union decided to do more and took a unilateral decision to reduce by 20 % the Green House Gases emissions by 2020. Furthermore, it is estimated that in Europe 40% of the required energy is used in buildings. Figures published by the Euro stat in 2012 indicated that the figures remained the same more or less. In fact, it is estimated that in 2010, 26.65% of the energy consumption was used in residential buildings, while 13.21% was used in the service sector. It should be noted that the service sector includes, but is not limited only to, schools, hospitals, hotels, commercial buildings or any building which is used by people to render a service.

Obviously, the European Union had to address these areas and therefore it implemented the EU Directive 2002/91/EC. Article 7 of this EU directive establishes the Building Energy Rating (BER) Certificate Scheme. Basically, this article stipulates that owners of properties or dwellings should provide a BER certificate, whenever the properties or dwellings change ownership, whether this occurs due to leasing or selling. This directive also obliges public buildings which are greater than 1000 m^2 and which are not older than 10 years to display this certificate in the public area. With the aid of a BER certificate, a high energy performance building is given a tangible added value. Now buyers with a BER certificate can differentiate between a high and low energy performance building and authorities can positively discriminate and reward high performance buildings. Inevitably, the BER certificate system will lower or increase the price of a building. Thus, the BER certificate system should be a secure system, verifiable, and trusted by people.

2.3 A Typical Building Energy Rating System

There are many BER systems implemented around the world. Some are quite complex such as, Leadership in Energy and Environmental Design (LEED) which takes under consideration the number of people living in a building, as well as, how far the building is from the necessary amenities. A typical building energy rating system predicts the annual energy usage of a building and expresses it in $kWh/m^2.yr$. Figure 2.1 shows a typical BER Certificate for Malta.

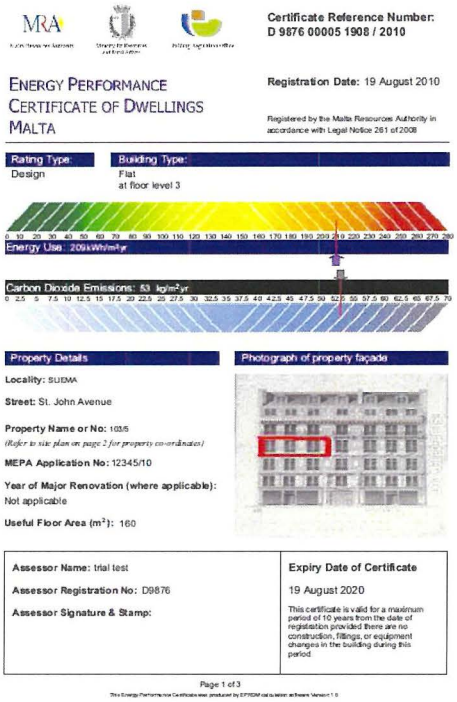

MRA

Certificate Reference Number:
D 9876 00005 1908 / 2010

ENERGY PERFORMANCE CERTIFICATE OF DWELLINGS MALTA

Registration Date: 19 August 2010

Registered by the Malta Resources Authority in accordance with Legal Notice 261 of 2008

Rating Type: Design

Building Type: Flat at floor level 3

Energy Use: 209kWh/m²yr

Carbon Dioxide Emissions: 53 kg/m²yr

Property Details

Locality: SLIEMA

Street: St. John Avenue

Property Name or No: 103/5

(Refer to site plan on page 2 for property co-ordinates)

MEPA Application No: 12345/10

Year of Major Renovation (where applicable): Not applicable

Useful Floor Area (m^2): 160

Photograph of property façade

Assessor Name: trial test

Assessor Registration No: D9876

Assessor Signature & Stamp:

Expiry Date of Certificate

19 August 2020

This certificate is valid for a maximum period of 10 years from the date of registration provided there are no construction, fittings, or equipment changes in the building during this period.

Page 1 of 3

Figure 2.1 A typical BER Certificate for Malta produced by the Building Regulation Office

Typically BER systems take many things under consideration, some of which are highlighted below:

- The type of lighting used in the building
- The types of heating and cooling systems that are used in the building
- The air infiltration and ventilation in the building
- The usage of secondary water in the building such as rain water for flushing
- The renewable energy used in the building such as photovoltaic installations
- The efficiency of the equipment used in the building
- The space heating and space cooling loads for predetermined set points

The last consideration is the most important and should be included in any BER certificate system. It is also the most difficult part to be performed accurately. To

determine the heating and cooling loads, it is required to carry out a thermal analysis of the building. The method that is widely adopted in the BER certificate schemes is the computation approach. This is done by an assessor who performs a site visit to the building in question to determine the thermal characteristics of the building. Then, the assessor will put this information into a program and the program determines the energy loads for a typical weather year and for a given internal set points. The assessor will input additional information such as the renewable energy equipment installed in the building. Based on the input information, the program computes the efficiency of the building. Figure 2.2 shows a screen shot of BER software provided by the Building Regulation Office of the Government of Malta's agency.

The benefit of using the computational approach is that it is very economical to carry out. On the other hand, this approach has the following draw backs:

- it is insensitive for the local variance
- it is prone for unintentional or intentional mistakes
- the input data is subjective

Due to the mentioned drawbacks, the building energy rating certificate might not reflect the actual performance. Two different assessors can rate the same building differently. This may lead people to lose their trust in the system and the rating will lose its effectiveness.

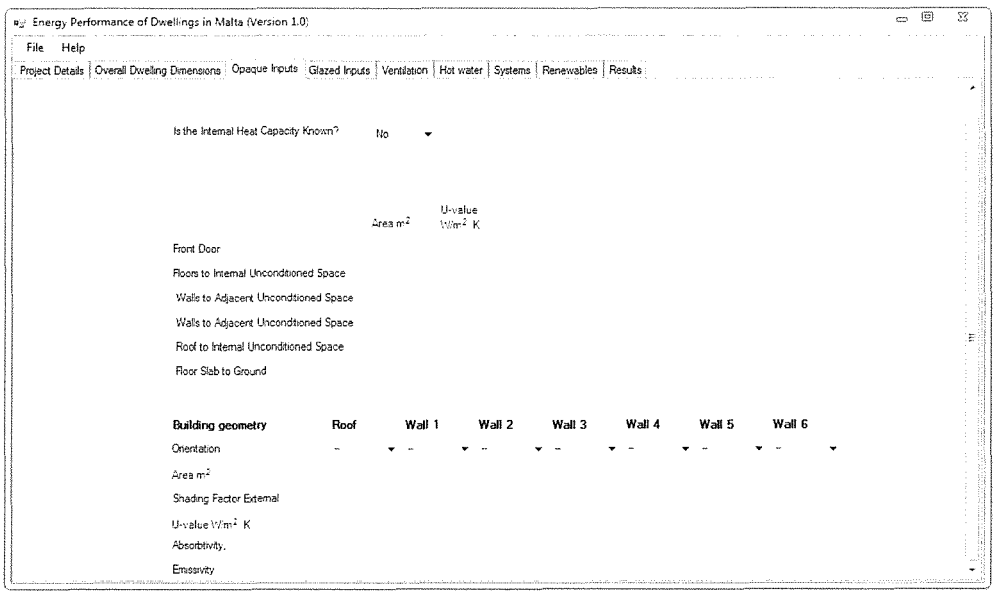

Figure 2.2 A screen shot of the BER software provided by the Building Regulation Office

2.4 Determining the Heat Energy flows in a Building

2.4.1 Introduction

To calculate accurately, the space heating and cooling annual energy requirements of a building is a complex task. First, it is necessary to determine, the various heat paths experienced by the building. Then, based on this information, the annual energy requirements for a typical weather year can be determined. This section will discuss some selected theories and the complexity in calculating the heat energy flows in a building. It will also explain the shortages involved when using the computation approach to determine such flows.

This section starts by introducing the energy balance of a typical residential building. Then, there is a focus on the various energy flows indicated in the energy balance. The section concludes with a summary of the various drawbacks identified.

2.4.2 Energy Balance in Building

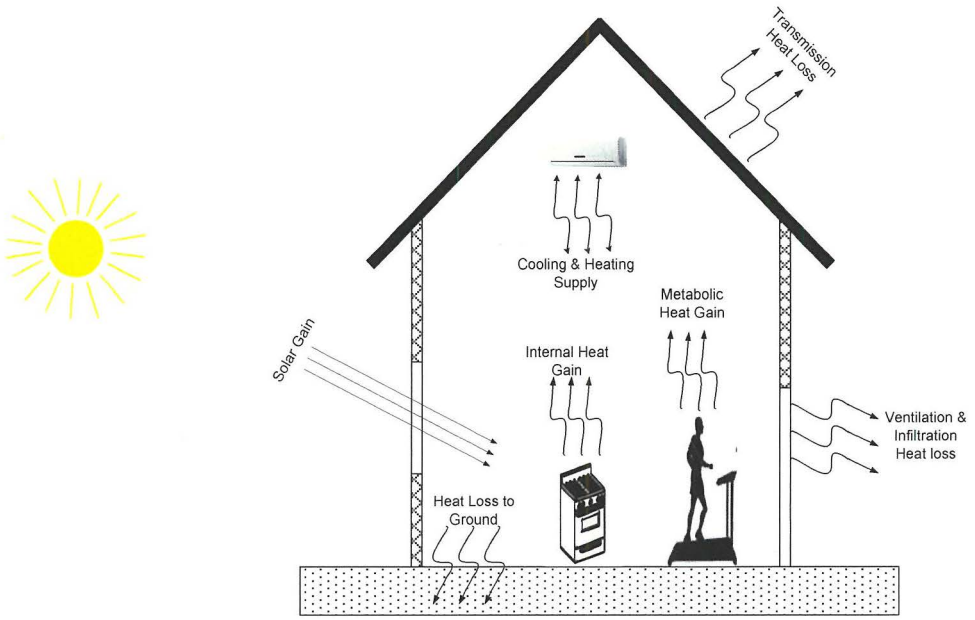

Figure 2.3 shows the various energy flows in a building

The Figure 2.3 shows the various energy flows that are acting in the building. The net result is temperature equilibrium. At this point, the net heat flow into the building is equivalent to the net heat flow out of the building. During the heating season the net heat energy flow in the building is made up of any heat source, solar gain, internal gain and the heat gained from the adjacent buildings, if applicable. While the heat energy flow out of the building is made of air infiltration and ventilation, heat loss to the ground, and heat loss due to transmission.

2.4.3 Solar Gain

Solar gain is one of the significant energy flows in a building. Heat from the sun reaches the Earth in the form of heat radiation. The amount of heat energy gain depends on many things. It depends on the location of the building on earth, on the time of the year and on the amount of shading that the building is experiencing. The solar gain depends also on the material used in the building, on the weather, and finally on the apertures in the building.

The position of the sun with reference to a point on Earth depends on the day and time of the year. The reason behind this phenomenon is because the Earth is orbiting around the sun in an ellipse path and furthermore, the earth is spinning on itself with its axis tilted about 23.45^{o} with reference to the path around the sun. This also has effects on the amount of solar radiation that a particular place can experience. The solar radiation levels are also affected by the weather conditions. By means of statistical analysis it is possible to forecast, with a good approximation, the effect of the weather on the solar radiation. A pyranometer can be used to measure global irradiation on site.

When the solar radiation hits a material, part of the energy is reflected back, another part of the energy is transmitted out of the material and the rest is absorbed in the material, in the form of heat. The amount of energy depends on the absorptivity, emissivity and transmittance of the material. For example, glass permits most of the energy to pass through, while opaque objects only absorb and reflect back some of the energy. The solar radiation that goes through the apertures of the building, instantaneously heat up the internal part of the building. In this case, the affects of the solar radiation is immediate on the internal temperature. On the other hand, when the solar radiation hits the opaque parts of the building the material absorbs some of the energy and stores it internally. By time, this energy is slowly released in the building. In this case, the effects on the internal temperature are retarded.

Nowadays, the position of the sun with reference to the Earth can be accurately calculated. This makes simulations possible, hence one can determine the amount of shading that the building is experiencing. Furthermore, simulations can also determine the effect of the solar radiation for the given shading on the building as well as the temperature inside the building. But this requires the implementation of a numerical model of the building along with that of its surroundings. This model requires skill and time and therefore a simpler but less accurate model such as Sol-air Temperature are generally adopted. Furthermore, the actual values of reflectivity, emissivity, absorptivity and transmittance of the material used, are generally not

known. As a consequence, the assessors had to deduct these values. This is generally done on the basis of their personal experience or on some sort of guidance. Such guidance is typically provided on a national level. Due to the latter, and due to the use of simple model, the results could be unacceptably different from the actual ones.

2.4.4 Internal gains

Internal gains are heat energies released internally in a building by an activity of an object or a living thing. For example, the primary role of an incandescent bulb is to light up the building but it also releases heat. Another example is that of fridges or freezers which are primarily used for cooling, however they also release heat in the building. The list of examples can be very long including every electrically operated equipment or appliance. Other sources of internal heat gains can come from adjacent buildings, from hot water usage and finally from living things such as humans. The latter is also known as metabolism heat gain. The heat released by humans depends from the activities conducted by the individual person, and can be up to 400W for a male doing heavy activities. Heat gains, can reduce the energy need during the cold season but in contrast they can increase the cooling load during the hot season. It is difficult to calculate accurately the internal gains and in many situations assumptions have to be made. The ASHRAE fundamentals [1] give a list of various components which contribute for the heat gain in the building along with their typical heat gain contribution.

2.4.5 Heat loss due to Air Infiltration and Ventilation

Heat energy flow due to air changes in a building could be significant. Air changes in buildings occur due to air ventilation or due to air infiltration. Ventilation is a necessity in a building but air infiltration is something undesirable. In case of air ventilation, heat recovery is possible but this is not the case for air infiltrations. Air changes in a building occur due to the pressure difference in the air inside the building and the air outside the building. This pressure difference is made of wind pressure, stack pressure and mechanical ventilation pressure.

When there is wind on a building a positive pressure is induced on the walls facing the wind. On the other hand, a negative pressure tends to form on the external walls opposite to the wind direction. This creates a differential pressure and hence air flow through the building. Stack pressure is created due to the difference between the exterior and the interior temperatures. If the building is supplied by mechanical ventilation, a positive pressure inside the building is created. In contrast, if in the building an extract mechanical ventilation is used, a negative pressure is formed inside the building. The energy flow due to air changes is dependent on the specific heat capacity of air which is 1.006 kJ/kgC for dry air. The heat energy flow due to air changes is best described by the following formula:

$$Heat\ Energy\ flow\ due\ to\ air\ changes = 0.33 * V * N * (T_{int} - T_{ext}) \quad (2.01)$$

Where V is the Volume of the building in m^3

N is the number of V changes per hour

T_{int} is the internal temperature in K

T_{ext} is the external temperature in K

As can be seen, the heat energy flow is proportional to the temperature difference and to the number of changes per hour. Furthermore, this formula also indicates that energy losses due to air changes are higher in cold countries.

It is possible to measure on site, the air leakage of a building envelope by using the blower door test [2] on site. Alternatively, to this test one can use Tracer gas [3] which can measure the air changes in a building envelop, whether these air changes occurred due to air infiltration or due to air ventilation. When these tests are not possible, the air changes can be estimated using some sort of guidance like ISO 13789:2007.

2.4.6 Heat loss by Transmission through Fabric

The heat loss through fabric is the heat energy that is conducted through fabric from the condition space to the external environment or to an adjacent building with a lower temperature. An example is the heat loss through the external walls of a building. Calculating the heat loss through the fabric of a building is possible but it is a long process and may be subject to assumptions. The highlights of this process along with selected theories are discussed below along with the complexity that can arise when this is done in practice.

Anything which resists the passage of heat can be presented as a thermal resistor in a thermal circuit. The resistance of a homogeneous layer shown in Figure 2.4 is calculated as follows:

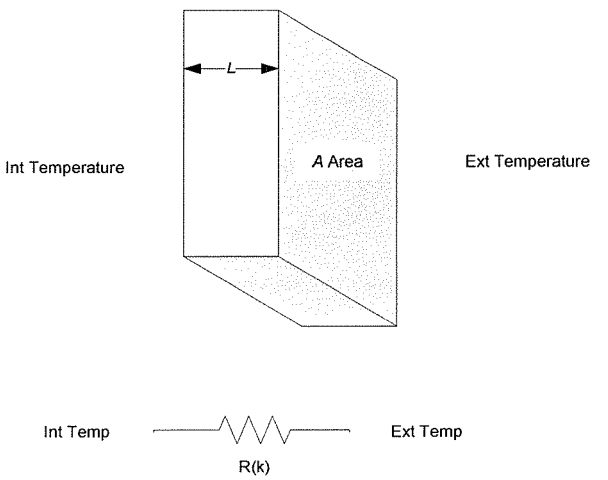

Figure 2.4 Shows Equivalent Thermal resistances for homogeneous layer

$$R_k = \frac{L}{kA}$$

Where: R_k is the thermal resistance in m^2W/k

A is the surface area in m^2

L is the length in m

k is the Thermal conductivity of the medium in W/m.k

Figure 2.5 shows a wall with two different layers and its equivalent thermal circuit. It is assumed that each layer is made from homogeneous material and the thickness is uniform throughout.

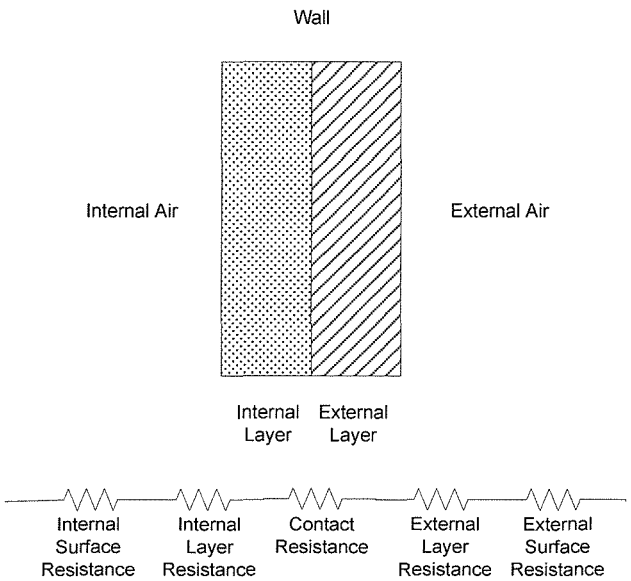

Figure 2.5 A two layer wall and its equivalent thermal circuit

As can be seen from figure 2.5, the thermal resistance circuit includes another three additional thermal resistances. These thermal resistances include an internal surface thermal resistance, an external surface thermal resistance and a contact resistance. The surface thermal resistance is created by a thin layer of stagnated air. This layer resists the passage of heat, therefore, it should be added in series with the fabric thermal resistance. Sometimes, the value chosen for the surface thermal resistance takes into account the convection and radiation effects. This is done for simplicity reasons. Typical values of the surface thermal resistance for exposed walls are 0.06 m^2 K/W for the external surface, and 0.10 m^2 K/W for the internal surface. The contact resistance is formed because the surfaces which are making contact are not perfectly smooth surfaces. As a consequence, the tiny gaps formed are filled with air and therefore they create a resistance to the flow of heat.

The overall heat transfer coefficient (U) of a building is calculated by:

$$R_{total} = R_1 + R_2 + \ldots\ldots R_n$$

$$U = \frac{1}{R_{total}}$$

Where R_i is the individual thermal resistance of each building component or sub-component exposed to the external environment. For example, if we have an exposed wall with a window, than at least there should be three R_i thermal resistances. One for the wall, one is for the window frame and one for the glass.

At a glance, this procedure seems simple, but it is not straight forward in practice, especially when no plans or other information are available on the building. Some of the problems encountered are highlighted below:

- The internal construction of the building components might not be known or might not be accessible. As a consequence, the thermal circuit derived might deviate heavily from the actual one.
- The materials used are not necessarily homogeneous, in which case, each non homogeneous part must be treated as sub-component. For example, if a brick absorbs water, its thermal conductance changes and should be treated as a separate component.
- The physical shape of a component might be complex and non uniform. In this case, calculating the thermal resistance becomes difficult.
- The thermal conductance assumed for various sub-components may vary from the actual ones.
- The effective surface resistance and contact resistance assumed may not reflect the actual ones.

As can be seen, finding the overall heat transfer coefficient of a building using the computation approach could become a very complex task. In order to simplify the process and make it viable, certain assumptions have to be made. For example, the individual components are assumed homogeneous and uniform. Other assumptions are taken on the national level and embedded in the BER protocol. An example of such assumptions, is the surface air thermal resistance and thermal conductance of various materials. This is good from the standardization point of view but the result could significantly deviate from the actual one.

It should be noted that direct measurements of the heat transfer coefficient of an individual building components are possible. The accuracy of such measurements vary between 5% to 10%. The procedure of such measurements is described by EN 12494.

2.4.7 Other Heat losses through Fabric

Further to the transmission losses, the building also experiences thermal radiation losses. Thermal radiation does not require any medium and the heat energy flows in the form of electromagnetic waves. Any object whose temperature is over the absolute zero temperature radiates heat to the surrounding objects. The rate of energy loss due to radiation depends on many factors mainly on the surface area and on the surface temperatures of the objects involved along with their emissivity. Of particular interest is the energy heat loss to the space. This is the heat radiation that an object exchanges with the outer space. In which case, the weather also plays its part. This is particularly important for flat roofs which exchange heat radiation to outer space only. A rule of thumb says that thermal radiation increases the heat loss by 15% for flat roofs [4]. The theory related to the thermal radiation is well established and therefore remodeling of such heat energy transfer is possible. Similarly, with the other cases, a balance between the complexity of the model used and the accuracy of the result should be found so that the process is a viable one. A problem commonly faced by the assessors is the lack of information about the

specifications of the material used like emissivity (ε). In such a case, these values are left to the assessor discretion.

Another source of heat loss through fabric occurs due to thermal convection. This is the heat transfer between a surface and a fluid. In the case of a building, the fluid is air. There are two types of air convection, one is natural and the other is a forced one. The natural convection occurs due to the temperature difference in the fluid, while in the case of a forced convection, the movement of air occurs due to the external force. The rate of heat energy flow due to convection is best described by the following formula:

$$q_c = \alpha_c(T_s - T_a) \tag{2.02}$$

Where:

q_c is the convection heat flow rate in W/m^2

α_c is the heat transfer coefficient W/m^2K

T_s is the surface temperature in ^oC

T_a is the environment temperature in ^oC

The heat flow due to convection is determined by multiplying the convection heat flow by the surface area. It should be noted, that the convective heat transfer coefficient is dependent on whether the convection is natural or forced, the speed of the moving air and its direction. The heat loss due to convection in building is primarily dependent on the wind speed and the wind direction. Another parameter which indirectly affects the convection heat transfer is the surface roughness. While a typical wind year is easily obtained by performing statistical analysis on the available weather data, the same thing cannot be said for the local surface roughness. The surface roughness is a local variance and should be determined locally. Finding the local surface roughness is possible but the process definitely is not a viable one for the BER scheme. In practice, when it comes to calculating the convection heat flow rate, the working can become complicated too. The reason behind these complications is that the different sections of the building may have different heat

transfer coefficient α_c for the same wind speed. To avoid these complications, assumptions have to be made.

Typically, where the surface to surface thermal resistance is high, both the radiation and the convection are included in surface thermal resistance. On the other hand, if the surface to surface is low, than the thermal convection and the thermal radiation should be dealt with separately [5].

2.4.8 Thermal Storage

An object that has a mass is able to store heat. The heat energy stored in an object is best described by the following formulas:

$$q = V * C_p * \rho * (T_{final} - T_{initial}) \quad (2.03)$$

$$C_{th} = V * C_p * \rho \quad (2.04)$$

Where: q is the sensible heat stored in J

C_{th} is the thermal mass of the object J/°C

V is the Volume of the object in m^3

C_p is the specific heat capacity of the material in J/kg°C

ρ is the density of the material in kg/m^3

T_{final} is the final temperature of the object °C

$T_{initial}$ is the initial temperature of the object °C

While the internal thermal mass of a building is calculated by:

$$C_{th\_building} = \sum_{k=1}^{n} C_1 + C_2 \ldots C_n \quad (2.05)$$

Where: C_n is the thermal mass of any building component or any sub-component or any object in the building.

In thermal equivalent circuits, the thermal mass is shown as a capacitor symbol (–| |–). In practice, the thermal mass of the building is generally calculated. It has the effects of retarding the heat changes in the building. Knowing the thermal mass of a building is particularly important if the temporal temperature variations have to be considered. Typically, the thermal mass of a building is calculated using a guidance such that of ISO 13786:2007.

Similarly, as with the thermal resistance of a material, the calculation of the global internal thermal mass is not a simple task. The same problems faced with the calculation of the overall heat transfer coefficient of a building are also encountered here. Basically, the main problems are: the actual specific heat capacity of the materials used is not known and the lack of information about the construction of the building. Other complications arise here because the materials used are not necessarily homogeneous or have a complex shape which makes calculations even more difficult. A further complication crops up here, because the thermal mass of a building includes the thermal masses of the objects housed in the building, for example furniture.

The internal thermal mass of a building is used along with the overall thermal transmittance to form the equivalent thermal network of a building or more precisely of a zone. When a building is relatively large, then it is divided into zones. Each zone is treated separately and the results are combined. When the building is small such as a flat, the whole building is treated as a single zone. Figure 2.6 shows the simplest form of model thermal network, more thermal networks are covered in Chapter 3 - Literature review.

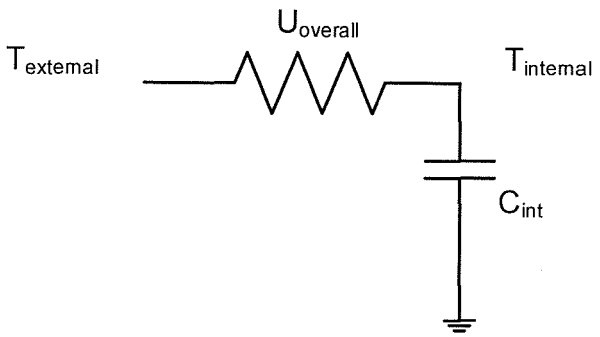

Figure 2.6 The simplest form of an equivalent thermal network

2.4.9 Typical Annual External Temperature Variations.

The external temperature and its annual variations have the most significant impact on the energy usage in a building. These variations are mainly caused by the earth orbiting around the sun and the fact that the earth is spinning on its axis. The external temperature variations are typically made from the seasonal variations added with the diurnal or daily variation. Both variations have sinusoidal like shape and can be approximated by:

$$T_e(t) \approx T_0 + T_1 * Sin\left(2\pi\left(\frac{day}{365}\right) - \theta_1\right) + T_2 * Cos\left(2\pi\left(\frac{hour}{24}\right) - \theta_2\right)$$

Where:

T_e	is the external temperature in °C
T_0	is the external annual average temperature in °C
T_1	is the maximum seasonal temperature variation °C
T_2	is the maximum diurnal temperature variation °C
θ_1	is a local constant
θ_2	is a local constant

The sinusoidal temperature variations have effect on the temperature penetration depth and hence on the energy flow in the object. Figure 2.7 shows the effects of the sinusoidal temperature on a 10cm wall over a 24 hour period. The y-axis shows the

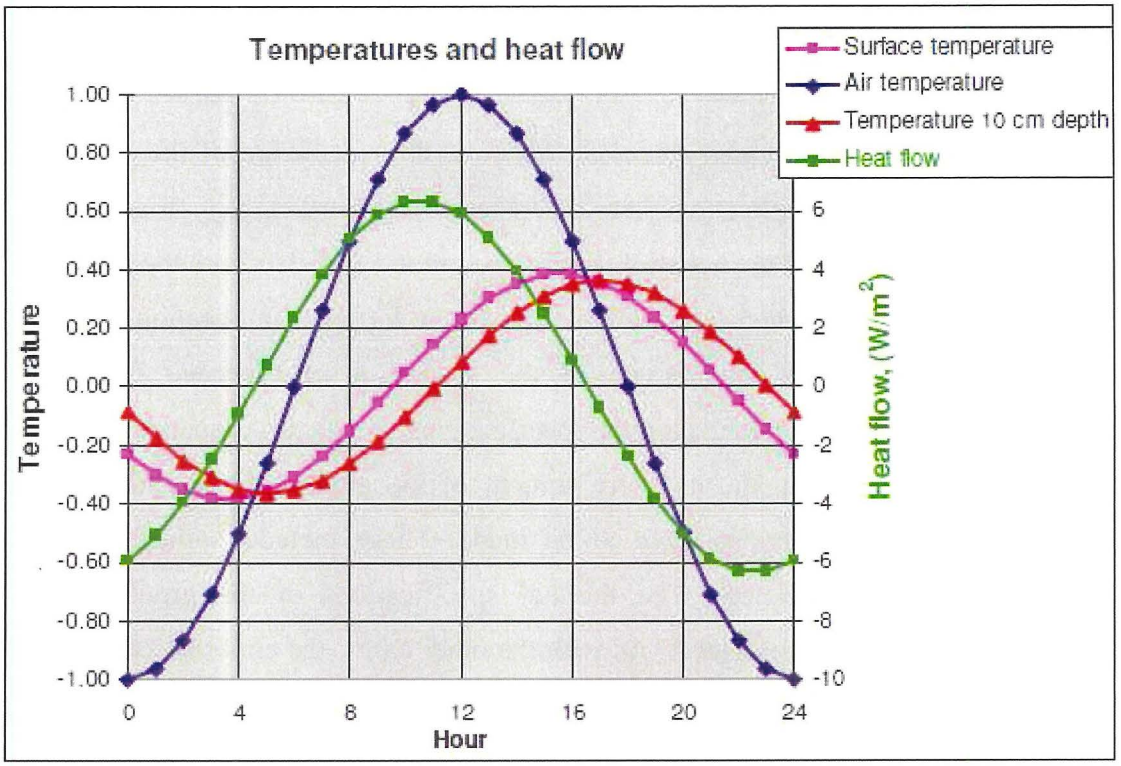

Figure 2.7 The effects of sinusoidal temperature on a 10cm wall. This figure was taken from a report "Heat capacity in relation to the Danish building regulations" by Lars Olsen [6].

temperature variation in Kelvin (K) from a reference temperature which the report did not specify, while the x-axis shows the time in hours.

2.4.10 Heat loss to the Ground

The heat flow from a building to the ground is considered to be significant especially if the ground in question is not insulated or the building includes a basement. The loss due to the ground should be treated differently from other components in the building. The ground has a massive thermal mass and can release or absorb heat energies for several days. In this scenario, one must take into consideration the seasonal external temperature variations. The thermal energy flow to the ground depends on the thermal conductivity of the materials used, on the geometry of the floor area and also on the thermal conductivity of the ground material. Another

factor which must be considered in estimating the heat energy flow to the ground is the temperature penetration depth.

Similarly, as with the other cases discussed till now, the calculation of the energy flow to the ground has complications here too. These complications may arise from the thermal specifications of the material used in the ground and also from the details of the floor construction which may not be known. A further complication arises here, because the thermal conductivity of the ground is also needed for the calculations. The ground's actual thermal specifications are locally dependent and their values are affected by the moisture content of the ground. To simplify the calculations certain assumptions have to be made. These include homogeneous material and uniform thickness. The thermal specifications of the ground are generally decided on a national level. As with the other cases, the correctness of the results depends on the assessors.

2.4.11 Computation Approach Drawback

Calculate the heating and cooling loads of a building, using the computational approach, is the most practical and cost effective way, provided that the process is simplified. For this reason, it is widely adopted in the BER scheme in place today, although other approaches are possible. Unfortunately, the computational approach has also its drawbacks as discussed in the previous sections. A summary of these drawbacks is given below:

1. Accurate calculations or simulations of the various energy heat flows in a building are possible but in most cases these require a detailed model of the building along with its surroundings. This is very time consuming and therefore a simpler, but less accurate approach, is generally adopted for the BER scheme.
2. Whatever model is adopted, an accurate thermal specification of the material used is required. This information is not always available, in which case the assessor has to deduct its values using his or her personal experience or using

some sort of guidance. Furthermore, the actual thermal specifications of a material used may differ from the official ones. This imprecise information will affect the accuracy of the results.

3. Sometimes, the lack of construction details can also pose a problem, because not all parts of the constructions are accessible. In such a case, certain assumptions have to be made. The wrong one will negatively affect the results.
4. Most calculations involve volumes, areas and thicknesses. If the correct plans are not available, then the assessor has to measure the building himself, a process which is subject to human errors. Furthermore, certain building components may have complex shapes which make measurements more tedious and therefore more prone to errors.
5. The individual building components are generally assumed to be homogeneous and have uniform shapes which are not true in reality. This assumption has to be made for practical reasons but it reduces the accuracy of the results.

All the five points mentioned above contribute in some way for the inaccuracy of the final result. They also make the computational approach insensitive for the local variance. But the worst is that the computational approach is prone for mistakes, whether these are made intentionally or unintentionally. Similar problems were mentioned by A Rabl in Parameter Estimation in buildings: Method for Dynamic Analysis of Measured Energy used [7].

2.5 The Heating and Cooling loads in Building

2.5.1 Introduction

Before one can perform any calculations of the heating and cooling energy loads, one has to decide which thermal network model to use, which calculation method to adopt and which internal set points to use. Furthermore, one has also to acquire a Typical Meteorological Year relevant to the building location. This section will discuss each of the mentioned elements.

2.5.2 Thermal network model

The thermal network models are used as a simple approximation of the building's thermal characteristics. They are frequently used along with the heat energy flows in the building which make the diagram more comprehensive. Figure 2.8 shows a simple thermal network model for unconditional space which is the minimal for a dynamic calculation method. Thermal networks are discussed further in Chapter 3 - Literature review.

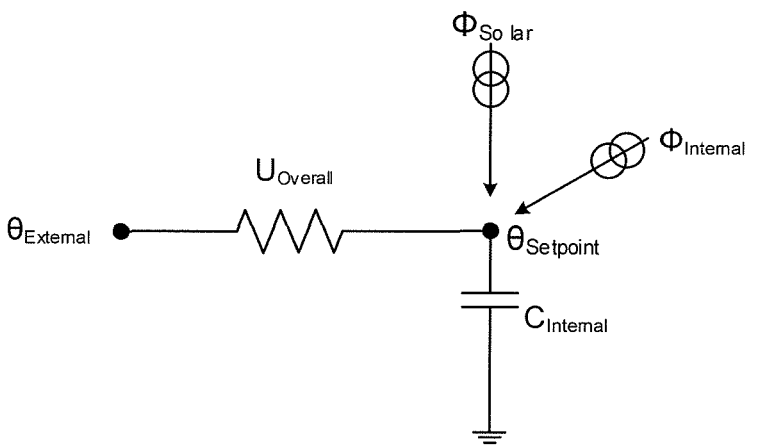

Figure 2.8 A simple thermal network model for an unconditional space

The $U_{Overall}$ incorporates the heat energy flow from fabric, from air ventilation and air infiltration. This can be done when no ventilation heat recovery is used. ϕ_{Solar} and $\phi_{internal}$ represent solar gain and internal gain respectively. $C_{internal}$ represents the thermal mass of the building. $\Theta_{Internal}$ and $\Theta_{External}$ are the internal and external temperatures and are discussed in sections 2.5.3 and 2.5.4 respectively. In the case of the BER scheme, the thermal network model is selected on a national level and is embedded into the scheme. This ensures a common methodology between the issued certificates.

2.5.3 The Thermal Comfort and the Internal Set points

The selection of the internal set point temperatures must satisfy the internal thermal comfort. The thermal comfort depends on several variables: the temperature, the humidity, the metabolic rate of the people, the air speed, the radiation temperature and the clothes worn. Several thermal comfort models were developed, one such model is the Predicted Mean Vote formula. It is a common practice to have two internal set points, one for the hot season and another one for the cold season.

In the case of a BER scheme, the internal temperature set points are decided on the national level and enforced into the BER procedures. This ensures harmonization between the BER certificates.

2.5.4 A Typical Meteorological Year

Apart from the external temperature, there are other weather attributes such as the solar radiation and the wind speed which are also required, especially if a detailed simulation method is used. A Typical Meteorological Year provides such information. It should be noted that a Typical Meteorological Year is typically derived from a 30 years weather data set, using a Statistic-based approach or a Simulation-based approach. An alternative approach is to use the multiyear data sets and then you take the average of their output. In the case of the BER scheme, the typical Meteorological year are provided by the authorities and are embedded in the BER program.

2.5.5 Calculation methods

The calculation methods used are classified in one of the following methods namely: the Steady-state method, the Quasi-steady-state method and the Dynamic method. The Steady-state methods are the simplest methods and assume no variations in the internal and the external temperatures. Furthermore, their methods do not take into considerations the thermal mass of the building into consideration. On the other hand, the Dynamic methods take into account the temporal temperature variations and the thermal mass of the building. The complexity of a Dynamic method depends

on the level of details used in the calculations. The Quasi-steady-state method is a Steady-state method which takes into account the dynamic effects by incorporating some correlation factors. These methods are more complex than the Steady-state methods but are less complex than the dynamic ones.

The type of method to be used in the BER scheme is selected on a national level. In most cases, this will adhere to a standard such as ISO 13790:2008. This standard mentions four methods which are the seasonal, the monthly, the simple hourly and the detailed simulation. The first two are quasi-steady-state methods while the last two are dynamic methods. The selection of the method is decided on a national level.

To ensure that the buildings are evaluated on common criteria the calculation method, the Typical Meteorological Year, the internal set points and the thermal network model should be decided on a national level. Furthermore, these elements have no effect on the local variances.

2.6 Main Objective of Research

2.6.1 An effective BER Scheme

The main idea behind the BER scheme is that people and authorities alike can distinguish between high and low efficient energy buildings. From the government's point of view, a high energy efficient building means less pollution, less burden on the country's infrastructures, greater possibilities of reaching obligatory targets as well as less dependence on foreign energy resources if it is the case. With the BER schemes in place, governments now can positively discriminate towards high energy efficient buildings.

From the public's point of view, now people may opt for high energy buildings for environmental reasons or for financial reasons. In such a scenario, a BER scheme may lower or increase the value of a property. As a consequence, a BER scheme should be robust and consistent. Furthermore, the BER scheme should allow reproducibility; it should be free, as much as possible, from any human error and

free as far as possible from subjective input data. Only in this way, can people trust a BER scheme and hence the scheme becomes more effective.

2.6.2 Finding the Building's Energy efficiency using a Measuring Approach

Section 2.5 discussed the elements of the annual energy heating and cooling loads which should be common to all certificates issued by a given BER scheme. These are:

- The calculation method
- The Typical Meteorological Year
- The internal set points temperature
- The thermal network model

The same thing applies if the measuring approach is used instead of the computational approach.

Section 2.4 discussed the various heat energy flows exerted on a building. It was also pointed out that these energy flows are unique to a particular building. Furthermore, section 2.4 showed that the computational approach which is widely adopted by the BER scheme around the world is insensitive for local variance, subject to human error and sometimes the input data is also subjective. All this could negatively affect the accuracy of the results, which indirectly influences the effectiveness of a BER schemes.

An ideal alternative for the computational approach is the possibility of measuring on site the energy flows in a building. This reduces human error and reduces the possibilities of ambiguous data input. Furthermore, the onsite measurement makes the process sensitive for the local variations. All this suggests that the results obtained by using a measuring approach are more realistic.

The various energy flows experienced by a building can be broadly classified to :

- Overall loss or gain through fabric
- Solar gain

- Internal gains
- Heat loss or gain due to air ventilation or air infiltration

The internal gains depend on the activities carried out in the building and have nothing to do with the efficiency of the building. For example, if a building is used for residential purposes, no changes are expected to occur in the building's efficiency if the same building is used for catering purpose. The only changes which are expected are the internal gains. While internal gains are important, for example, when calculating the size of the air-conditioners, they should not be considered in a BER scheme.

As explained in section 2.4 - Determining the Heat Energy Flows in a Building, there are established procedures to measure the air ventilation rates or the air infiltration rates. But the actual air changes depend heavily on the behaviour of the people or on the activities carried out inside the building. As with the internal gains, the BER schemes should not be influenced by the behavior of the occupants or the activity carried out inside the building. This suggests that any onsite energy flow measurements should be carried out with the building unoccupied and without any internal activities.

To use the measuring approach for a BER scheme is not an easy approach because up to now very little research has been dedicated for in situ measurements of the solar gain and of the overall heat loss coefficient. There are no established and approved procedures which can measure in situ the solar gain or the overall heat loss coefficient. The procedures that exist are still on an experimental level or too complex to implement on regular basis. Further details on these procedures are covered in Chapter 3 – Literature Review.

2.6.3 Objective

The Objective of this research is to develop a system that is able to predict the energy use in unoccupied residential buildings by in situ measurements with minimal user intervention and minimal energy intensive use.

This involves the development of an energy performance protocol based on in situ measurements along with the necessary hardware and software. Since the building is unoccupied the internal gain is assumed to be 0 and hence no measurements are done. The energy performance protocol will measure the effective heat loss coefficient, the thermal storage of the building, the solar gain and finally the air exchanges rate. The latter is not a priority because the procedure which measures the air exchange rate in a building is already developed and in use. The software and hardware was developed in such a way to minimize the installation and inconvenience to the owner of the property.

3. Literature Review

3.1 Introduction

This chapter goes through some of the techniques and methods used to forecast the energy consumption in a residential building. There are many techniques and method but this literature review will concentrate mainly on the data driven ones. This chapter starts by going through an equivalent thermal network commonly used for the thermal analysis. Then it continues with the classification of the methods used for the forecasting of the energy usage in residential buildings. Following the classification of the methods, the chapter continues to cover some energy performance protocols and methods which are data driven. This chapter concludes with a discussion and a conclusion.

3.2 Equivalent thermal network for models

Equivalent thermal networks are used to conceptually approach a very complex thermal circuit of a building into a more simplified thermal network. This section will present and discuss the most commonly used equivalent thermal networks for buildings. Starting from the most simple ones to the more complex ones. The more complex the equivalent thermal network is, the more it represents the characteristics of the building. One of the most simple thermal network is the 1R1C equivalent thermal network [7] which is represented in Figure 3.1.

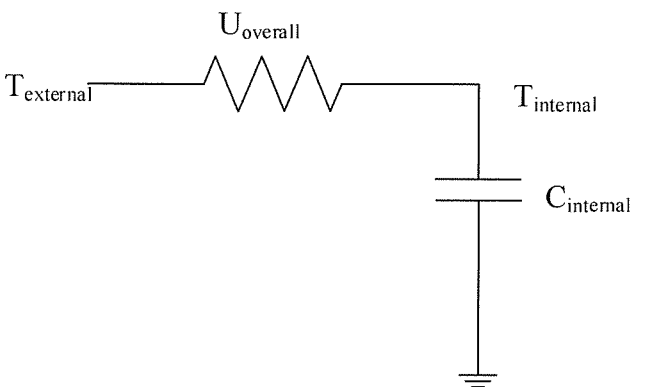

Figure 3.1 The 1R1C equivalent thermal network

This description model of the building is represented by only two components, the internal thermal capacitance $C_{internal}$ and the overall heat loss coefficient $U_{overall}$. In this model the thermal mass temperature is assumed to be equal to the internal air temperature $T_{internal}$ which in reality is not realistic. This is because some thermal resistance is always present between the building components and the air. One thermal resistance is the surface thermal resistance. It should be noted that this was evident in the experiments which were carried out as part of this study. This problem is addressed in the next equivalent thermal network. Figure 3.2 shows the 2R1C equivalent thermal network [7].

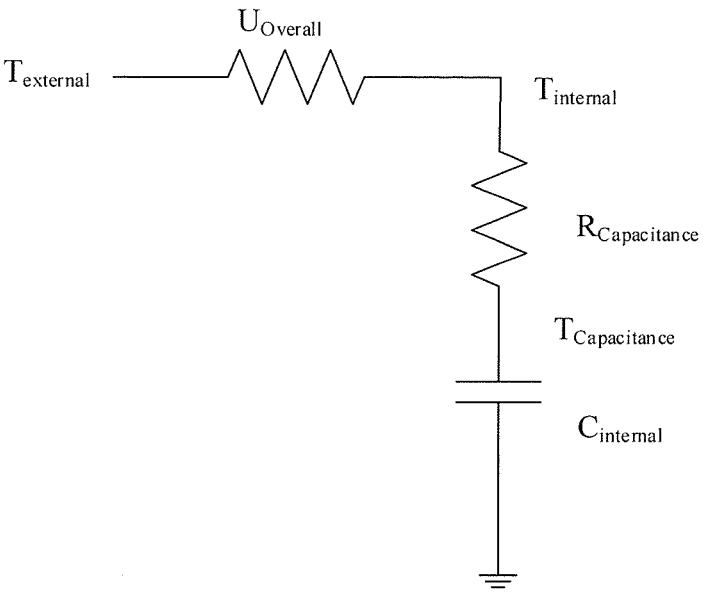

Figure 3.2 The 2R1C equivalent thermal network

The above equivalent thermal network is nearly identical to the previous one with the exception that another thermal resistor $R_{capacitor}$ is added to the network. This thermal resistor conceptually represents all the thermal resistance that exists between the building components and the air. It should be noted, that the air has a very low thermal capacitance as compared with the other building components or other objects housed in the building. As a consequence, its response for the heat energy supply is instantaneous and its thermal capacitance is ignored in the overall internal thermal mass. The 2R1C equivalent thermal network differentiates between the internal temperature $T_{internal}$ and the thermal mass $T_{Capacitance}$. The 2R1C equivalent thermal

network does not make a difference between the building components which completely contribute for the total effective internal thermal mass and those that partially contribute for the total effective thermal mass. For example, the thermal mass of the internal walls and the furniture contributes completely to the internal thermal mass. But unfortunately, this cannot be said for the boundary walls because only part of the heat energy stored in the boundary walls is released internally. As a consequence, they are partially contributing for the overall internal thermal capacitance. This same thing can be said for the 1R1C equivalent thermal network. This shortage is addressed in the next thermal network. Figure 3.3 shows the 4R2C equivalent thermal network [7].

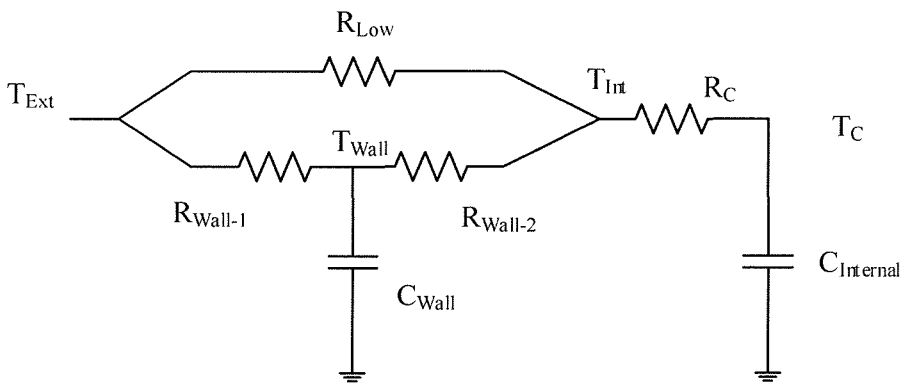

Figure 3.3 The 4R2C equivalent thermal network

As can be seen, this equivalent thermal network is the most complex of the three thermal networks presented so far. It differentiates between the internal thermal capacitance and the thermal capacitance of the boundary walls. $C_{Internal}$ represents the internal thermal mass of the building, R_c is the thermal resistance that exists between the internal thermal mass and the air, while T_c represents the thermal mass temperature. R_{Low} approximates the thermal resistance offered through the mass less the building components and air exchanges. An example of such a building component is a window. The thermal characteristics of the external walls are approximated by R_{Wall-1}, R_{Wall-2} and C_{wall}. R_{Wall-1} and R_{Wall-2} indicates the total thermal resistance offered by the external walls while C_{wall} represents the thermal capacitance of the walls. If the walls are made from homogenous material then $R_{Wall-1}$is equal to

$R_{Wall\text{-}2}$. This thermal model differentiates also between the internal temperature and the temperature of the walls' thermal mass. There are many other possibilities of the equivalent thermal networks model. For example, figure 3.4 shows model 3R2C which is a variant of thermal model 2R1C [7].

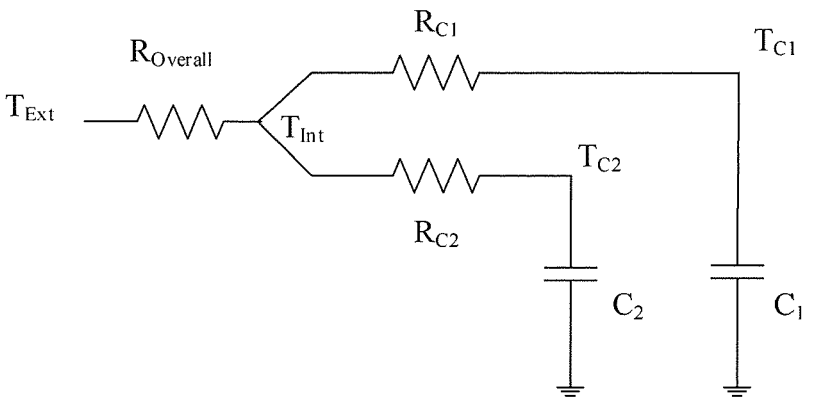

Figure 3.4 The 3R2C equivalent thermal network

In this model the internal mass is divided into two parts. One part approximates the internal mass which is made from the internal building components and which is denoted by C_1. Another part which approximates the internal mass, is made from objects housed in the building and is denoted by C_2. R_{C1} and R_{C2} represent the thermal resistance between the inner air and C_1 and C_2 respectively. $R_{Overall}$ is the overall thermal resistance of the external structure of the building. This model is especially useful for buildings which house many objects with high thermal mass.

A variant of the 1R1C is shown in figure 3.5. Here, the overall heat loss coefficient is divided in two parts. The first part represents the heat loss coefficient through the transmission loss denoted by U_A. The other part represents the heat loss due to ventilation and is denoted by H_v. $C_{Internal}$ represents the internal thermal mass of the building.

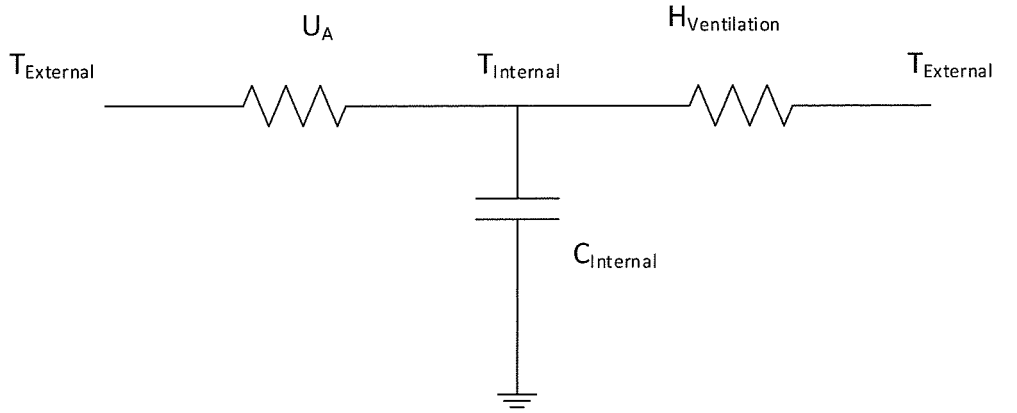

Figure 3.5 A Variant of the 1R1C equivalent thermal network [8]

3.3 Classification of the Analysis methods

There are many methods which estimate the energy usage in a building. The ASHRAE handbook Fundamentals [9] classifies them into a number of categories. These are listed and briefly explained below.

Dynamic or Steady-state methods: The ASHRAE handbook Fundamental classifies these methods into two types. The methods which take into account the thermal mass of the building and other methods which do not consider the thermal mass of the building. The first group of methods are referred to as dynamic methods and the latter group of matters are referred to as the steady-state methods. The dynamic methods are expected to give more accurate results.

Forward or Data-driven: Another classification that is found in the ASHRAE handbook Fundamental is the Forward approach or the Data-driven (inverse) approach. In the forward approach the prediction of the energy usage is based on a mathematical model which describes the behaviour of the building. This approach does not require the building to be physically built. In contrast, the Data-driven methods require the building to be complete. Data-driven methods require on site measurements. From these measurements, a mathematical description of the building is obtained and used to predict the energy usage in the building.

Data-driven categories: The ASHRAE handbook Fundamentals categorizes further the Data-driven methods into three more categories. These are **Empirical** also known as the **Black-Box,** the **Calibrated Simulation** and the **Physical** which is also known as the **Gray-box.**

Empirical: In Empirical methods the mathematical model is derived solely from the measurements conducted in the building under analysis. These tend to be less accurate than the calibrated simulation or the physical approach ones. With the exception of neural networks which give quite accurate prediction. Neural networks are discussed further in the following sections.

Calibrated Simulation: Here, the building in question is first simulated on a computer and the predicted energy usage is compared to the actual energy used. Then, the various inputs to the simulator are calibrated until the energy predicted matches the actual one. Once this process is complete the predictions are more reliable. These type of methods are labour intensive and require skilled people who are knowledgeable in the simulation programs [10].

Physical: In this approach, the building is first formulated into a physical model and then the coefficients are aggregated with the important parameters, using statistical analysis to determine these coefficients. These type of methods show great potential but they need high level of expertise[10].

Now that the classification of methods is known, it is possible to go through these categories and identify the category which is suitable for this research. The forward methods cannot be used, because they are based on calculations only and in this research we need to measure the building performance. The physical or the calibrated simulation data-driven methods require expert people and they are labour intensive methods and thus make the proposed system not viable. This leaves only one option that is the empirical data-driven methods. ASHREA handbook Fundamentals identifies seven methods of this category which are described in the following sections.

3.4 Empirical data-driven method for energy use

The ASHREA handbook Fundamentals list seven empirical Data-driven methods. Only one method is classified as a dynamic method, the rest are classified as steady-state methods [9]. The dynamic method uses the artificial neural networks to solve the problem. This is discussed in section 3.5. The rest of these methods are discussed in this section.

The most simple method is the simple linear regression using energy as the dependent parameter and the external temperature as an independent parameter. The accuracy of this method is regarded as low. The multiple linear regression method is a more complex method with medium accuracy. It has energy usage as the dependent variable and it has as the independent variable any combination of temperature, humidity, solar radiation, wind and time. The data-driven bin method is an adaptation of the ASHRAE bin method for a measured value. The accuracy of this method is regarded as medium [11].

Another method is the 3-P changing point model. This is a single-Variate model with the energy as the dependent variable and the temperature or degree-days as the independent variable. The accuracy of this method is regarded as medium [11]. Figure 3.6 shows the three-parameter changing-point for cooling. It shows a typical energy profile for cooling only.

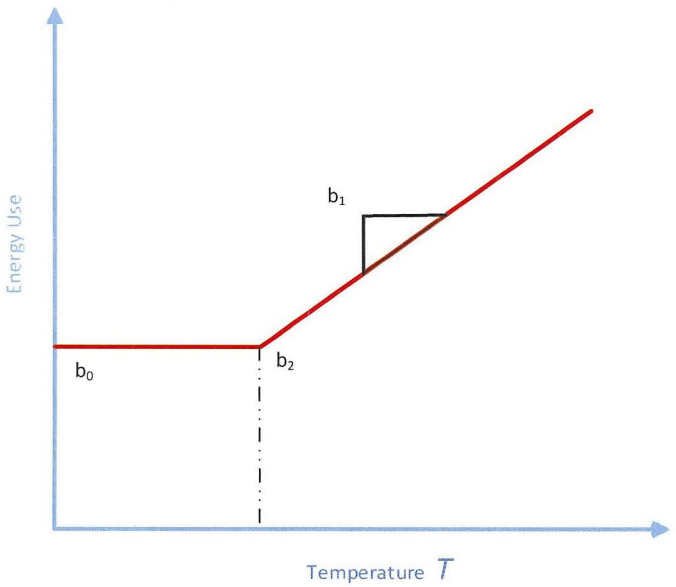

Figure 3.6 A Three-Parameter change-point, cooling [12]

This profile is typical for a building which uses electricity for cooling. The red line represents the electrical energy supplied to the building and is attained by performing regression analysis on the data. Parameter b_0 indicates the electrical energy needed when no cooling is needed in the building. Parameter b_2 indicates the changing point temperature. This is the temperature when the cooling process is started. Parameter b_1 is the slope of the regression. The energy E is estimated by

$$E = b_0 + b_1(b_2 - T) \tag{3.01}$$

The fifth method is the four-parameter change point. It is very similar to the three-parameter changing point with the difference that it has two regression slopes, one for the temperatures over the base temperature and another one for the temperatures under the base temperature. The last method is the five-parameter change point method. It is similar to the three-parameter change point method but it has two change point temperatures where one indicates the temperature when the cooling process is started and the other one indicates when the heating process is started. It has also two regression slopes, one for the cooling period and the other one for the heating period [12].

All the steady-state methods discussed in this section can be used to estimate the energy requirements of a building, but unfortunately they cannot differentiate between the energy used for the space heating and the space cooling or the energy used to make up for the inefficiency of the heating and cooling systems. Furthermore, the energy requirements of a building depends also on the behavior of the occupants which is difficult to predict and hence difficult to correct.

The objective of this research is to measure the efficiency of the building structure which excludes the occupant's behaviour and the inefficiencies of the cooling and the heating systems. As a consequence, none of the methods discussed above is suitable for the proposed system. This leaves only one option to investigate, that is, the neural network method which is discussed in the next section.

3.5 The Artificial neural network method for energy use

This section will discuss the artificial neural network as a method to predict the energy use in a building. An artificial neural network is made up of an input layer, an output layer and a number of hidden layers. Each layer is made up from a number of neurons. Each neuron has a number of weighted inputs which are fed to transfer function and then the result is passed to an active function. Typically, the transfer function is a summation function. The number of the weighted input of the neuron depends on the position of the layer in which a neuron is placed. Before an artificial neural network can be used, it should be trained by using an algorithm such as the back-propagation algorithm.

The implementation of an artificial neural network for practical solutions comes with a lot of challenges. The implementer has to decide on the number of inputs and outputs of the neural network, on the number of hidden layers to use, on the number of neurons that are in the hidden layers, the type of active functions to use in the neurons, the algorithm to use to train the neural network and finally the training set to use. Each problem has its own ideal configurations. Few rules exist which can

guide the implementer on how to configure the artificial neural networks, therefore, the design of the artificial neural networks is more art than science. The main advantage of the artificial neural networks is that it can adapt for a specific scenario. The characteristics of the artificial neural networks make them sensitive to the local variance and gives them an edge over the other methods.

The ASHRAE handbook Fundamentals classified this method as a dynamic one with high accuracy [12,13]. There is a lot of literature which describes the success of using an artificial neural network for applications involving the prediction of energy use or related to. Some of this literature is discussed here.

Mikael Lundin et al [14] used artificial neural networks to determine the heat loss coefficient, the thermal mass and the gain factor. The experiment was carried out in a test cell with dimensions 365x400x400 mm. The root means square error RMSE was 2.5 to 9.4% for the total heat loss coefficient, and the total heat capacitance had an average error of 9.8%. A.E Ruano et al [15] used artificial neural networks to predict the air temperature for air condition control systems. The energy predictions derived from an artificial neural network are considered to be so reliable that scientists are using them as a benchmark. Abraham et al [16] used the energy prediction from an artificial neural network as a benchmark to evaluate four commonly used simulators which are the GBS Website, the Energy_10, the eQUEST and the EnergyPlus.

An interesting investigation was done by T.Olofsson and S. Anderson [17]. They used neural networks to predict the annual energy used for single family buildings. The experiment was carried out on six units. The measured parameters were the domestic energy, the heating demands and the internal and external temperatures. The monitoring period varied between two to five weeks. The outcome of this experiment showed that the deviation from the actual annual energy used was about 4%.

Another use of the artificial neural networks is in the predictions of energy saving after performing retrofits. Melek Yalcintas [18] used the artificial neural networks to

predict the energy saving from two projects involving retrofitting of the building equipment. The RMSE varied between 6.81% and 16.4%.

Probably, the most interesting event which showed the power of the artificial neural networks in prediction of the energy use was "The great energy predictor shoot-out I" . The competitors were given four months of historical data and they had to predict the energy used for the next two months. Five of the six most successful contenders used artificial neural networks [19].

As can be seen, from the above literature the artificial neural network could be used for this research. But unfortunately the artificial neural network requires training data to predict the energy use in a building. This data should be at least two weeks long and therefore this takes too long for getting the results. Furthermore, similar to the steady-state methods discussed previously, the predicted energy use is not limited to the heat transmission loss only. It includes energy losses due to the inefficiency of the cooling and heating system and due to the behaviour of the occupants. A possible solution for this problem is to create a training data with the building closed and unoccupied using fan heaters as a source of heating. But this in practice is not likely to be a feasible solution because the training data is expected to be at least two weeks long to get the required accuracy. Using a general data for training is also not a solution because the artificial neural networks need data for training which originates from the building under analysis. Furthermore, this type of method requires highly qualified personnel which does not make it feasible and cost effective to perform on a regular basis.

The next section discusses briefly a physical data-driven method which influenced the design of the proposed protocols.

3.6 STEM & PSTAR method

In this section a brief description of the Short Term Energy Monitoring (STEM) and the Primary and Secondary Term and Renormalization calculation procedure

(PSTAR) can be found. This method is classified as a dynamic physical data-driven method. It has quite good accuracy [20]. This method begins by an audit visit to the building. By this audit a descriptive model of the building is obtained and expressed in the following equation:

$$0 = Q_{int} + P_1 * Q_{AU} + P_2 * Q_{sun} + P_3 * Q_{C\_in} + Q_{C\_out} + Q_{inf} + Q_{Sky} + Q_{aux}$$

Where:

Q_{int} is the internal gain term which is measured on site.

Q_{AU} is the heat energy loss due to transmission. This is a calculated term which is calculated by using the overall U-value from the descriptive model and from the difference in temperature between the internal and external environment.

Q_{sun} is the heat gain due to the solar radiation. This term is obtained by performing a simulation of the audited building.

Q_{C_in} is the heat energy that goes in the internal thermal mass of the building. Its value is calculated from the descriptive model and the internal temperature.

Q_{C_out} is the heat energy that goes in the thermal mass which is in contact with the external temperature. Its value is calculated by the descriptive model and from the external temperature.

Q_{inf} is the heat energy loss due to air infiltration. This is a measured term which uses for example a blower door test.

Q_{sky} is the heat energy loss caused by sky temperature depression. This term is obtained through simulation.

Q_{aux} is the supplied heat energy in the building to maintain the required temperature. This is a measured term.

P_1, P_2 and P_3 are renormalization parameters. Q_{ua}, Q_{sun} and Q_{C_in} are primary terms whose values affect the accuracy of the results. The rest are secondary terms whose values have a lesser effect on the accuracy of the result. The primary terms are tuned

by the renormalization parameters P_1, P_2 and P_3 whose values are obtained by using linear least-squares regression. The necessary data required for the normalization process is attained by following test protocol. This test protocol is run over a period of three days. The building has to be unoccupied with all the appliances turned off. The external, internal and unconditioned temperatures are monitored together with the external weather conditions including the solar radiation. In the night of the first day the building is heated up to a pre-defined set point. The needed energy is measured and recorded. On the second or third night the heating is turned off allowing the temperature to decay. The data obtained during the temperature decay is used to determine P_3, the data obtained during the first night is used to determine P_1 while the data obtained during the days between day one and two are used to determine P_2. [21,22]

As can be seen, the whole process is quite complex mainly due to the descriptive model. Therefore, this method is not suitable for the proposed system. But the test protocol used to determine the normalization parameters is of interest for this research. In fact, the principle used here to separate the dominant forces was partially adapted in the proposed protocol. Next section will list some of the protocols which were investigated but not discussed here. It will also conclude this literature review.

3.7 Discussion

There were other energy performance protocols which were investigated but were not discussed in this literature review. These are the Energy Barometer, the House Energy Labeling Procedure (HELP) and Monitored Energy Protocol. The objective of these protocols were different from the objective of this research. These protocols predict the total energy used and not the energy required for cooling and heating only. Furthermore they do not consider the behavior of the occupants. The objective of this research project is to measure the overall heat loss coefficient of the building.

As can be seen from the previous sections none of the methods or protocols which were investigated are suitable for achieve our target. The data-driven methods are either too complicated to be conducted regularly or they predict the total energy use and not the energy required due to the heat transmission loss. As a consequence a new protocol had to be developed. The development of this protocol is covered in the next two chapters.

4. Analysis of Humidity, Temperature and Solar Irradiance

This research is divided into two main tasks. The first task is to develop a protocol which measures the energy performance of an unoccupied Maltese residential building. The protocol should be able to measure the energy performance of a Maltese residential building. The second task is to develop the necessary hardware and software for the implementation of this protocol or other energy performance protocol.

4.1 The Energy Performance Protocol

The development of the energy performance protocol consists of two phases. In the first phase an energy analysis of a typical Maltese building was carried out. In the second phase, the protocol was developed, based on the data attained in the analysis and with a number of evolving experiments. For these purposes, a room with a typical Maltese characteristics was identified and used.

4.2 The Test Room

The Test room is situated at the back of a house which was built in the beginning of the eighties. The original purpose of the room was to keep and breed green finches, therefore some retrofitting was carried out in order to make the room similar to a room in a residential building. This room is ideal for the purpose of the analysis. It has the roof and 50% of the walls exposed to the outside environment. The orientation of the room is WSW, therefore its external walls are subject to direct solar radiation in the afternoon, while the adjacent building provides some shade. Figure 4.1 shows photo of this room.

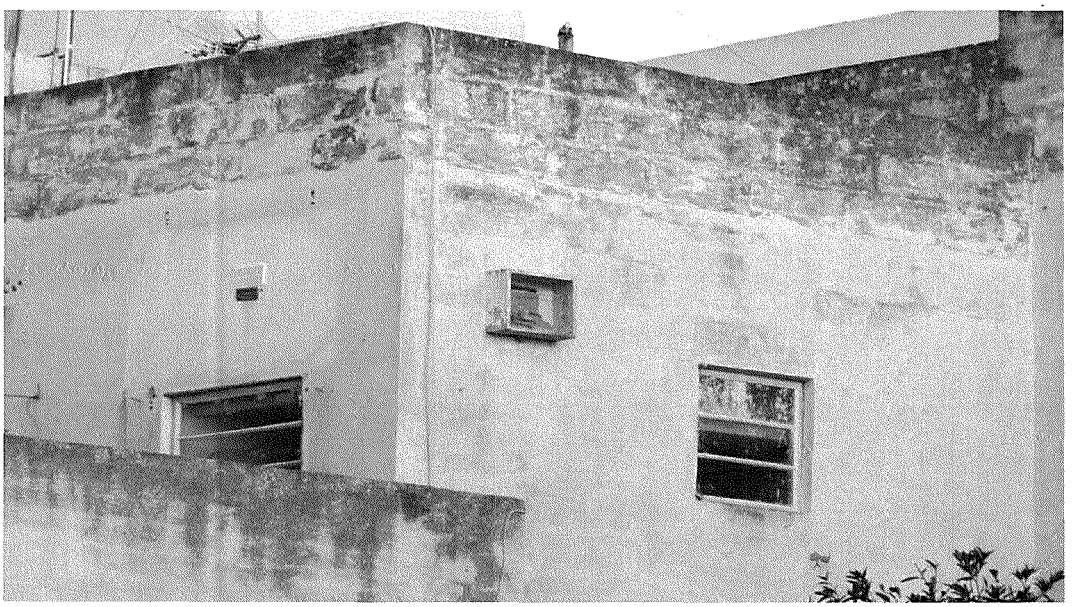

Figure 4.1 Picture of the Test Room

A detailed inspection of the test room and an interview with the builder was carried out. This provided the following information:

Size of the room:	Length: 3.7m Width: 1.14m Height: 2.91m
Door size:	0.89m X 1.90m made from wrought iron and glass.
Window size:	0.8m X 0.69m made from wrought iron and glass.
Ventilation:	0.15m X 0.15m.
Common walls:	Bricks 0.23m and with cement mortar finishing.
External walls :	Most of the bricks are 0.15m with some limestone and with cement mortar finishing.

Roof: Concrete Slab 0.18m + 0.13 Limestone + 0.10 Concrete + membrane.

Floor: Concrete Slab 0.18m + 0.10 Limestone + Tiles.

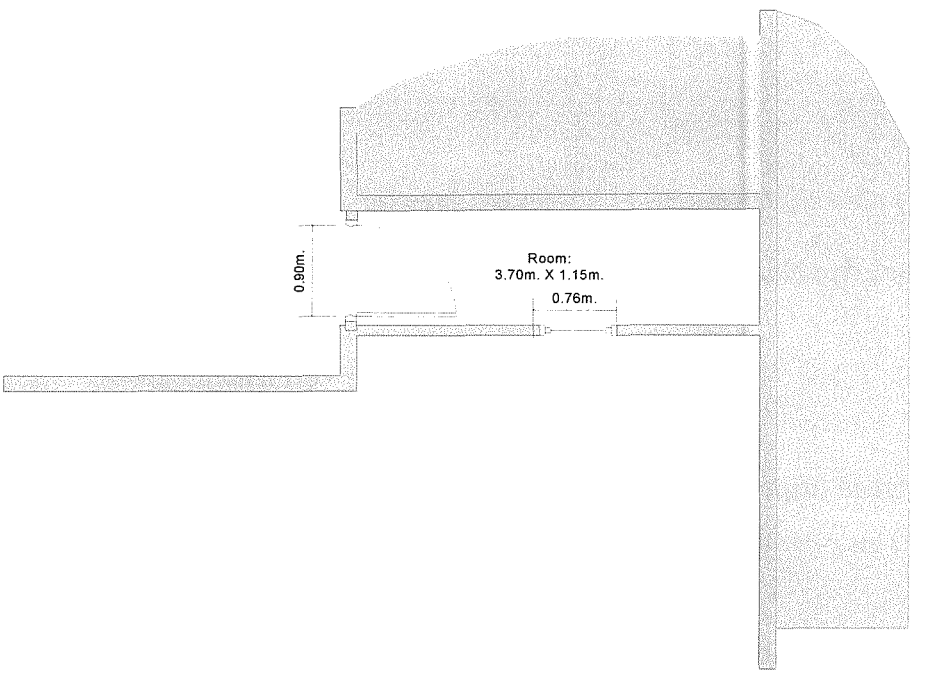

Figure 4.2 Plan View of the Test Room

4.3 Test Room Energy Analysis

The main objective of these analysis is to identify how the internal environment of a typical local residential building is effected by the external environment. This required the monitoring of the external weather conditions together with the internal conditions of the test room. For this reason, an industrial type, wireless weather station was installed outside on top of the test room with its console placed inside the test room. The weather station used was a Davis Vantage Pro 6152. Its external sensor suite provides temperature, humidity, wind speed, wind direction and rainfall while the console provides humidity, temperature and barometric pressure. In addition, a solar radiation sensor, which provides the global radiation

readings, was installed in the external sensor suite. Figures 4.3 shows a picture of the external sensor suite installed on top of the test room.

Figure 4.3 Davis Vantage Pro 6152.

Furthermore, a data logger was added to the console. The latter provides 128 Kbyte of non-volatile memory, which means that the weather station can record 8 days of weather data with 5 minutes intervals. The data logger provides a USB port which allows the users to download data to a PC. The supplier, supplies for free a Weather Link software together with the data logger. This software archives all the downloaded data in a database on the PC and provides utilities to analyze the archived data. Figure 4.4 shows a screen shot of one of the utilities.

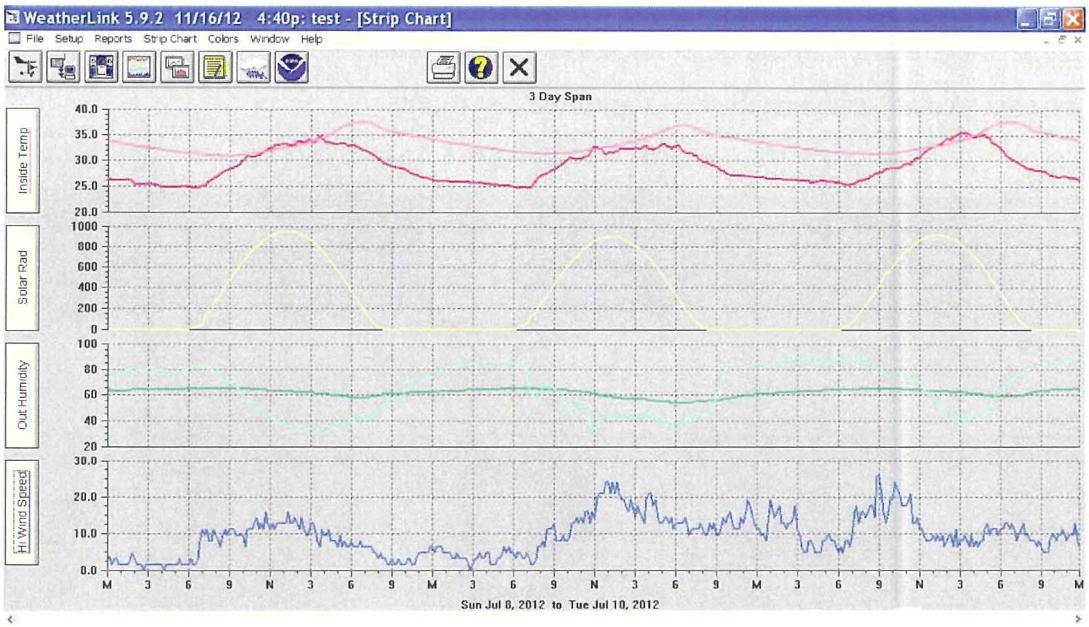

Figure 4.4 The Weather Link Software

The monitoring of the test room was conducted for one whole year. This ensured that the effects of the seasons were captured in the analysis. The monitoring period was started on the 2nd September 2011 and was completed by the 3rd September 2012.

4.4 Salient Points From the Analysis

4.4.1 Humidity

The humidity in the air has little significance on the energy performance of the building but on the other hand, it has a significant impact on the heat index and the thermal comfort inside the building. Consequently, humidity could indirectly have considerable effect on the energy consumption if the thermal comfort is a must. For this reason, an analysis on the internal and external humidity was carried out. It should be noted that the test room does not contain any water or living things which can contribute to the moisture balance in the air. The only source of moisture in the test room was from air infiltration and from the building itself.

4.4.2 Relative Humidity

The air surrounding us can hold water vapour. As a consequence, it continuously absorbs and loses water molecules to the surrounding environment. At some point in time, the mix of air and water vapour reaches equilibrium. In this state of equilibrium, the air looses the same amount of water vapour that it manages to absorb from the surroundings. There is a limit on how much water the air can hold water vapour. This limit depends from the dry bulb temperature and from the atmospheric pressure and it is generally referred to as water vapour at saturation. One way to express the Relative Humidity is to compare the water vapour pressure in the air to the water vapour pressure at saturation for the given dry bulb temperature. This is given by :

$$RH = \frac{Water\ Vapor\ Pressure}{Water\ Vapor\ Pressure\ at\ Saturation} X\ 100\ \% \qquad (4.01)$$

Water vapour partial pressure at saturation (p_{ws}) can be estimated by:

$$p_{ws} = e^{(77.3450 + 0.0057\ T - 7235\ /\ T)} / T^{8.2} \qquad (4.02)$$

Where T is the temperature in Kelvin.

It should be noted that with an increase in temperature, the water vapour pressure will also increase. This causes the relative humidity to decrease if no additional water vapour is induced in the given air.

Density of Water Vapour (ρ_w) is calculated by

$$\rho_w = 0.0022\ p_w / T \qquad (4.03)$$

where p_w is partial pressure water vapour and T is the temperature in Kelvin.

4.4.3 The External Relative Humidity

The external relative humidity for the whole year which started on the 2nd September 2011 and ended on the 3rd September 2012, was visually observed. It

was observed that during the night the relative humidity was significantly higher than during the day excluding some exceptions. This was also confirmed statistically as shown in figure 4.6. Figure 4.5 shows the external humidity and the temperature data for the period which started on the 1st June 2012 and ended on the 8th June 2012.

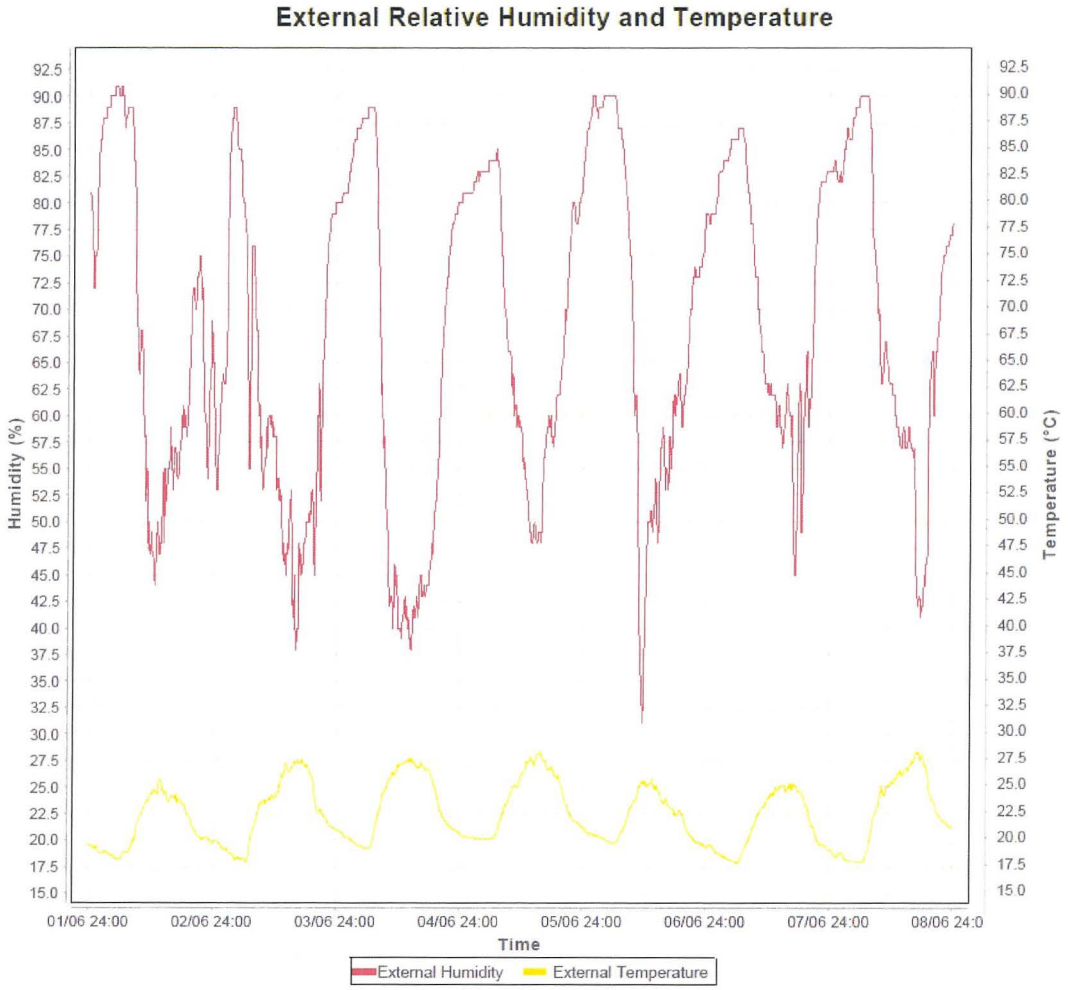

Figure 4.5 The External Relative Humidity and Temperature

As can be observed in figure 4.5 there is a correlation between the external temperature and the external humidity. In a 24 hour period, the humidity is at the lowest point when the temperature is at its warmest, while the humidity is at the highest point when the temperature is the coldest. As was explained in section 4.4.2 of the Relative Humidity, the relative humidity is effected by the change in temperature. There are other conditions which effect the relative humidity but in

this case it seems that the external temperature has significant impact on the external relative humidity.

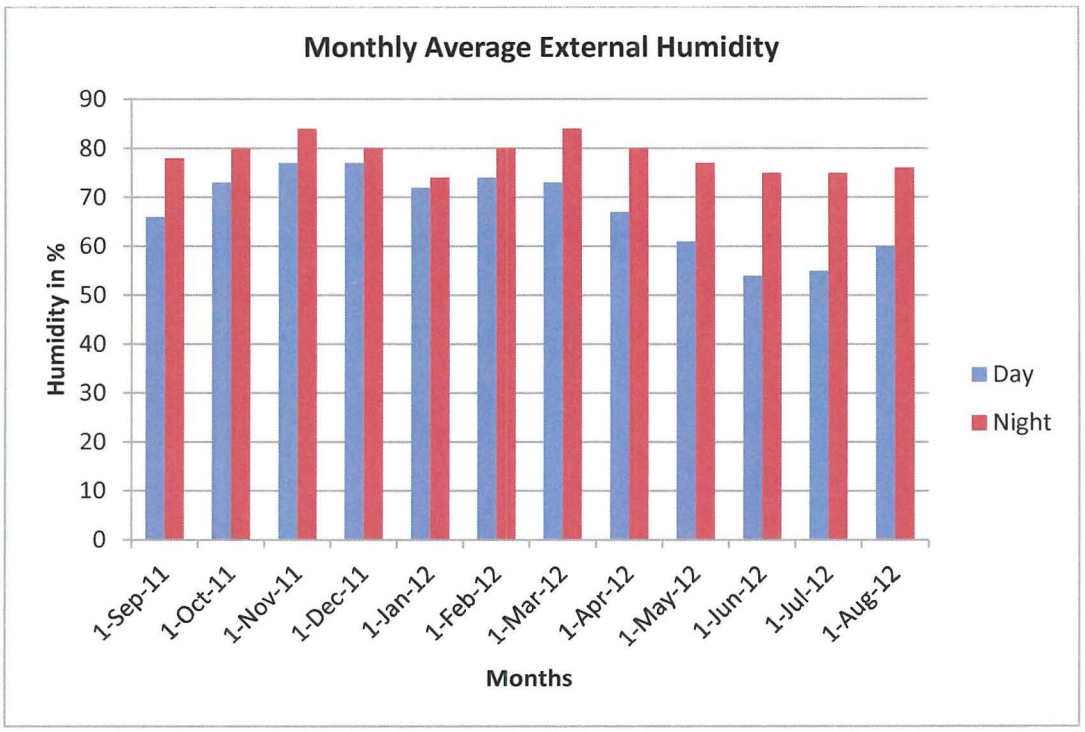

Figure 4.6 The Monthly External Average Relative Humidity during the day and night

Figure 4.6 shows the monthly averages for the external humidity. The blue bars represent the averages during the day, while the red bars represent the averages during the night. The averages during the day were calculated from 7.00 to 19.00 hours, while the averages during the night were calculated from 19.00 to 7.00 of the next day. As can be seen in the bar chart of Figure 4.6, the monthly average of relative humidity is always higher during the night time than during the day time. It was also observed that this difference was smaller during the rainy season. Inevitably, the rain will increase the sources of water vapour in the air which in turn increases the relative humidity.

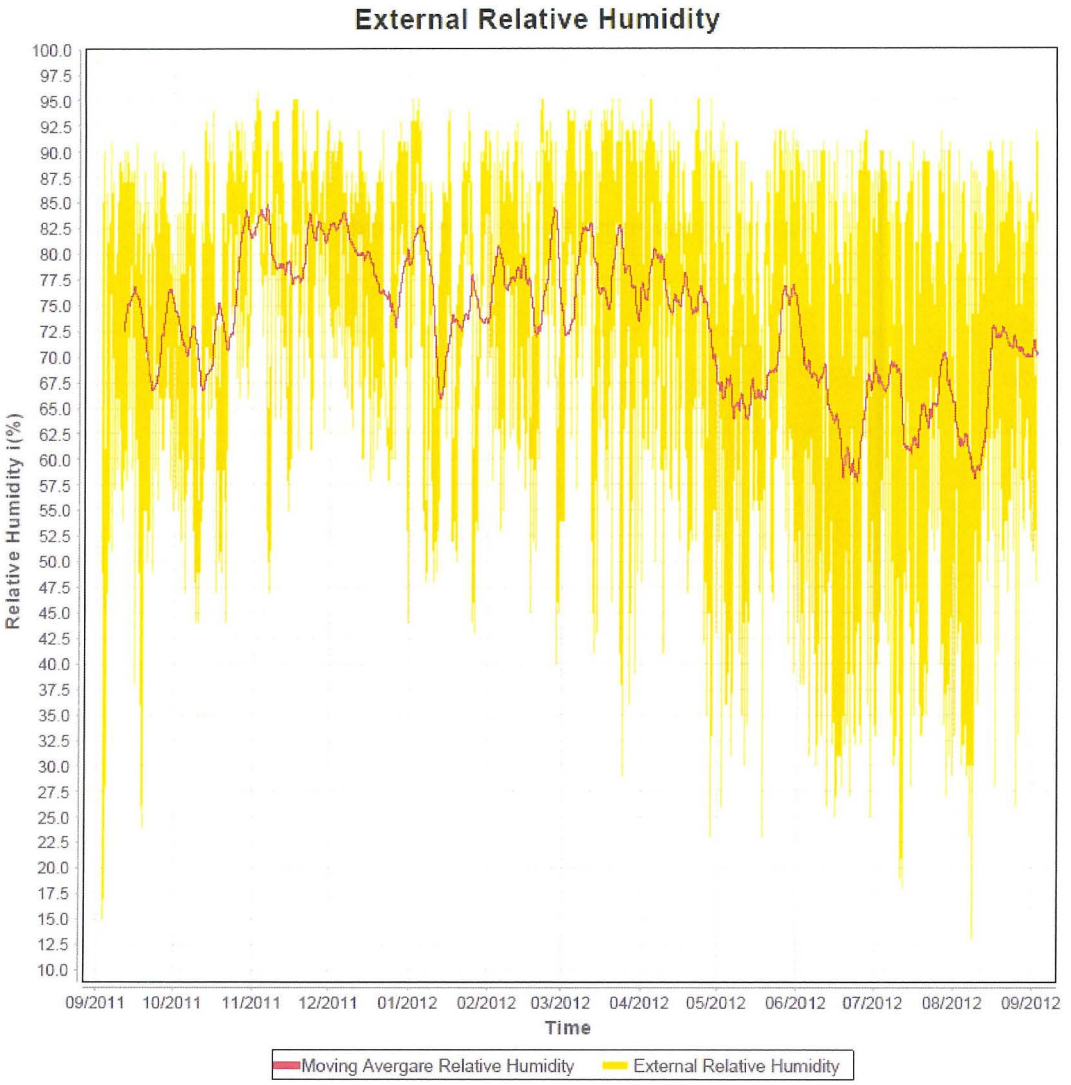

Figure 4.7 The External Relative Humidity

Figure 4.7 shows the external relative humidity for a whole year which started on the 2nd September 2011 and ended on the 3rdSeptember 2012. The orange line represents the actual external relative humidity, while the red line represents the rolling average of the actual relative humidity data. The step is of 10 minutes while the averaging period is of 7 days. The latter indicates that the fluctuations in the relative humidity are small.

4.4.4 The Internal Relative Humidity

The internal relative humidity was also visually observed for the whole observation period. The findings were quite different from the external ones. It should be recalled that the test room does not contain any water sources or living things. Therefore, the only water vapour sources which were available were from the building itself and from the air infiltration. It was observed that the fluctuation of the internal relative humidity from the night period to the day period were very small when compared with the external ones. Furthermore, the fluctuations throughout the one year period were significant. Figure 4.8 shows the internal humidity and the temperature data for the period which started from the 1st June 2012 and ended on the 8th June 2012.

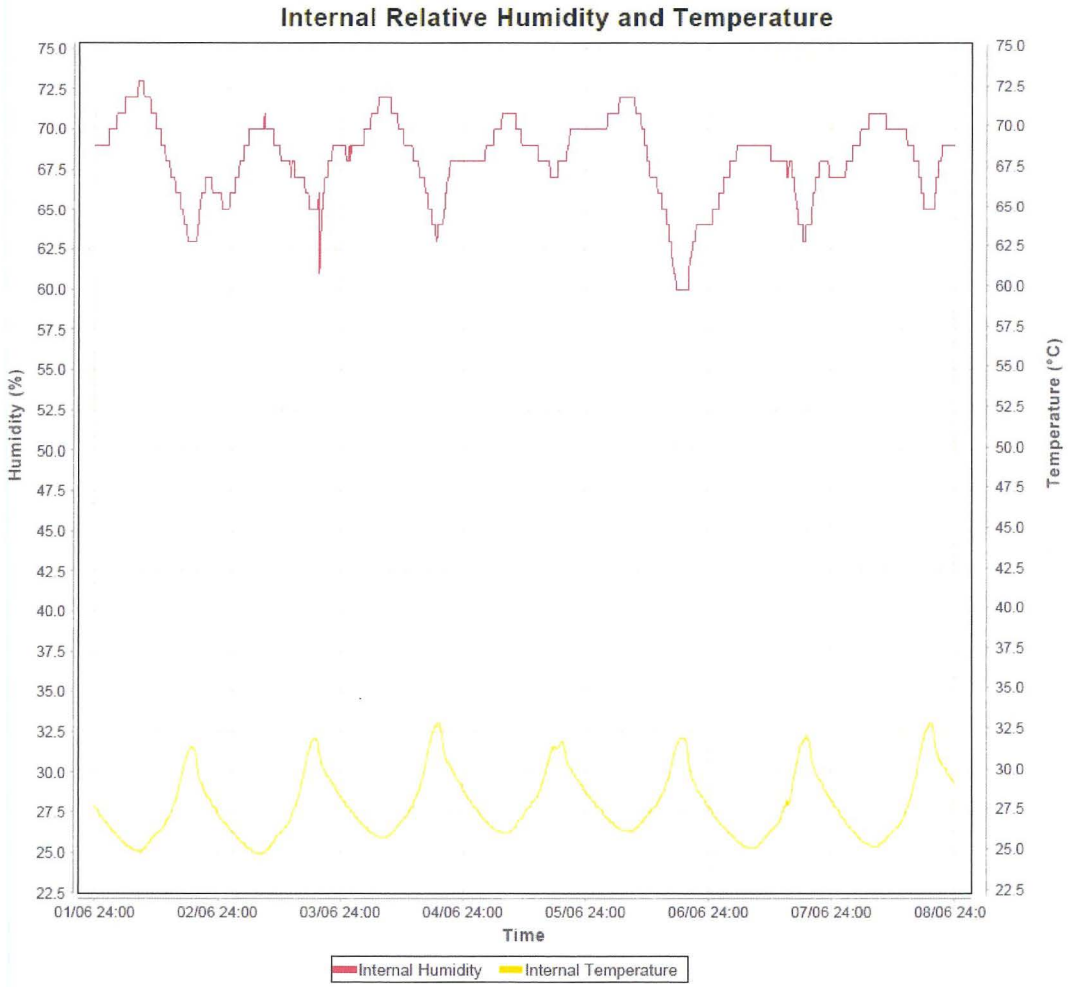

Figure 4.8 Internal Relative Humidity and temperature

Similarly to the analysis of the external relative humidity, it was noticed that there is a correlation between the internal temperature and the external relative humidity. The correlation is: when the temperature is the warmest, the humidity is in the lowest point and when the temperature is the coldest, the relative humidity is in the highest point. The difference here seems that the temperature has much less affect on the relative humidity.

Figure 4.9 is showing the internal relative humidity for a whole observation year.

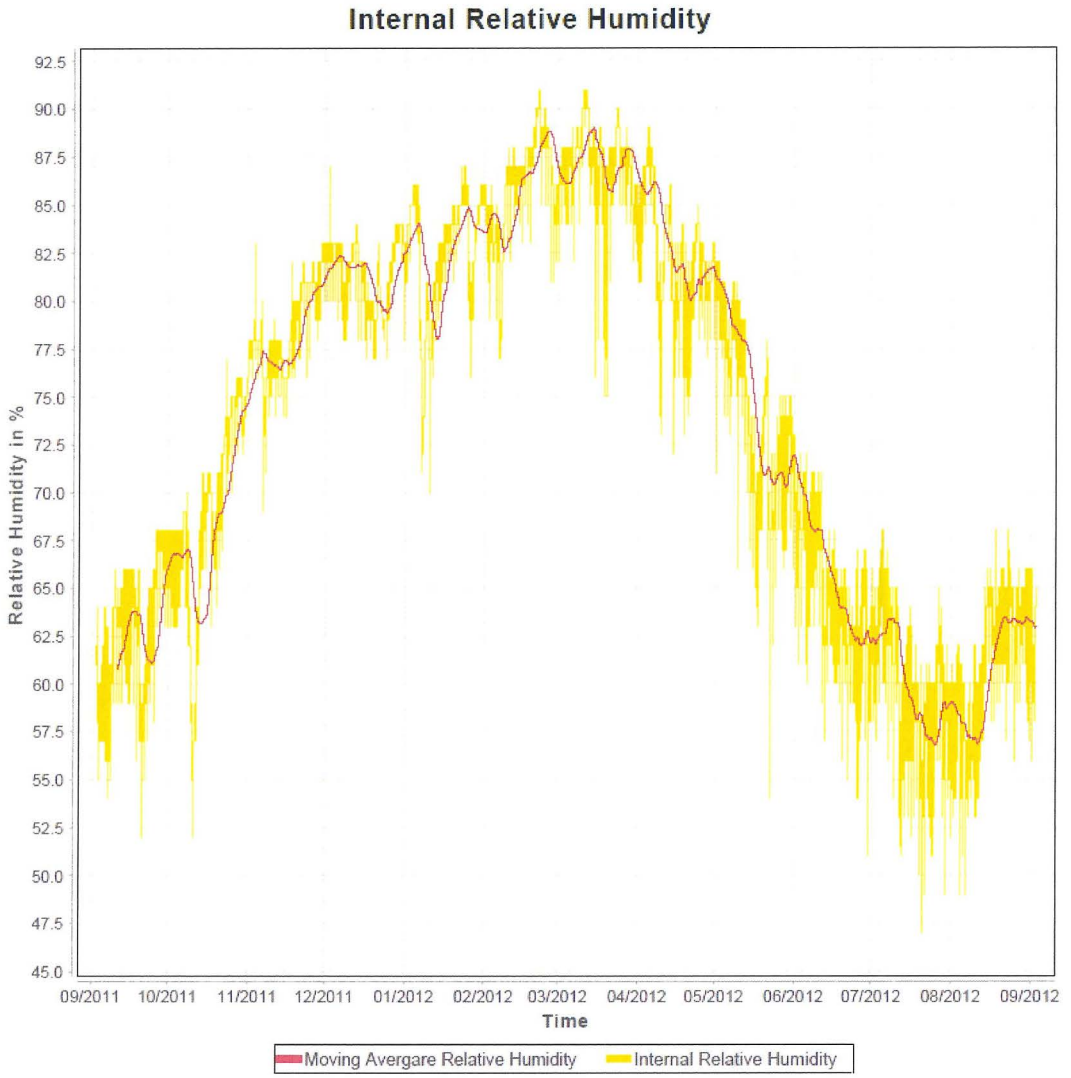

Figure 4.9 The Internal Relative Humidity

The orange line represents the internal relative humidity samples which were taken every 10 minutes, while the red line represents the moving average. The step size of the rolling average is 10 minutes while the averaging period is of 7 days. As can be seen in the line graph of Figure 4.9 the changes of the internal relative humidity are

relatively small during the one day period but on the other hand, the seasonal changes are quite significant. It may be observed that the internal relative humidity is significantly higher during the rainy season and during the months that follows. For better comparison the rolling averages of the external and internal relative humidity are shown in the line graphs of Figure 4.10.

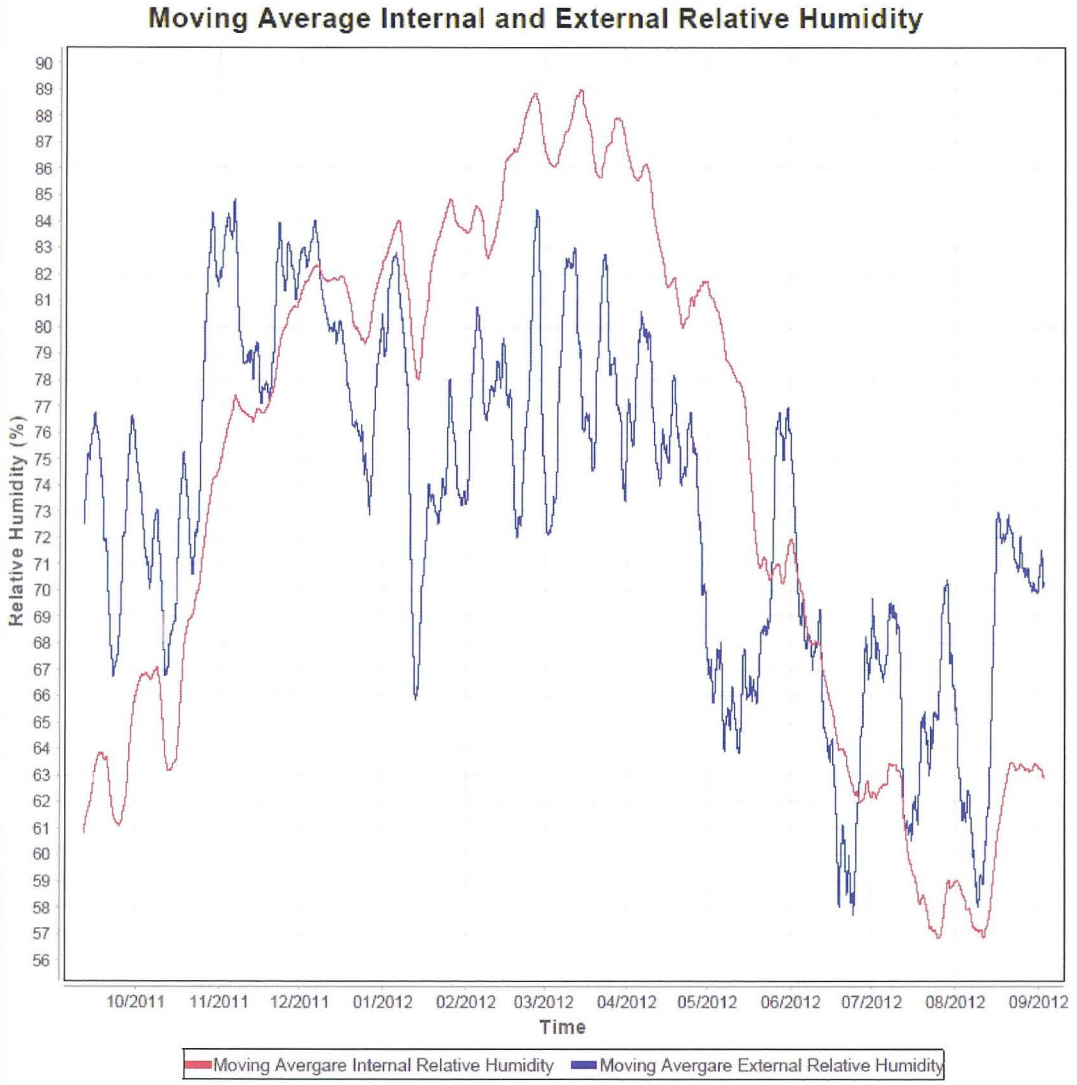

Figure 4.10 Moving Average Internal and External Relative Humidity

The red graph represents the internal relative humidity while the blue graph represents the external relative humidity. In both cases, the step size is 10 minutes, while the average period is of 7 days. As can be seen, there is no direct correlation between the internal and external relative humidity. This was not expected since

because there was substantial air infiltration in the test room from the outside air. This air infiltration changes the water vapour content of air and hence changes the level of relative humidity in the test room. It is evident, that there was a difference in the Absolute humidity of the air inside the test room and of the air outside. Consequently, analysis of the Absolute humidity (which is also referred to as water vapour density) of both the inside and the outside air were carried out. Absolute humidity, indicates the amount of water in grams present in one cubic meter of air. The aim of these analysis was to explore the possibility of estimating the air changes within a room by simply monitoring the Absolute humidity of both the inside and the outside air. The estimation of the air changes in a building is considered as an important parameter when measuring the energy performance of a building. This is especially true in cold countries like the Scandinavian ones. By having the estimation of the air changes in a building, it is possible to know the energy loss due to air infiltration and air ventilation, if no heat recovery system is used.

The Absolute humidity (kg/m^3) was calculated through the following steps:

1. Calculate the water vapour pressure at saturation point using formula (4.02) for the given temperature.
2. Calculate the water vapour pressure for the given temperature using formula (4.01).
3. Determine the water density of the water contained in the air or the Absolute humidity using the formula (4.03).

The red line in figure 4.11 shows the Absolute humidity of the air inside the test room for the period which started on the 1st June 2012 and ended on the 7th June 2012. The orange and blue line represent the relative humidity and the temperature respectively, inside the test room for the same period of time.

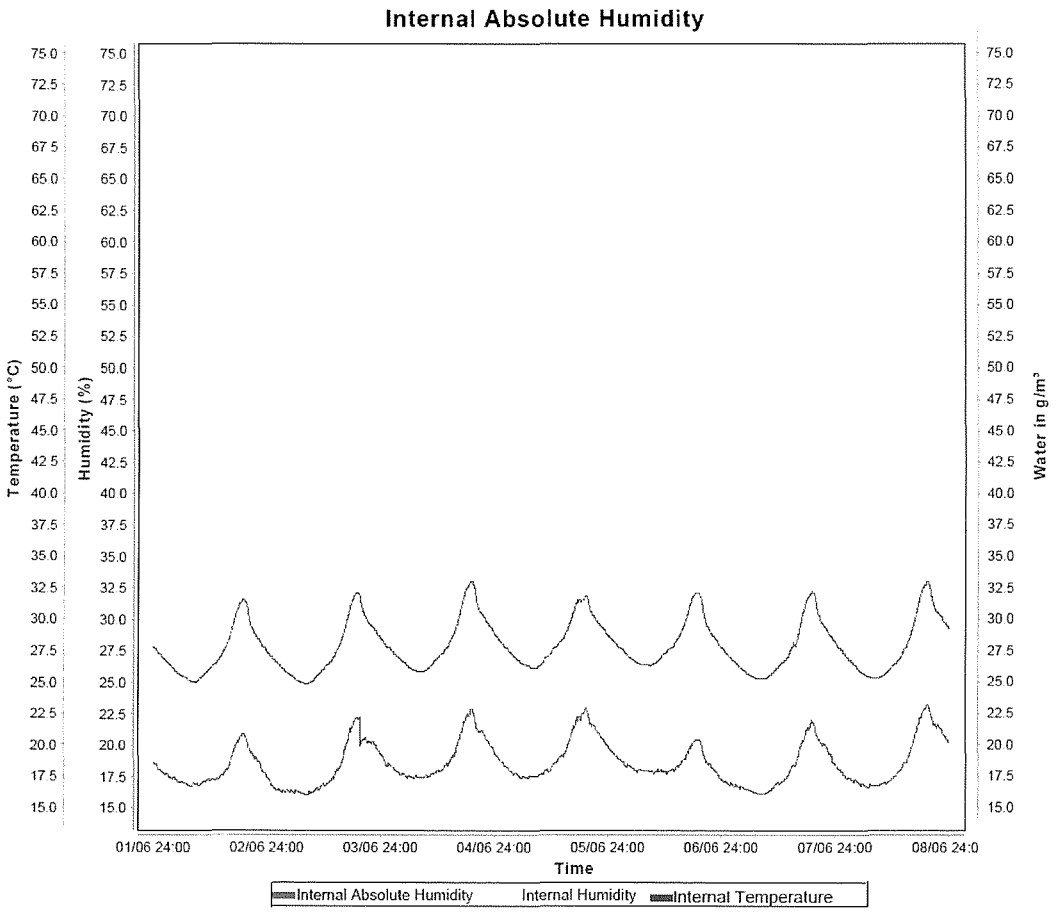

Figure 4.11 The Absolute humidity in the air inside the test room

As can be seen in the above line graph, the Absolute humidity is fluctuating quite uniformly for the given period. Furthermore, there is a direct correlation between the inside temperature and the inside Absolute humidity in the air. This is caused by the fluctuations of the relative humidity inside the test room, which were relatively small.

The same analysis for the same period of time were carried out on the data for the external environment. The findings with respect to the Absolute humidity were quite different. Figure 4.12. shows a line graph for the relative humidity, temperature and Absolute humidity for the outside environment. The orange line represents the relative humidity, the blue line represents the temperature, while the red line represents the Absolute humidity.

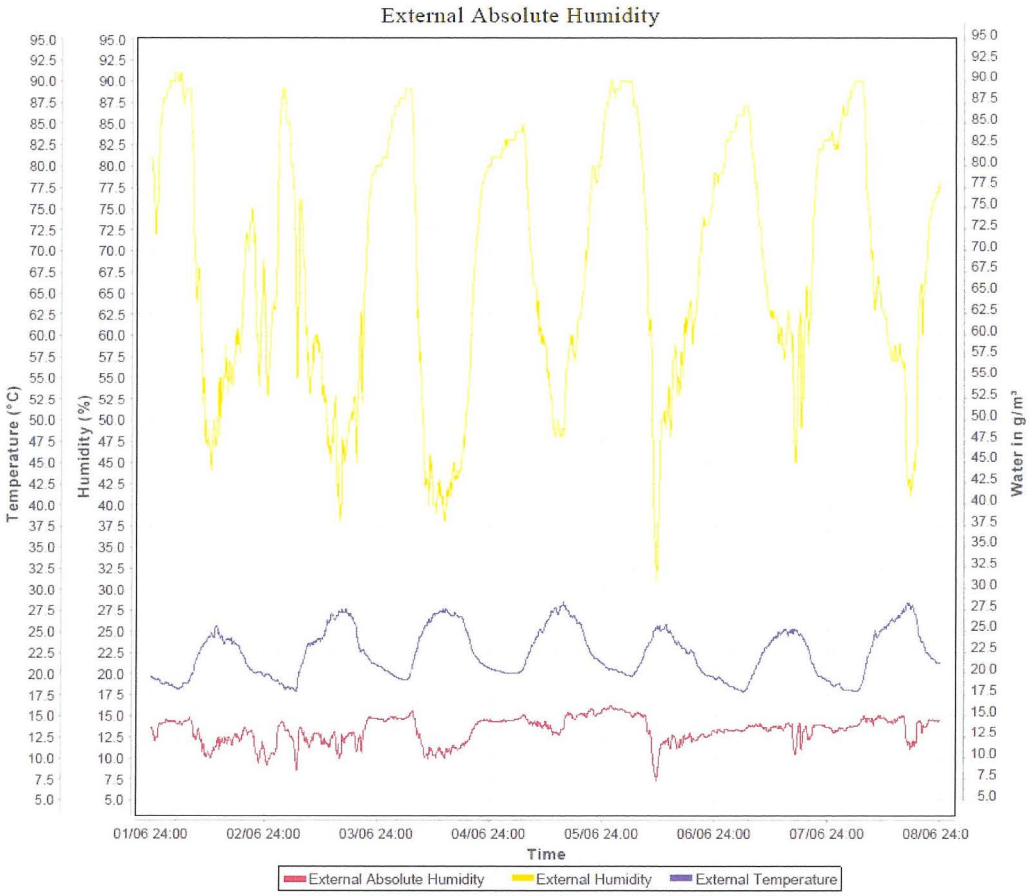

Figure 4.12 The Absolute humidity of the outside air

The results with regards to the Absolute humidity of the outside air were quite different from that of the previous analysis. As shown in figure 4.12, Absolute humidity was not uniform along the given period. For a better comparison, the Absolute humidity for both the inside and the outside environment are shown in the line graph of figure 4.13.

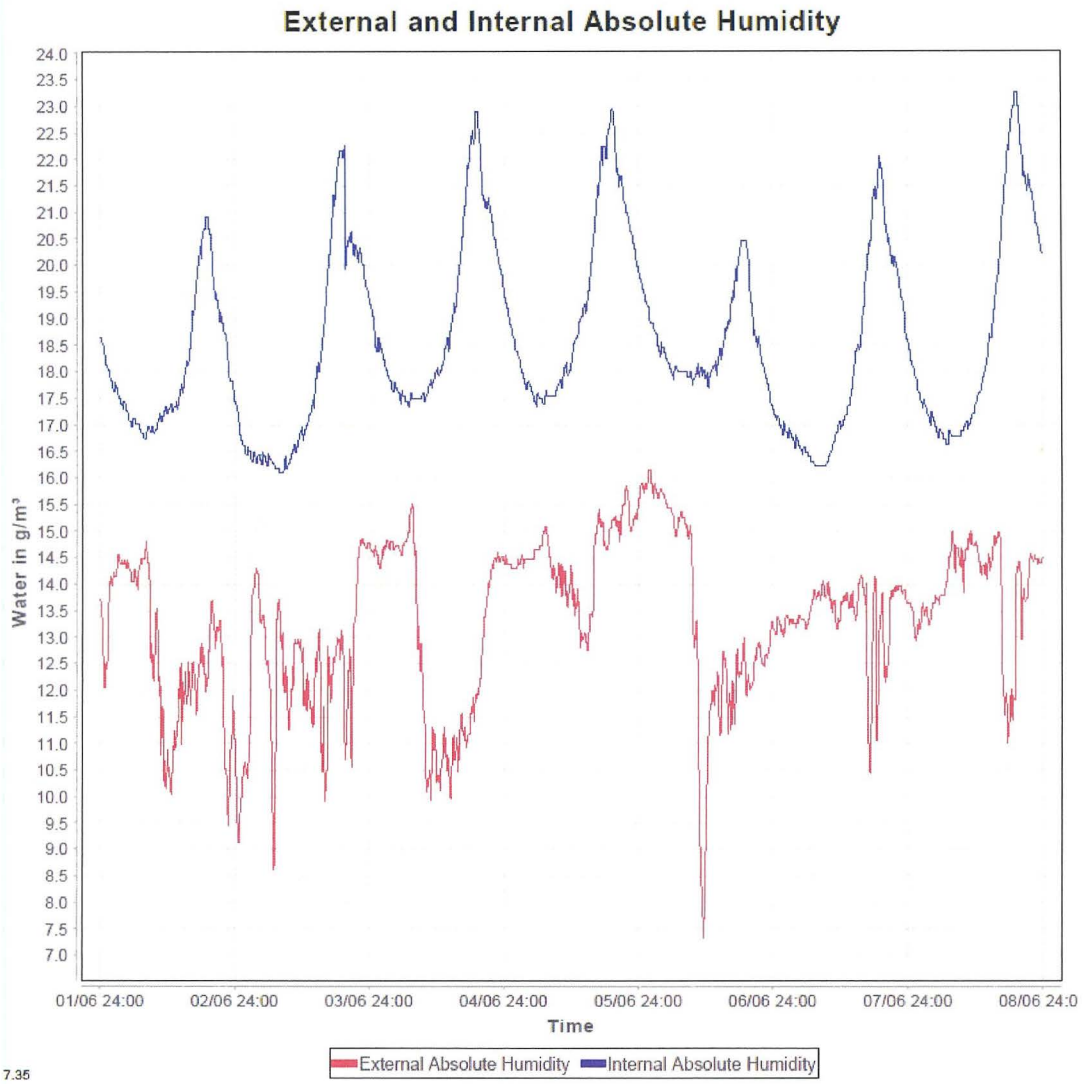

Figure 4.13 The Absolute humidity for the internal and external air

The red line represents the Absolute humidity of the outside environment, while the blue line represents the Absolute humidity inside the test room. It is clear from the line graph that the Absolute humidity is higher inside the test room. The Absolute humidity analysis, up to this point, were carried out only for a short period and during the warm season.

So further analysis were carried out for all the seasons. The details of these analysis are shown in the line graphs of figures 4.14, 4.15 and 4.16. The time period of the investigation started on the 2nd September 2012 and terminated on the 3rd September 2012. In figures 4.14 the yellow line represents the Absolute humidity

inside the test room while the red line represents the simple moving average for the Absolute humidity inside the test room. In the case of figure 4.8, the yellow line represents the Absolute humidity in the external environment, while the red line represents the simple moving average for the same data. In both cases of the moving averages, the step was taken as 10 minutes, while the average window period was taken as 7 days.

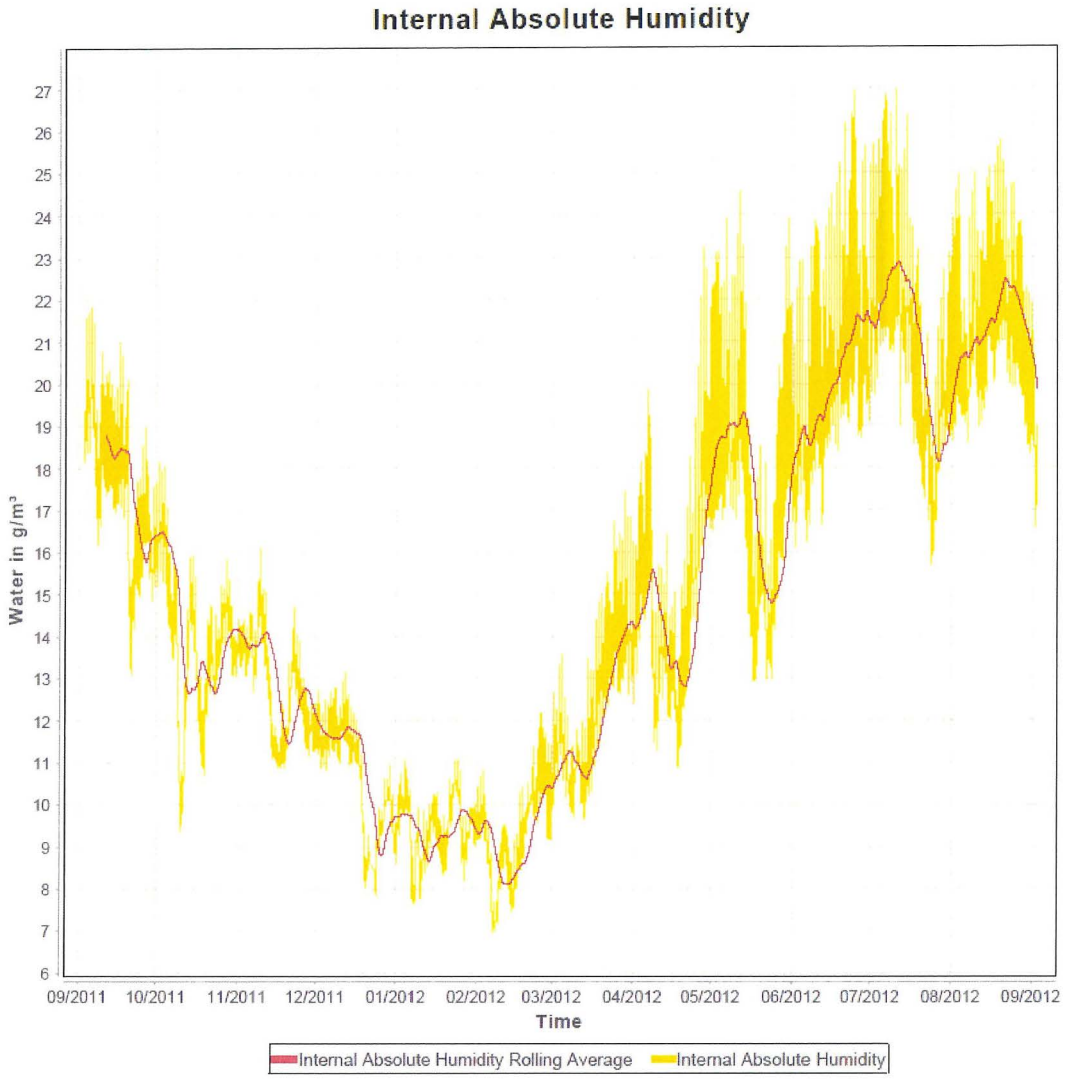

Figure 4.14 The Absolute humidity of the internal air

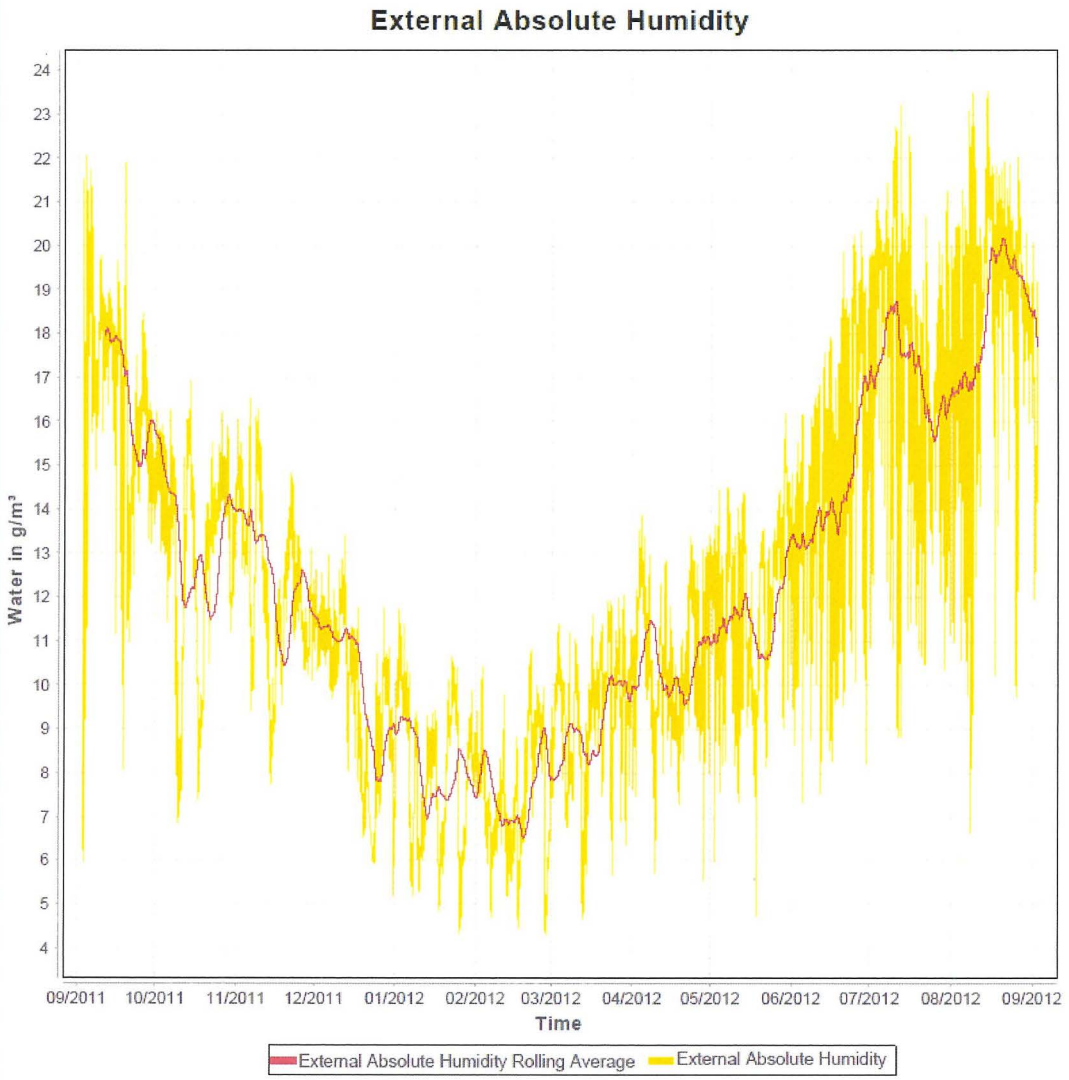

Figure 4.15 The Absolute humidity of the external environment

For a better comparison, the two moving averages of figure 4.14 and figure 4.15 are shown together in line graph of figure 4.16. The red line represents the external data, while the blue line represents the data inside the room.

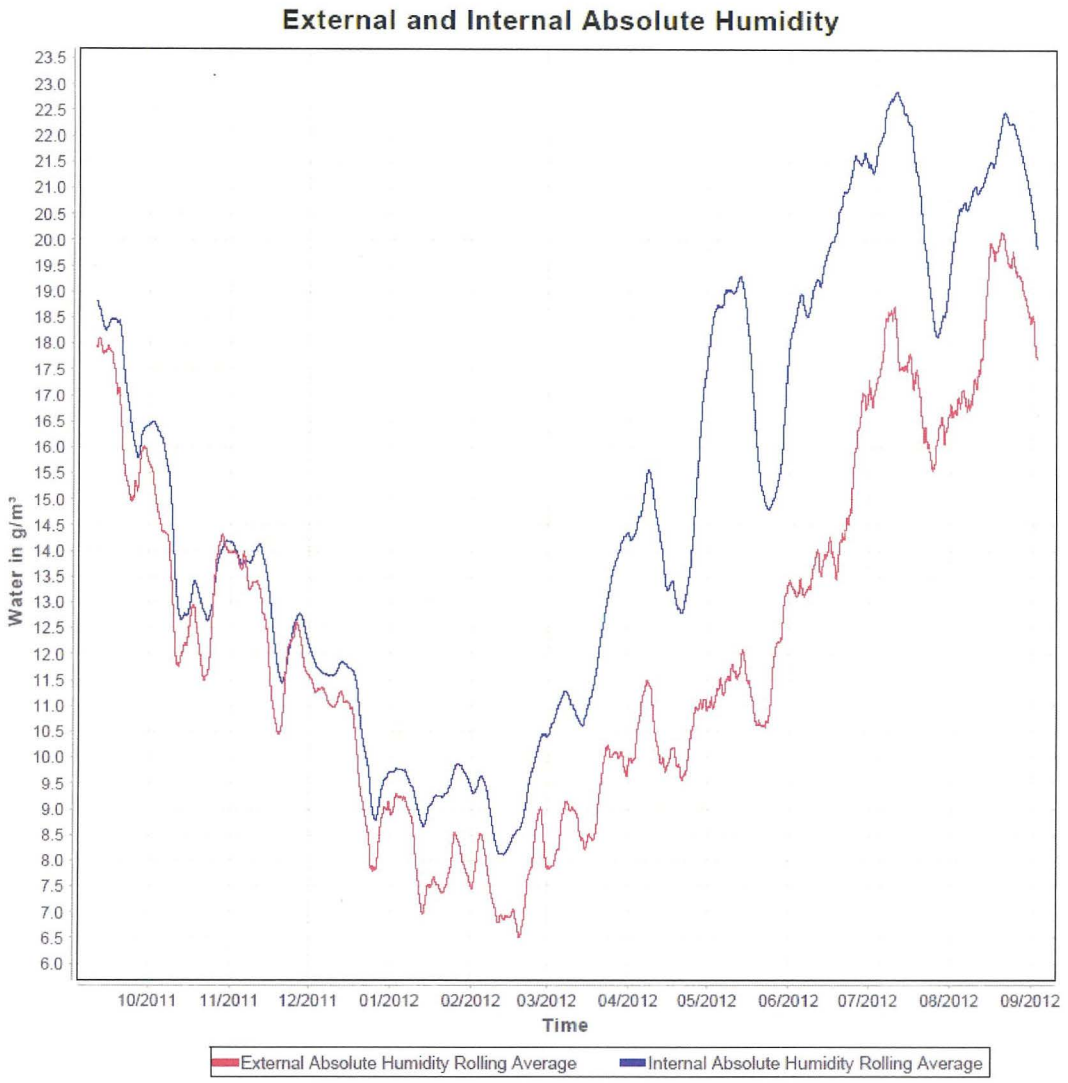

Figure 4.16 The Absolute Humidity of the external environment

There a number of unmistakable observations in figure 4.16 which are outlined below:

1. In both cases the Absolute humidity was higher during the warm seasons.
2. For the entire period of the observation, the Absolute humidity of the air inside the test room was almost always higher than the one found in the external air environment.
3. The greatest difference between the internal and the external data occurred after the raining season.

4. The two line graphs are very similar in shape. Both line graphs follow the same trend.

5. The blue line graph which represents the data inside the test room is following the red line graph which represents the data of the outside environment.

As regards to observation 1 as shown in section 4.4.2, warm air can hold more water vapour at saturation point than in a colder temperature. As a consequence, warm air tends to absorb more water vapour and hence it is likely to contain more water vapour. The temperature profile, for the same period of observation, for both the inside environment of the test room and for the external environment is shown and discussed in section 4.5.

With regards to observation 2, the air inside the room can be exchanged with the external air only. This suggests that there must be some sort of water vapour sources inside the room. But as already stated there are no water sources or living things in the test room. Furthermore, the test room is situated on the first floor which eliminates any dampness from the ground. All this indicates that the water vapour sources must originate from the surrounding building material and from the objects inside the test room.

This phenomena is best explained through some selected moisture theories. Porous materials can hold moisture in their pores. For example, concrete can hold up to 140 Kg/m^3 [23]. Moisture can be transferred through a material by means of diffusion or by the capillary suction. In diffusion, air which contains water vapour fills up the pores of a material, which then the vapour condenses within the material and partially fill the pores with water. This process continues until some pores are completely filled up. Then, the capillary suction kicks in and the water starts to move from one pore to another. Capillary suction will also occur when the material is in direct contact with water, such as, when condensation is formed or when there is rain. This process continues until an equilibrium in the moisture content is reached. This equilibrium depends on many factors such as the water sources, humidity and temperature. Changing any of these factors causes a change in the

equilibrium of the moisture content in the material, which in turn causes the material to absorb more moisture or release moisture in the form of vapour. It should be noted, that the capillary suction causes a higher moisture absorption into the material. As can be seen from above, the building itself and the objects that it contains are acting as a moisture storage. Moisture can accumulate in the building even if there is no rain. This moisture is then slowly released in the form of vapour inside the test room. This is causing a higher average of Absolute humidity in the air inside the test room as compared to the outside environment. Furthermore, the water content stored in the form of moisture in a building is higher than the water that can be stored in the air inside a building. This is causing a higher average of Absolute humidity in air inside the test room for almost all year round.

With regards to observation 3, the test room has its roof and 50% of its wall exposed to the environment. Therefore these walls are subject to rain, which in turn causes the outer walls and the roof to absorb lot of water due to the capillary suction as explained above. It is assumed that the maximum moisture content in the building occurs during the rainy season. This stored moisture is then gradually released during the months that follow the rainy season. It should be noted, that the external walls are also exposed to direct solar radiation, which increases water evaporation from the walls and hence increases the moisture source inside the test room. All this causes an increase in Absolute humidity inside the test room.

Observations 4 and 5 suggest that there is a good correlation between the Absolute humidity in the air inside the test room and the air in the external environment. This correlation must be related by the following formula [24]:

$$v_i(t) = v_e + \frac{G}{nV} * (1 - e^{-nt}) \tag{4.04}$$

Where:

$v_i(t)$ is the internal humidity by volume in g/m^{3}at a given time in seconds

v_e is the external humidity by volume in g/m^3 fixed

G is the internal moisture source in kg/s

V is the volume of the room in m^3

n is the air exchange rate from the external to the internal in V/s

t is the time in s

At time 0, the internal and external humidity by volume are equal. The humidity by volume is another term which refers to the Absolute humidity in the air. Furthermore, at time 0, the internal moisture source is activated. The external humidity by volume assumed is fixed.

In an ideal situation where all the parameters are fixed, it is possible to find the rate of exchange of air only if the external and internal humidity by volume and the internal moisture source are known. But in practice, these parameters are changing continuously. From the above findings, it is evident that it is possible to estimate the air exchange rate by monitoring the required parameters. But there are a number of challenges to overcome in order to determine the moisture sources in a building. This deserves further investigation and experimentation but due to time restrictions it is left for future study.

4.4.5 Deductions for Relative Humidity

The findings of the analysis with regards to the relative humidity are outlined below:

1. The external relative humidity is higher during the night time than during the day.
2. The behaviour of the external relative humidity is fairly constant during a one year period.
3. The diurnal internal relative humidity changes are quite small.
4. The internal relative humidity is the highest during the rainy season and during the months which follow.
5. There is no evident correlation between the internal and external relative humidity.
6. There is a correlation between the internal and external Absolute humidity in the air.

7. The correlation mentioned above could be used to estimate the air exchanges in a building. But this possibility should be confirmed by further experiments and analysis.

4.5 Temperature and Solar Radiation

The external and the internal temperatures are by far the most important parameters which determine the energy usage in a building. Likewise, solar radiation can have considerable effect on the temperatures inside a building. Consequently, the temperature and solar radiation are discussed together. First, the external temperature is discussed followed by the internal temperature along with the solar radiation.

4.5.1 External Temperature

The external temperature is investigated for its periodical variation namely diurnal variation and seasonal variation. These variations are particularly important if a dynamic model is adopted for the energy performance calculations. The seasonal variations can be useful in the estimation of energy transfer through the ground, while diurnal variation can be useful in the estimation of energy transfer through the building from the external environment.

The external temperature can be described by the following equation:

$$T_e(t) = T_0 + T_{season}(t) + T_{diurnal}(t) + T_{dev}(t) \quad [25] \qquad (4.05)$$

$T_e(t)$ is the external temperature in °C at a given time (t)

T_0 is the annual average in °C

$T_{season}(t)$ is the seasonal variation in °C at a given time (t)

$T_{diurnal}(t)$ is the diurnal variation in °C at a given time (t)

$T_{dev}(t)$ is the deviation temperature in °C at a given time (t)

The last term represents the deviation temperature which is caused by the real weather conditions such as the clouds' density. This term is very complex to

determine and normally it is left out [25]. Therefore, the approximate external temperature is calculated by:

$$T_e(t) \approx T_0 + T_{season}(t) + T_{duinal}(t) \quad (4.06)$$

It should be noted, that all terms in the equation are unique for a particular location in the world. The next section describes each term for the local environment.

4.5.2 Local Periodic Variations

The local periodic variations were determined with the aid of Matlab along with the external environment data obtained during the period of observation. The period of observation started on the 2nd September 2011 and concluded on the 3rd September 2012, exactly one year. Each term of equation 4.06 was therefore determined

T_0

The term T_0 was determined by calculating the average external temperature for the whole period of observation. The calculated average T_0 was 19.34 °C

T_{season}

The seasonal periodic variation was determined by performing a sinusoidal curve fit to the entire external temperature data for the whole period of observation. The following is the sinusoidal curve type selected for this fit:

$$A * \sin\left(\left(2\pi * t_{day}/365\right) + d\right) + C \quad (4.07)$$

where;

A is amplitude; in this case it is 8.391°C

t_{day} is the day of the year, in this case day 1 is 2nd September 2011

d is the phase shift; in this case 2.1

C is the annual average external temperature; in this case 19.34°C

The seasonal periodic variations T_{season} are described by:

$$T_{season} = 8.4 * sin\left(\left(2\pi * \frac{121+t_{day}}{365}\right) + 2.1\right) \quad (4.08)$$

where t_{day} is the day of the year starting from 1st January.

Figure 4.17 is showing the curve fit determined

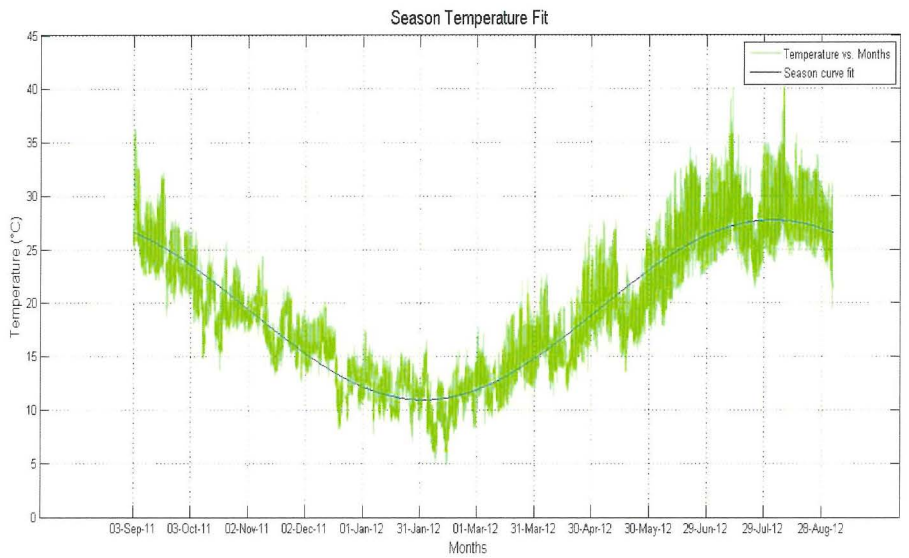

Figure 4.17 The external temperature along with the sine curve fit

T_{duirnal}

The diurnal periodic variations were determined by performing a sinusoidal curve fit to the external temperature data. But this time, the curve fitting were performed on the daily external temperature data. The sinusoidal curve type selected for this fit was:

$$A * \cos\big((2\pi * t_h/24) + d\big) + C \quad (4.09)$$

where;

A is the daily amplitude

t_h is the hour during the day where hour 0 is midnight

d is the phase shift

C is a constant which is made from the other two terms and which is ignored in this case

This process was repeated 50 times on different days which were proportionally spread along the period of observation. Then, the averages of A and d were calculated to produce the following formula.

$$T_{duirnal} = 2.62 * cos\left(\left(2\pi * \frac{t_h}{24}\right) + 0.9\right) \quad (4.10)$$

Figure 4.18 shows a curve fit for day 4th September 2011

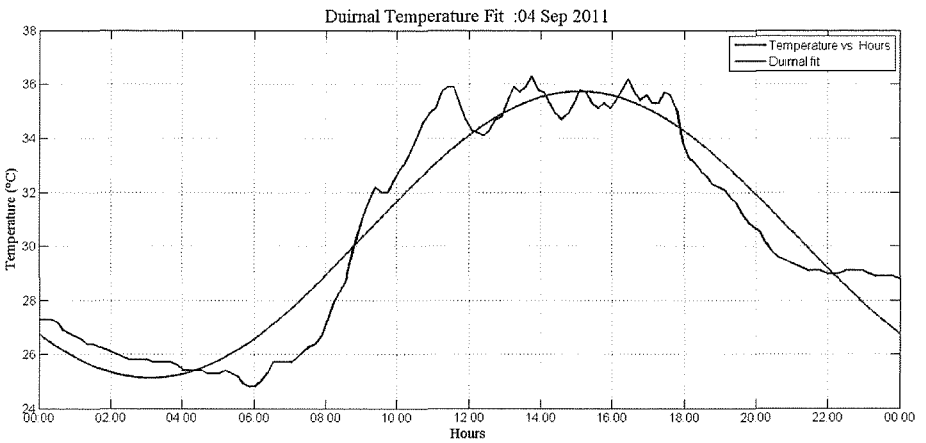

Figure 4.18 A typical cosine curve fit

So the final equation is:

$$T_e(t) \approx 8.4 * sin\left(\left(2\pi * \frac{121+t_{day}}{365}\right) + 2.1\right) + 2.62 * cos\left(\left(2\pi * \frac{t_h}{24}\right) + 0.9\right) \quad (4.11)$$

The above equation is derived from a one year data. A more accurate approximation is possible by using more data. Figure 4.19, shows the moving average of the external temperature. The averaging period selected is that of 7 days, while the step size selected is just of 10 minutes. As can be seen in Figure 4.19 the moving average line is following a sinusoidal path.

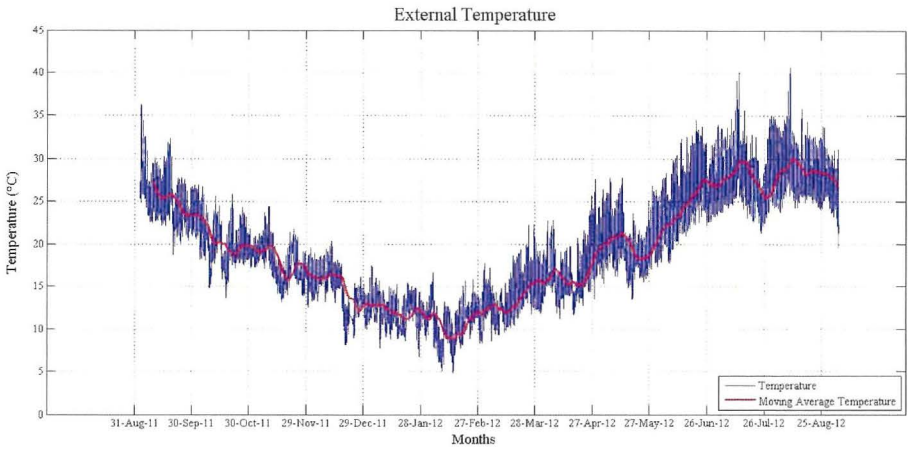

Figure 4.19 The external temperature along with its moving average

4.5.3 External Temperature variation between 12.00 AM and 6.00 AM

During the visual analysis of the external temperature graphs, it was observed that the external temperature variation between midnight (12.00 AM) and 6.00 AM were minimal in the majority of the cases. This fact can be useful in the development of the energy performance protocol. Therefore, a statistical analysis was conducted and consequently, confirmed this fact. Figure 4.20 shows a typical external temperature profile for the local environment.

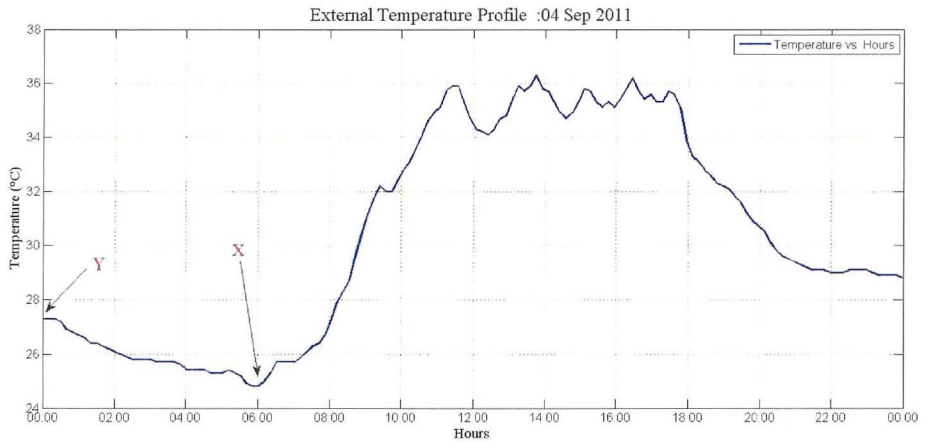

Figure 4.20 The external temperature profile of the 4th September 2011

The statistic analysis was conducted by calculating the temperature difference between midnight and 6 o'clock in the morning for each day during the observation period. The difference in temperature was calculated by Y - X where Y is the

temperature at midnight and X is the temperature at 6 o'clock in the morning. Figure 4.21 shows a histogram of the temperature differences along with the normal distribution fit, with the mean equal to 0.8466 and the standard deviation equal to 0.8594.

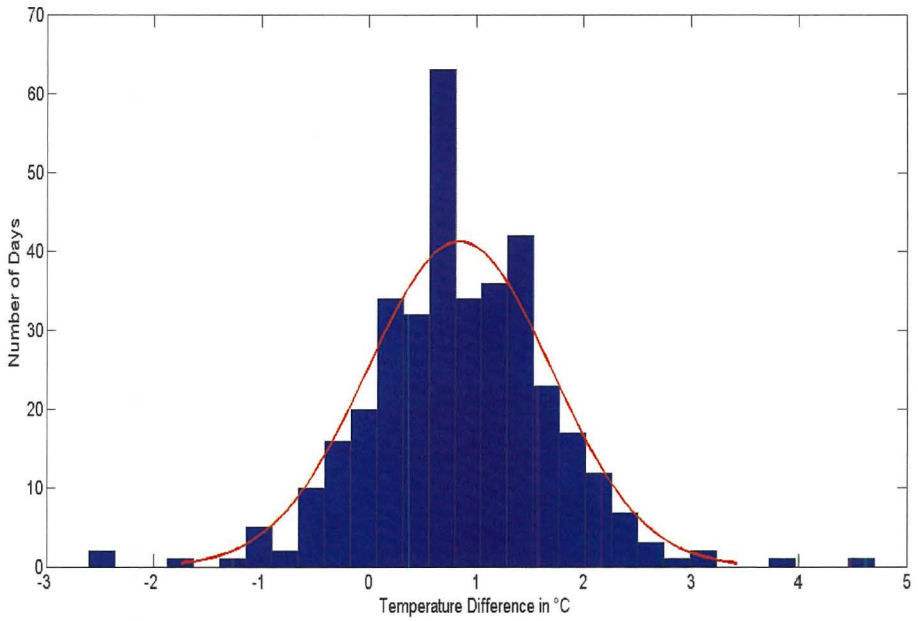

Figure 4.21 The internal temperature difference between midnight and 6:00 am for a one year period which started on the 2nd September 2011

4.5.4 The Internal Temperature and the Solar Radiation

The internal temperature was investigated to see how it is effected by the solar radiation and to see the correlation with the external temperature. This investigation is important for the development of the energy performance protocol because it is the resultant temperature inside a building which determines the required energy needed to keep the temperature inside that building to the desired set point. Figure 4.22 shows the external temperature along with the solar radiation and the internal temperature for the period between the 1st and the 5th July 2012. The solar radiation is measured by means of a pyranometer which is mounted horizontally. Throughout this document, all the measurements referring to the solar radiation, refer to a measurement performed by a pyranometer which is mounted horizontally.

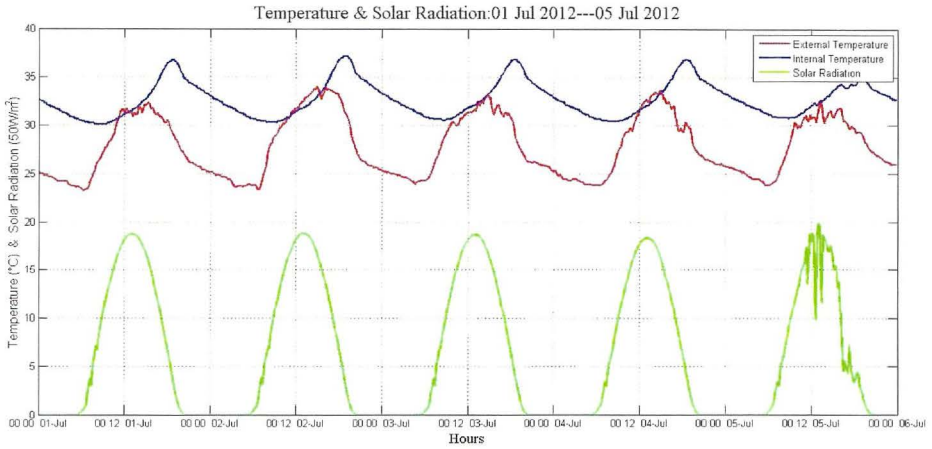

Figure 4.22 The temperature and the solar radiation between the 1st and the 5th July 2012

With the presence of the external solar radiation, the internal temperature starts to rise due to the solar gain. The solar gain in a building depends on many factors such as the building orientation, the shade, the emissivity of the material used and the thermal resistance of the building material used. During the night, without any solar gain the thermal heat stored within the building starts to dissipate out the heat. In turn, this causes a decrease in the internal temperature. The decrease in the internal temperature continues until the next sunrise where the cycle is repeated.

As can be seen, the internal temperature is almost always higher than the external temperature. Based on the second law of thermodynamics which states that, heat always flows from a hot region to a cooler region, one can conclude that the heat is flowing from the inside of the test room to the external environment. There were no heat sources inside the test room, the heat is only from the solar gain. From this it was concluded that the diurnal fluctuations in temperature inside the test room are caused by the solar heat gains. This can be seen clearly in Figure 4.23. The green line indicates the daily accumulative solar radiation energy per square meter, while the red line represents the moving average of the daily accumulative solar radiation energy. The averaging period was of 21 days while the step size was of one day.

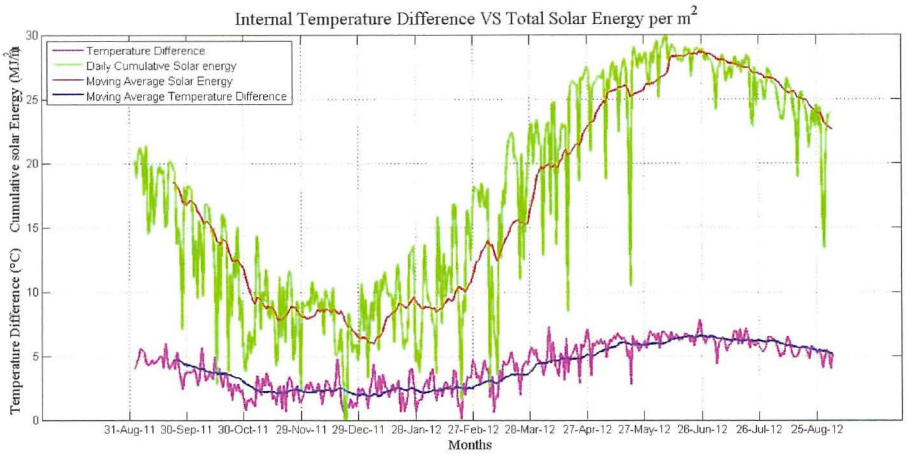

Figure 4.23 The Internal Temperature Difference and the Daily Accumulative Solar Energy for a one year period which started on the 2nd September 2011

The accumulative daily solar radiation energy (Z) is calculated by summing the areas between the samples:

Let $S_1, S_2, S_3, S_4, \ldots\ldots S_{142}, S_{143}, S_{144}$

where S is a sample of solar radiation in W/m^2 at every 10 minutes.

$$Z = \sum_{n=2}^{144} ((S_{n-1} + S_n)/2) * 600$$

which is equivalent to

$$Z = \sum_{n=2}^{144} (S_{n-1} + S_n) * 300 \qquad (4.12)$$

The 600 is computed according to the sample rate in this case (10 min X 60 sec).

The magenta line in figure 4.23 represents the temperature difference between the maximum internal temperature during a given 24 hour period starting from midnight and the minimum internal temperature of the next successive 24 hour period. These references are shown in figure 4.24 by Y and X respectively. This temperature difference is caused by the solar gain in the test room. The bigger the difference the greater is the solar gain.

There are two interesting observations in Figure 4.23. These are outlined below.

1. The accumulative daily solar energy moving average line has a sinusoidal like shape. This is caused by the earth orbiting around the sun.
2. The internal temperature difference moving average line has also a sinusoidal like shape. Furthermore, this sinusoidal like shape is in phase with the daily solar energy moving average line. This indicates that both trend lines are correlated. It is also an indication that the internal temperature fluctuations are proportional to the daily total accumulative solar energy per m^2. It should be noted that this proportionality depends on the solar gain, hence it depends on the characteristics of the building, such as the orientation and shade level.

Figure 4.24 shows a typical internal temperature profile of the test room during the warm season.

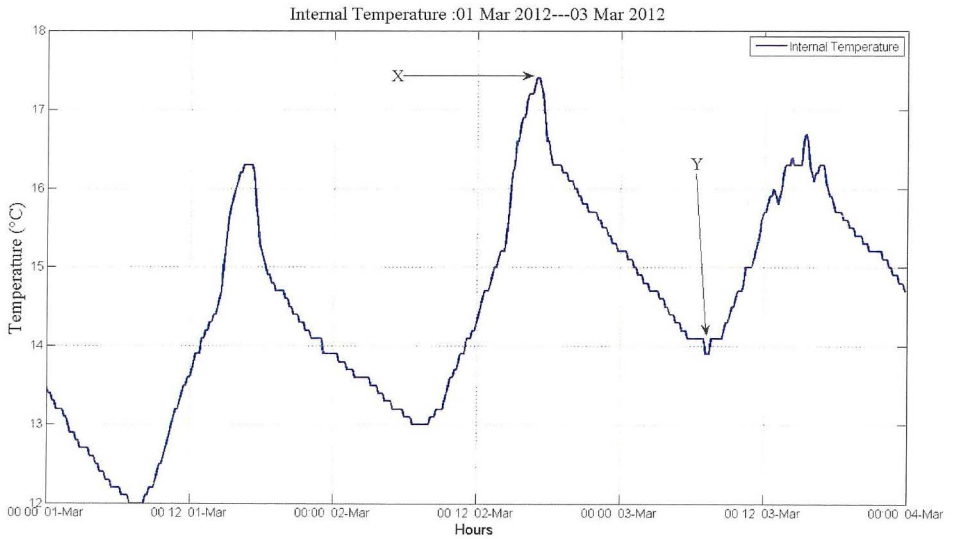

Figure 4.24 The internal temperature taken from the 1st to the 3rd March 2012

The temperature variations inside the test room for the whole period of observation are shown in figure 4.25. The red line shows the moving average for the internal temperature. The averaging period in this case is of 7 days while the step size is of 10 minutes.

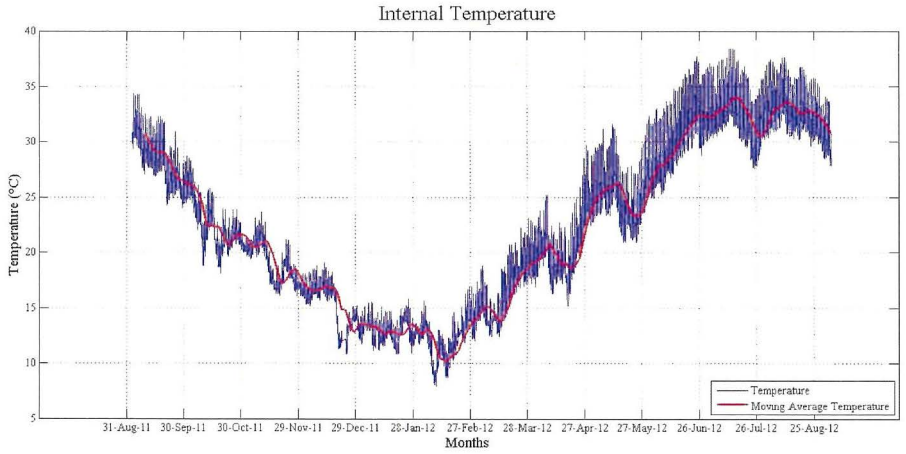

Figure 4.25 The internal temperature along with its moving average

Once more, the moving average has a sinusoidal like shape. Figure 4.26 shows the moving averages for both the temperature inside the test room and the external temperature. In both cases, the averaging period was of 7 days while the step size was of 10 minutes.

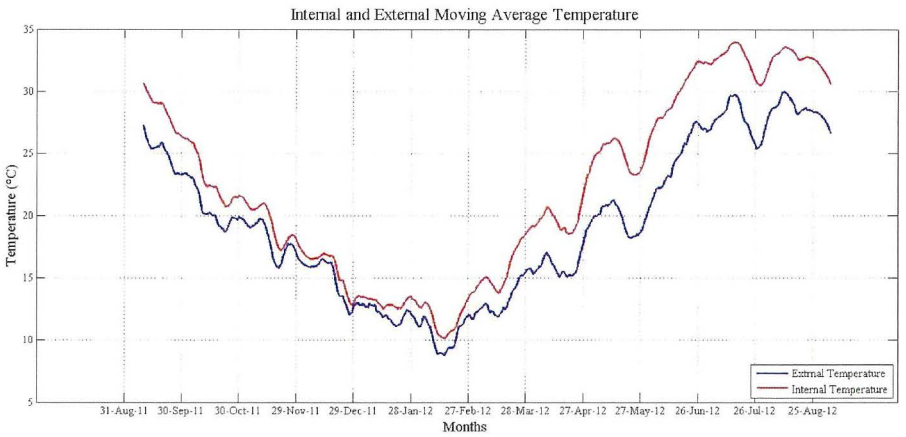

Figure 4.26 The internal and external temperature moving average

From figures 4.26 and 4.23 one can conclude that:

1. The internal temperature was always higher than the external one.
2. The difference between the external and internal temperature increases with an increase in the daily cumulative solar energy. This is caused by the fact that with an increase in solar radiation, the solar gain also increases and hence it causes an increase in the internal temperature.

3. Both moving averages are very similar in shape. This suggests that both temperature moving averages are well correlated. Furthermore, as can be seen, if the graphs are closely examined, the internal moving average is leading a little bit the external moving average. This is caused by the thermal storage of the building.
4. Both the internal and external moving averages are relatively in phase with the cumulative daily solar radiation, although proper comparison is not possible. This suggests that there is a correlation between the three entities.

4.5.5 Deductions on Temperature and Solar Radiation

The findings of the analysis with regards to the external temperature, the temperature inside the test room and the solar radiation are outlined below:

1. An approximation of the external temperature in the case observed is given by:

$$T_e(t) \approx 8.4 * sin\left(\left(2\pi * \frac{121+t_{day}}{365}\right) + 2.1\right) + 2.6 * cos\left(\left(2\pi * \frac{t_h}{24}\right) + 0.9\right) \quad (4.13)$$

   A more accurate approximation is possible if the above formula is based on more than one year of data.
2. The variations in the external temperature between midnight and 6 o'clock in the morning is a normal distribution with a mean of 0.8466 a standard deviation of 0.8594.
3. The external and internal seasonal temperature variations have sinusoidal like shape. Moreover, they are very similar in shape with the internal temperature leading the external temperature. This suggests that they are very well correlated. The internal temperature is always higher than the external temperature.
4. The higher internal temperature is attributed to the solar gain in the test room. The higher the daily accumulated solar energy, the higher the difference between the internal and external temperatures.

5. The seasonal daily cumulative solar radiation energy variations have a sinusoidal like shape. With an increase in the daily cumulative solar radiation energy, there will be an increase in the internal temperature variations.

5 Thermal model for building performance analysis

5.1 Introduction

This chapter begins by identifying the equivalent thermal network which is used later for the proposed energy performance protocol. Four possible methods to identify the parameters in the equivalent thermal network are discussed. Experiments which validate these methods are also presented.

5.2 The Equivalent thermal network adopted

The equivalent thermal network adopted for the proposed energy performance protocol is shown in figure 5.1. This equivalent thermal network was selected because it is the simplest model and provides all the necessary information.

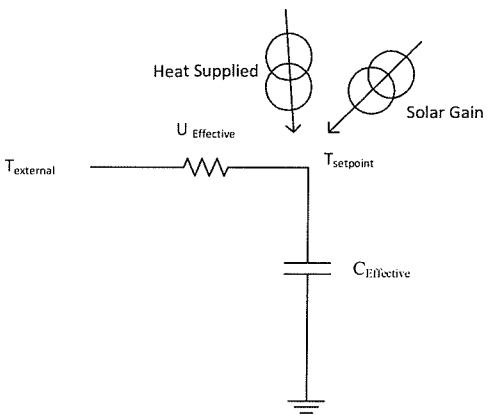

Figure 5.1 The equivalent thermal network adopted for the proposed energy performance protocol

Where:

$T_{external}$ is the external temperature

$T_{setpoint}$ is the set point internal temperature

$C_{effective}$ is the effective steady state thermal capacitance of the building

$U_{effective}$ is the effective steady state heat transmission loss or U-Value of the building

The $U_{effective}$, $C_{effective}$ and the solar gain are all unknown parameters. These parameters are measured by one of the methods developed in this research. Each method is described in detail in the following sections along with the experiments on which they are based. It should be noted that $U_{effective}$ is not the global U-Value which is calculated by adding together the individual U-Values of the components in a building envelope. It is the heat transmission loss out of the building for a temperature difference of 1 ^{o}C between the external and internal temperatures and which is expressed in W/ ^{o}C . The $U_{effective}$ can be used to calculate the annual energy usage or the energy efficiency of a building. When the $U_{effective}$ is used to measure the energy efficiency of a building, it should be divided by the building's volume or by the building's area and it should be expressed in W/^{o}Cm^{3} or W/^{o}Cm^{2} respectively. This should be decided on a national level. The next section gives details of the setup used for the experiments.

5.3 The setup equipment used for the experiments

These experiments were carried out before the ideal hardware and software were developed. Therefore, an alternative equipment had to be used for these experiments. The equipment needed for the experiments consisted of several temperature sensors, an external temperature sensor, an external solar radiation sensor, a temperature controller and a precise energy consumption profile for the heater.

The temperature sensors used were supplied by Abertax Kemtronics. These are wireless temperature sensors and require an online PC. The external temperature and the solar radiation data were obtained from a weather station whose details are found in section 4.3. The temperature control was performed by an Omron E5GN temperature controller which switches on and off a fan heater by means of a solid state relay. The electrical energy used was measured by an Iskra single phase energy meter. Its details are found in section 6.5.1. An interface which connects the output of the energy meters to the parallel port of the PC was built and an on-line program was written in Java which checks continuously the parallel port for an energy pulse. When an energy pulse is received, the program registers its time in a text file. Another program which was also written in Java, processes this text file and calculates the energy usage in 30 minute intervals. The data acquired was manually arranged and sorted so that the analysis could be performed.

5.4 Method one for measuring $U_{Effective}$

The purpose of this method is to determine the $U_{Effective}$ in the equivalent thermal network. Before describing method one in more detail, it is better to go through the experiment on which this method is based. Figure 5.2 shows the data obtained from experiment number 1 in a line graph format.

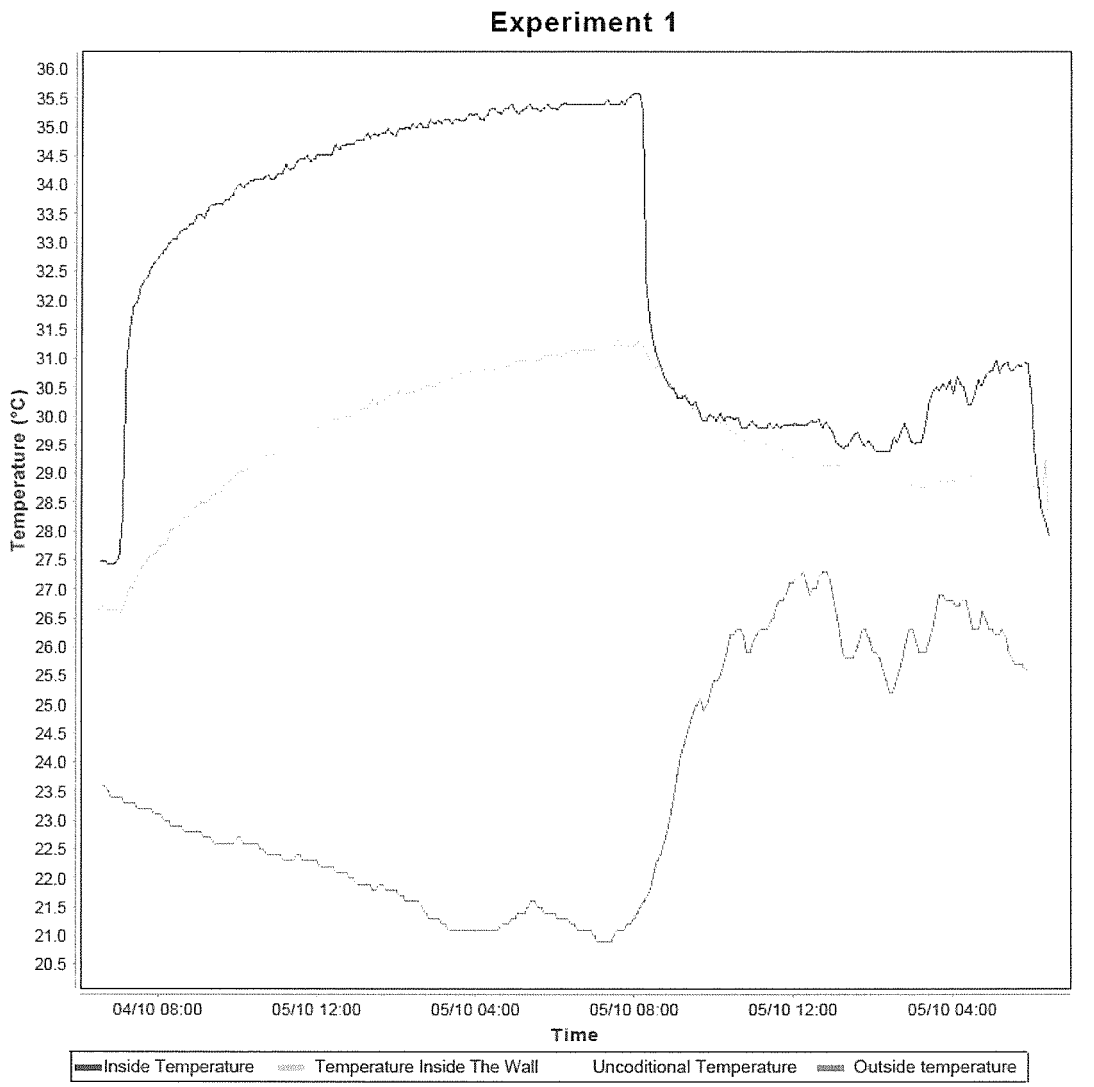

Figure 5.2 The temperatures of experiment 1

The curves in line graph of figure 5.2 represent the temperature readings from various sensors placed inside and outside the test room. In this experiment, a fan

heater was switched on at full power without any control. The power of the heater was measured and recorded.

The blue curve represents the data from a temperature sensor which is placed inside the test room at 1.8m above the floor. As can be seen, the blue curve is following an exponential path and it is near the saturation point. When the saturation point is reached the heat supplied by the fan heater is equal to the heat transmission loss out of the test room. Now, since the efficiency of the fan heater approaches unit, then the heat transmission loss is equal to the electrical energy supplied to the heater.

In this method, a temperature sensor is placed inside the room while another one is placed outside the building. The fan heater was placed inside the room and switched on. The electrical power to the heater is measured and recorded. When the saturation temperature is reached, then the $U_{Effective}$ is found by:

$$\frac{Heater\ electrical\ power\ input}{(Saturated\ internal\ temperature - average\ external\ temperature)} \qquad (5.01)$$

The main problem with this method is that the time constant of the building is normally several hours long, which means that the saturation temperature is reached after several hours of heating. Furthermore, as the temperature inside the building approaches the saturation point, changes are expected to be small which makes it harder to identify the proper saturation temperature.

An alternative solution to this problem is to use a smaller time window for heating and to perform an exponential curve fit on the internal temperature. This will extrapolate a saturation temperature which can be used to calculate the effective U-value of the room. Four different exponential curves fits were performed on the temperature data which is indicated by the blue line in figure 5.2. Each curve fit had a different sample size. The results are shown in Table 5.1.

Sample Data (Hours)	Extrapolated Stable Temperature (°C)	Average External Temperature (°C)	Heat Transmission loss (Watts/°C)
4	34	22.5	110
6	34.2	22	104
8	34.6	21.5	97
12	34.8	21.5	95.5

Table 5.1 Different heat transmission loss for different data sample size

In all cases, the sample data starts from the 4th October at 18:30. As can be seen, the sample size affects the result. As will be shown later, the result of the 12 hour sample data gave the most realistic results. On the other hand, extending the heating period can affect negatively the results. This is due to the external influences such as sudden changes in the external temperature which can disturb the data and hence the result. This method can be applied easily to a single room but it is very difficult to apply it to a whole building. In a building with multiple rooms, one expects to have rooms with different sizes. Using heaters with the same power in all the rooms will make the smaller rooms' temperatures higher. This will cause a heat energy transfer among the rooms which negatively effects the accuracy of the result.

It is possible to carry out this measurement in each room separately but the combined results does not reflect the real one. If the measurements are performed in one room at a time, heat will also be lost in the conditioned adjacent rooms. This should not be the case in practice because these rooms are expected to be heated and therefore such losses should not occur. If, on the other hand, the measurements are conducted in all the rooms concurrently, each room is likely to have a different saturation temperature which could negatively affect the combined result. This problem was addressed in method two.

5.5 Method two for measuring $U_{Effective}$

The purpose of this method is to determine the $U_{Effective}$ in the equivalent thermal network. This method is based on controlling the internal temperature to a pre-determined set point temperature and wait until the internal thermal capacitance is saturated with heat energy. At this point, the electrical energy supplied by the heater is equivalent to the heat transmission loss out of the building. By using the latter information and by calculating the temperature difference between the inside and the outside temperature of the building, one can calculate the U-Value of the building. If the measurements are conducted in the first 6 hours after midnight the dynamic effect is also minimized. The latter is due to the fact that the least external temperature variations occur in this time window. (Refer to section 4.5.3 for more details).

Figure 5.3 shows the data from experiment number 2 which confirms the arguments given above. In this experiment the internal temperature was kept constant at 32°C for a duration of 12 hours. This includes a time window between midnight and 6 o'clock in the morning.

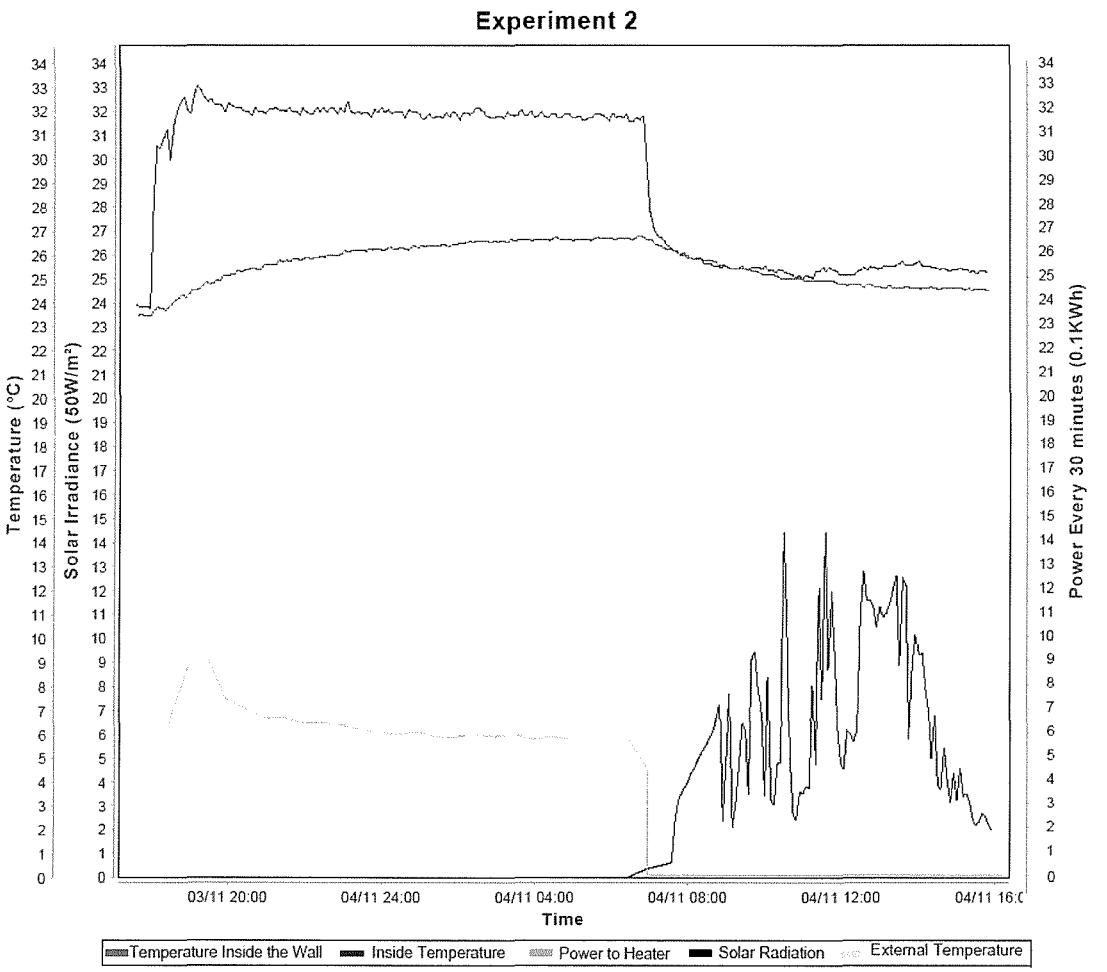

Figure 5.3 The temperature, power and solar irradiance of experiment 2

The blue curve in the above graph represents the temperature inside the test room, while the red curve represents the temperature 20mm inside the wall. The light pink curve indicates the external temperature, while the black curve represents the solar irradiance. The green curve represents the average electrical energy supplied to the heater every 30 minutes.

As can be seen, the temperature inside the wall is following an exponential path. Even the average electrical energy supplied to the heater is following an exponential path although this time it is decaying. In both cases, the saturation point is reached at the same time. This is a clear indication that the initial excess energy usage is stored in the thermal mass. Now, since the thermal mass is saturated with the heat energy

and the internal temperature is kept constant any additional heat supplied in the test room will result into heat transmission loss.

5.5.1 The Test Procedure adopted in method 2

The procedure of method 2 is as follows:

1. A temperature sensor was placed outside the building and protected with a proper solar shield.
2. A temperature sensor was placed inside the building.
3. A temperature sensor was placed 20mm inside one of the internal walls.
4. The temperature inside the building was kept constant and about 7°C higher than the outside temperature. A fan heater was used to control the internal temperature.
5. The electrical energy supplied to the heater was monitored.
6. It was ensured that the temperature inside the wall reached a stable state before midnight.
7. The heating inside the building was turned off before sunrise.
8. The average inside temperature and the average outside temperature were calculated, as well as, the average electrical energy supplied to the heater. The averages were calculated for a period of time which started at midnight and ended at around 6 o'clock in the morning.

All sensors are monitored and recorded at pre-determined intervals.

The $U_{Effective}$ is found by:

$$\frac{Average\ power\ supplied\ to\ the\ heater}{(Average\ internal\ temperature - Average\ external\ temperature)} \quad (W/°C) \quad (5.02)$$

This method can be applied concurrently into two adjacent rooms without affecting each other.

5.6 Method three for measuring $U_{Effective}$

The purpose of this method is the same as that of the other two methods, that is, to determine the $U_{Effective}$ in the equivalent thermal network. This third method is intended to improve over method 2 and to capture some effects of the solar gain. Similarly to method 2 the internal temperature is kept constant and higher than the external temperature by means of a fan heater. The main difference is the time window for heating and the time window to calculate the averages. The dynamic effect is minimized by saturating the internal thermal mass and then by performing the measurement over a time window of 24 hours. The latter is best explained in the data of experiment number 3. In experiment number 3, the internal temperature was held constant at about 32°C.

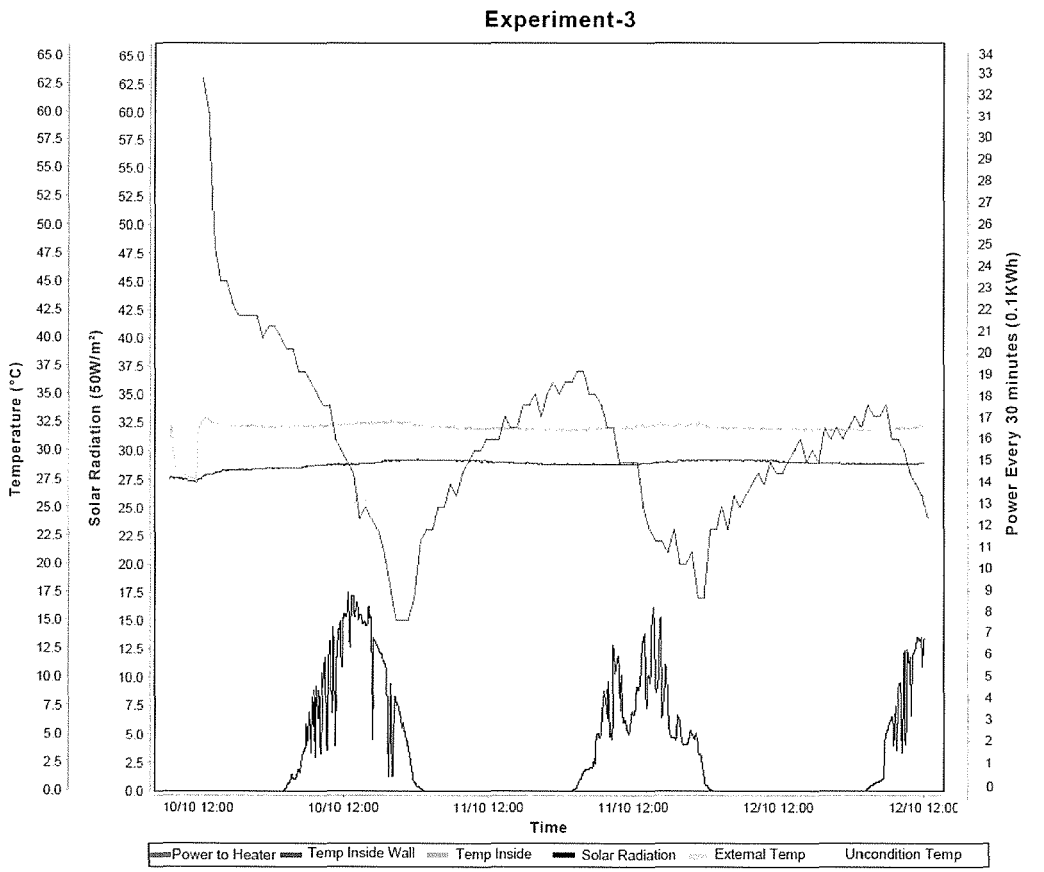

Figure 5.4 The temperatures, power and solar irradiance for experiment 3

Figure 5.4 shows the data of experiment 3 in a line graph format. The green curve and the light pink curve indicate the internal and external temperatures respectively. The blue curve and the yellow curve represent the temperature inside the wall and the temperature in the unconditioned space respectively, while the red curve and the black curve represent the electrical energy supplied every 30 minutes and the external solar irradiance respectively.

As can be seen, both the external temperature and the supplied energy are following a sinusoidal like path with a 24 hours time period. Another observation is that the supply energy is lagging the external temperature. This lagging is caused mainly by the thermal mass of the building. Another factor which contributes to this lagging is the orientation of the test room. The test room receives most of the solar irradiance in the afternoon.

In a pure steady-state environment, the energy supply must be in phase with the external temperature which is not the case in experiment 3. When the external temperature increases in the morning, the electrical energy does not react immediately. This is a clear indication that some of the applied energy is going in the thermal mass. The opposite happens in the evening when the external temperature starts to go down. Here, the electrical energy supply does not react immediately, as expected. This is an indication that the thermal mass is releasing heat energy in the room. In a typical day where the external temperature varies in a sinusoidal like path, the extra energy supplied due to the thermal mass in the morning is balanced by the energy released in the afternoon. As can be seen, if the average electrical energy supplied is calculated over a 24 hour period, the effect of the thermal mass on the average energy supplied is minimized. A similar approach was adopted by Hammarsten in his work [25].

Another factor which can affect the accuracy of the final result is the starting time on which the averages are calculated. If the starting time is selected just before sunrise, there will be enough time during the night for the thermal mass to release the stored heat energy from the previous day. In other words, this minimizes the dynamic effects, as well as, the solar irradiance effects from the previous day. Similarly to

this, the effects of the solar irradiance received during the measuring time window are reflected in the $U_{Effective}$.

5.6.1 The Test Procedure adapted in method 3

The procedure for method 3 is given below. As one can see, it is almost identical to that of method 2.

1. A temperature sensor was placed outside the building and it was protected with a proper solar shield.
2. A temperature sensor was placed inside the building.
3. A temperature sensor was placed 20mm inside one of the internal walls.
4. The temperature inside the building was kept constant and about 7°C higher than the outside temperature. A fan heater was used to control the internal temperature.
5. The electrical energy supplied to the heater was monitored.
6. It was ensured that the temperature inside the wall reached a saturated state before sunrise.
7. The heating inside the building was left on for further 24 hours.
8. For the above 24 hours time window the average inside temperature and the average outside temperature were calculated. The average electrical energy supplied to the heater was calculated as well for the same time window mentioned at 7.

All sensors are monitored and recorded at pre-determined intervals

The $U_{Effective}$ is found by:

$$\frac{Average\ power\ supplied\ to\ the\ heater}{(Average\ internal\ temperature - Average\ external\ temperature)} \quad (W/°C) \quad (5.03)$$

As with method two, this method can be applied concurrently to two adjacent rooms without affecting each other.

5.7 Method four for measuring $U_{Effective}$

This method is also used to determine the $U_{Effective}$ in the equivalent thermal network. This method is intended to capture the effects of the solar gain in the building. Similar to method two and three, the internal temperature is kept constant and higher than that of the external temperature by means of a fan heater. The time window for the heating is not changed from method 3. In method 3, the internal temperature and the solar irradiance are monitored for 5 complete days before the heating up of the building is started. There are also major changes in the calculations of the $U_{Effective}$. Before describing this method in detail, it is better to go through the experiments on which this method is based. Experiment number 4 and experiment 5 are intended to demonstrate the effects of the solar irradiance and the shading on the internal temperature of the building. Experiment number 5 was carried out in the test room, while experiment number 4 was carried out in a different room which from now on will be referred to as **test room 2**. Both rooms are found in the same floor of the same building but they are few meters apart. Both rooms have approximately about 50 % of their boundaries exposed to the external environment. The main difference is that test room 2 is well shaded while the test room is not.

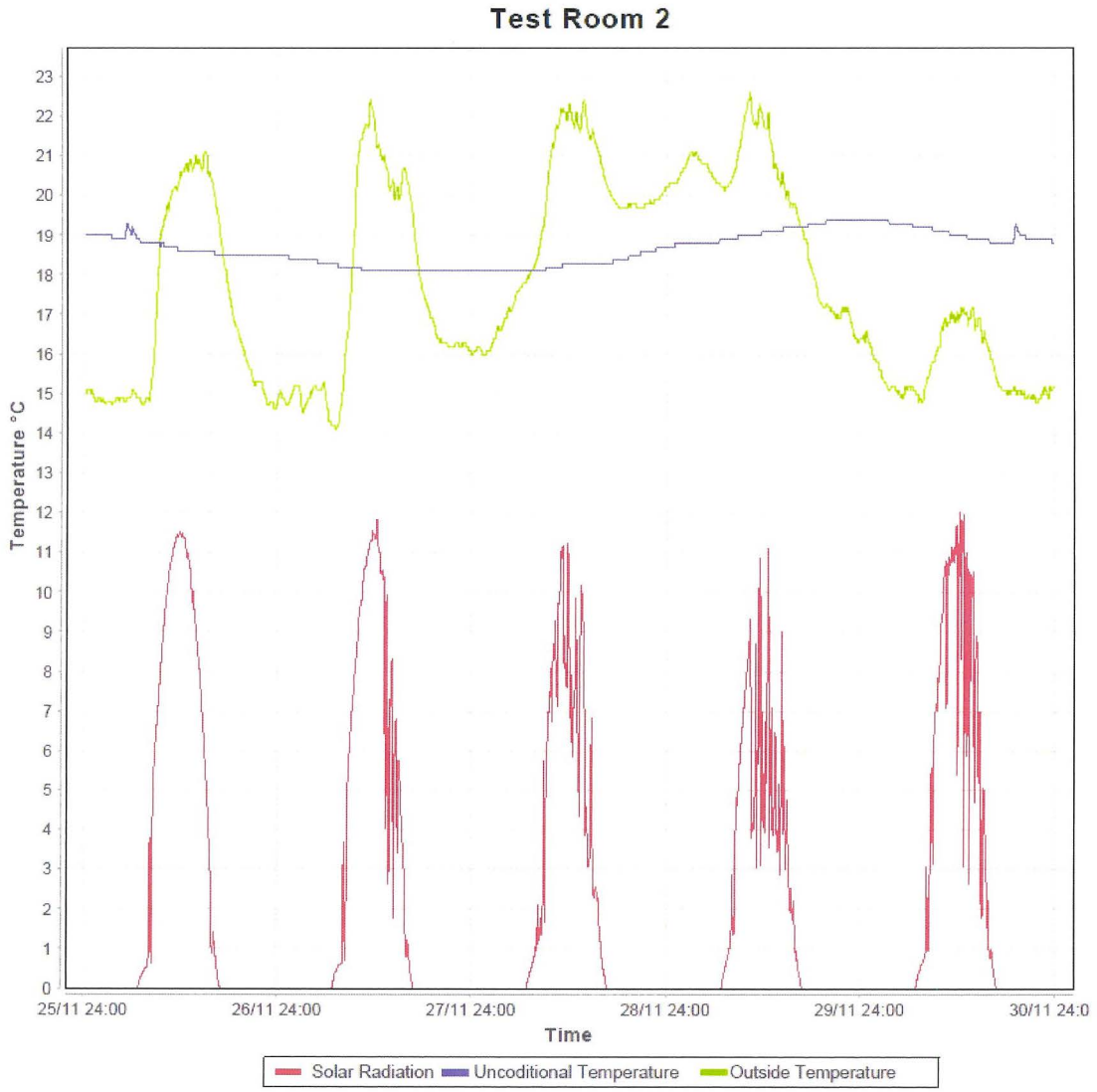

Figure 5.5 The temperatures and solar irradiance for experiment 4

Figure 5.5 shows the data of experiment 4. The blue curve and the green curve represent the internal and the external temperature respectively. The red curve represents the solar irradiances.

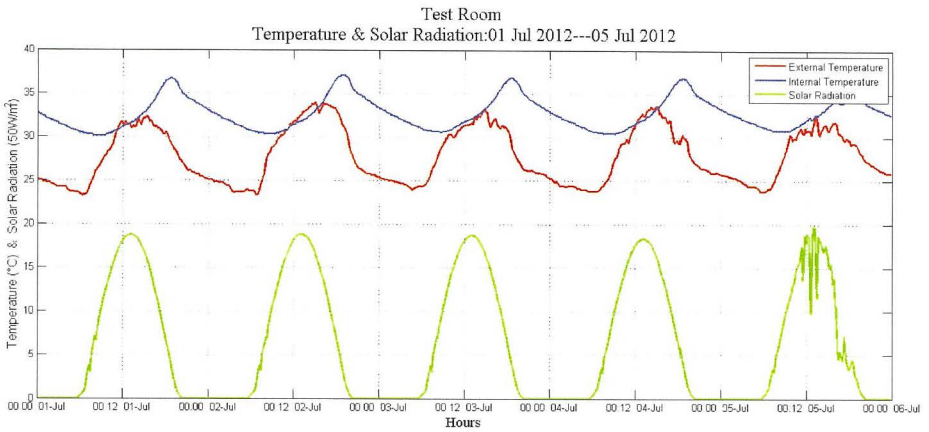

Figure 5.6 The temperatures and solar irradiance for experiment 5

Figure 5.6 shows the data of experiment 5. The blue curve and the red curve represent the internal and external temperature respectively, while the green curve represents the solar irradiance.

As can be seen, the internal temperature variations were minimal in the case of test room 2, while the internal temperature variations for experiment number 5 were substantial. The main difference between the two rooms is that test room 2 is well shaded, while the test room is not. This is a clear indication that the daily temperature variations in the test room are attributed to the solar gain. The study of section 4.5.4 which was carried out for one complete year, gave the same conclusions. This study concludes also that there is a proportional correlation between the accumulative solar irradiance to the temperature variation in the test room.

An interesting observation is the line graph of figure 5.7. Here, the red curve represents the electrical energy supplied to the heater, the green curve represents the internal temperature, while the black curve represents the external solar irradiance. The blue curve represents the temperature inside the test room as it was exactly one year before. As expected, the latter does not represent the actual present internal temperature because the external environment was different and the heating is taking place in the test room. On the other hand, the orientation of the building and the solar path are not changed. What is most important with regards to the old data is the shape.

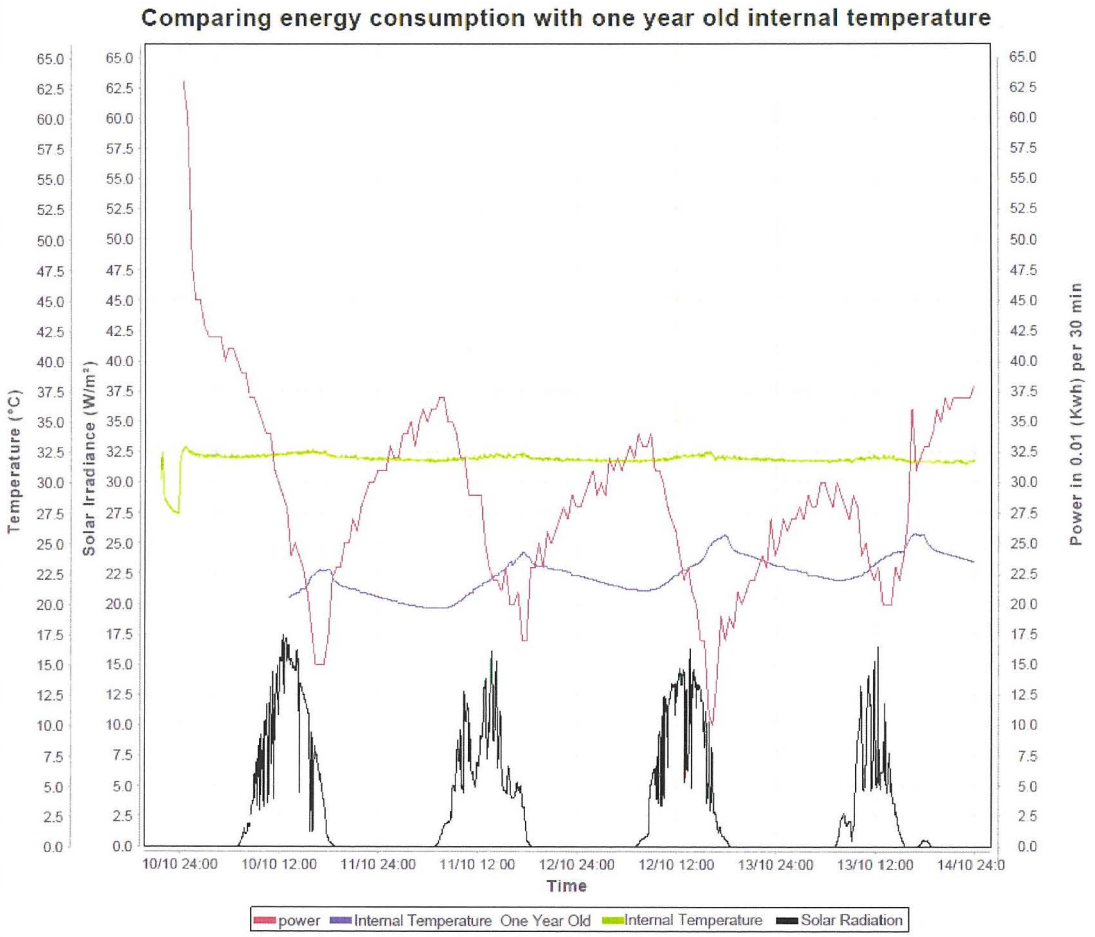

Figure 5.7 The data of experiment 3 compared with the internal temperature of exactly 1 year before in the test room

As can be seen in figure 5.7, there is a correlation between the internal temperature from the previous year (the blue curve) and the electrical power supplied (the red curve). When the internal temperature is maximum, the energy consumption is minimum with the exception of the 13th October, where the solar radiation was relatively low. Even the shapes are well correlated when considering that the external environment conditions are different.

From the above, it was concluded that by monitoring the internal temperature variations, one can anticipate the reduction in the energy requirements of the building. Now as shown in the study of section 4.5.4, in chapter 4, the daily temperature variations are directly proportional to the daily accumulative solar

energy. By using this fact, it can be argued that the daily average temperature increase inside the test room is directly proportion to the daily accumulated solar energy. Therefore the relation can be expressed as:

$$K = \frac{Daily\ Accumulative\ Solar\ Energy}{Average\ Temperature\ increase} \quad (5.04)$$

Where K can be determined by monitoring the solar irradiance and the internal temperature for a number of days and then by calculating on an average K. Once the average internal temperature increase can be estimated, then it can be used to correct the energy requirements. Unfortunately, this model does not cater for the random variation in the solar radiation which sometimes can affect the accuracy of K.

5.7.1 The Test Procedure adopted in method 4

The procedure for method 4 is given below:

1. A temperature sensor was placed outside the building and was protected by a suitable solar shield.
2. A temperature sensor was placed inside the building.
3. A pyranometer sensor was placed outside the building.
4. A temperature sensor was placed 20mm inside one of the internal walls.
5. The internal temperature and the solar irradiance were monitored for at least 5 days.
6. The temperature inside the building was kept constant at about 7°C higher than the outside temperature. A fan heater was used to control the internal temperature.
7. The electrical energy supplied to the heater was monitored.
8. It was ensured that the temperature inside the wall reached the saturated state before sunrise.
9. After sunrise the heating was left on for a further 24 hours

10. The $U_{Effective}$ and K were calculated according to section 5.7.2.

5.7.2 The calculation procedure for method 4

The main changes are found in the calculation of the effective U-Value. The first thing to do is to calculate the average temperature increase inside the test room and the accumulative solar energy for a whole day. The average temperature increase during a 24 hour period is calculated by identifying the reference temperature T_{ref} first. This is the temperature taken just before sunrise and it is used to determine the temperature increase. The reference temperature is indicated by x in figure 5.8

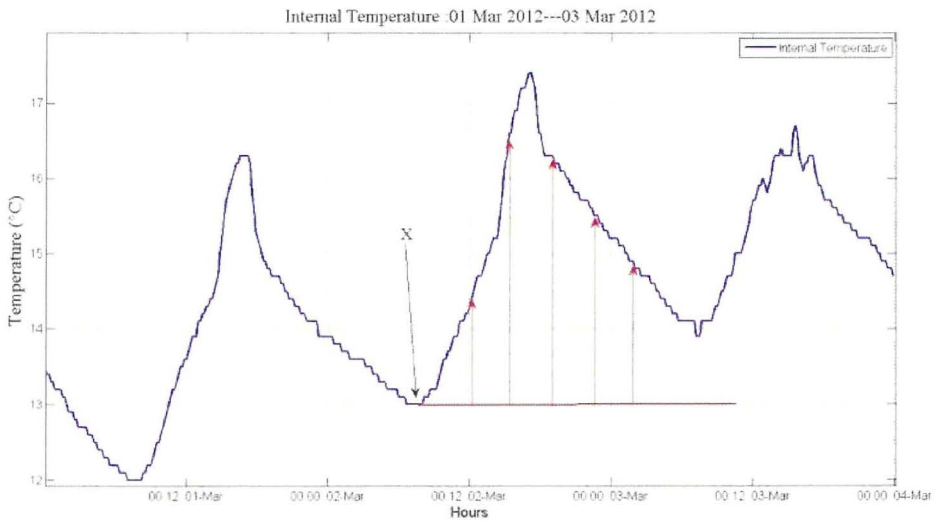

Figure 5.8 A normal temperature variation inside the rooms

$$ATI = \frac{1}{L} * \sum_{n=1}^{L} (T_n - T_{ref})\ for\ positive\ value\ only \quad (°C) \qquad (5.05)$$

Where;

ATI is the average temperature increase

n is the sample number

L is the last sample

T_n is the internal temperature at sample n (°C)

T_{ref} is the reference temperature (°C)

The accumulative solar irradiance is calculated by:

$$Daily\ Accumulative\ Solar\ \ Energy = T * \sum_{n=1}^{n} S_n \qquad \left(\frac{J}{m^2}\right) \qquad (5.06)$$

where;

T is the sample time in seconds

S is solar irradiance in (W/m^2)

n is the sample number

The relation between the solar radiation and the temperature increase inside the test room is determined by:

$$K = \frac{Average\ Temperature\ increase}{Daily\ Accumulative\ Solar\ Energy} \qquad (°Cm^2/J) \qquad (5.07)$$

The above procedure is performed for each complete day during the temperature and the solar irradiance monitoring period. Then, an average K (K_{avg}) is calculated.

The Effective U-Value is calculated by:

$$U_{Effective} = \frac{P_{Avg}}{T_{Avg\ Internal} - (K_{avg} * S_{acc} + T_{avg\ External})} \qquad (5.08)$$

The power requirement is calculated by:

$$P_{Required} = U_{Effective} * (T_{Avg\ Int} - (K_{avg} * S_{acc} + T_{avg\ Ext})) \qquad (5.09)$$

where;

$U_{Effective}$ is the Effective U-value (W/°C)

$P_{Required}$ is the power needed to keep the internal temperature to a given set point (W)

P_{avg} is the average power supplied to the heater over 24 hours (W)

$T_{avg\ int}$ is the average internal temperature over 24 hours (°C)

$T_{avg\ ext}$ is the average external temperature over 24 hours (°C)

K_{avg} is the average proportional relation between the accumulative solar radiation and the average internal temperature increase over 24 hours ($°Cm^2/J$)

S_{acc} is the accumulative solar energy over 24 hours (J/m^2)

5.8 Comparison of method two, three and four

This section will compare method two, three and four which measure the effective U-Value. Method one is excluded because it cannot be used in a building with more than one room. Therefore, method one is not adapted to any of the final protocols.

Method	Heat Requirements (hours)	Time to Complete (hours)
Two	12	12
Three	36	36
Four	36	156

Table 5.2 Comparison of methods two three and four

Table 5.2 compares the methods with their heat energy requirements and the time required to complete. As seen in the above section, method four is the only one which specifically caters for the solar gain, although the other methods indirectly

include some element of the solar gain. The performance of these methods in the final protocol is discussed in the next chapter.

5.9 Method for measuring $C_{Effective}$

In this research, a method which measure the $C_{Effective}$ was developed but its correctness was not validated. The details of this method along with its investigations are found in Appendix C.

6. Implementation of the Hardware and the Software

6.1 Introduction

This chapter covers mainly the development part of the system. It should be noted, that the final version of the hardware and software was developed after the analysis of the room under test were complete. This helped to identify the requirements and to establish the specifications. This chapter does not go in too much detail of the implantation but a good overview of the system is given. The discussion will concentrate mainly on the various features implemented in the system and how they are related to the established goals.

This chapter starts by defining the goals and the priorities for the proposed system and continues with the system requirements. An overview of the system along with some details of the hardware and software implementations follows. Finally this chapter concludes with a discussion of the system.

6.2 Goals and Priorities of the system design

The first required task was to identify the system requirements, features and functionality that must be included. These were a lot and due to time restrictions a compromise had to be reached. As a consequence, a list of goals was established. This list prioritized the goals according to their importance. The lower the number associated with the goal, the higher the level of the importance.

1. The system must include all the sensors and control requirements to enable the proper implementation of the energy performance protocols. Without these requirements the protocol cannot be executed accurately.
2. The system must contain features and functionality to make the execution of the energy performance protocols as easy as possible and hence reduces the laborious part of the protocol execution. This will make the adoption of the protocol a cost effective one.

3. The system must include a provision for automation. This will reduce the human interactivity in the process and hence reduce the errors in the results
4. The design of the system should support a considerable number of sensor nodes. This will ensure that the system is not restricted by the size of the building.
5. The system must include the requirements, and the flexibility to allow implementation of future improvements identified during the test room analysis and during the evolving experiments. This should make the improvement of the protocol easy to implement.
6. The system should also cater for the existing energy efficient protocols identified in the literature review.
7. The software should be structured in such a way that it allows other future building blocks to be integrated easily. The system should be user friendly as far as possible. This will reduce human errors.

6.3 System Requirements

Once the goals and their associated priorities are established, the next task is to identify the system requirements. This section will discuss these requirements along with their importance as established by the goals in the previous section.

6.3.1 External Sensors

The energy performance protocols proposed in this research requires two external sensors. These sensors are the external temperature sensor and the global solar radiation sensor. Without these two sensors the energy performance protocols proposed here cannot be executed. Another external sensor which is good to have in the system is the external humidity sensor. The external humidity sensor is really important if further research is to be carried out on the relationship between humidity and air infiltration, as suggested in section 4.4.4. Other external sensors which may be useful are the anemometer, the rain collector and the barometric pressure sensor. As mentioned in the literature review section, such data can be used in conjunction

with neural networks to forecast energy usage in a building. All these sensors are widely available in commercial weather stations. So it was decided to include an interface to a commercial available weather station. Ideally the weather station should be a wireless one, so it will reduce the labour requirements.

6.3.2 Internal Sensors

Further to the external sensors mentioned in the above section, the energy performance protocols developed here require an energy meter and four temperature sensors in each of the enclosed rooms in the building under analysis. A more accurate and detailed analysis is possible if more temperature sensors are used. For this reason, it is suggested that each sensor node should have the possibility of having eight temperature sensors. Another option would be to have a humidity sensor in the sensor node. The humidity sensor can be used for further analysis on the relationship between air infiltration and humidity level in the building, as mentioned in section 2.

6.3.3 Control

The proposed protocols stipulate that each room in the building under test is heated up to a predetermined constant temperature. For this reason, fan heaters controlled by a close loop controller should be used. In an ideal situation, the air temperature in the rooms should be homogenous as far as possible. This can be achieved by using the fans to circulate air inside the room. Too much air circulation in the room could affect the surface thermal resistance on the walls or affect the air infiltration in the building. This could have a negative effect on the result. Although this problem is not investigated, it is recommended that the sensor node provides a provision for fan control.

6.3.4 Functionality

The system should provide a means of exporting the collected data in the form of comma-separate value (CSV) file. Nowadays, CSV files are widely used to import and export data. For example CSV files are used to import data to MatLab and to

many other available databases. Another necessary function of the system is the ability to perform a temporal action or a conditional action. Examples of such actions are the switching on and off of a heater or the setting of the temperature set point to $5^{o}C$ above the external temperature. The latter function is especially useful to automate the process. Another useful function that the system should have is the ability to display the data in line graph form. This will help the users to capture trends in the data.

6.3.5 Processing and data requisition

The communication among the sensor nodes should be wireless. This will make the system more user friendly and less intrusive. The whole system should be controlled by a Personal Computer (PC) which will give the system many advantages. Some of these are listed below:

1. A PC in conjunction with a mobile internet key and a remote access software such as Team Viewer, will provide access to the system from all over the world.
2. A PC will also provide the necessary processing power and other resource if needed.
3. A PC provides data storage for the data collected from the sensor nodes.
4. A PC will allow the user to use the system in conjunction with many other available applications such as MatLab. This will give great flexibility to the user and allows him/her to be more productive.
5. PCs nowadays are inexpensive, easily available and easily upgradable.

6.4 System Overview

Figure 6.1 shows a birds' eye view of the proposed system. As can be seen in this figure, the proposed system is centered on a PC. The main purpose of the PC is to run the system's software and to provide storage for the data acquired. The PC provides also remote access to the system through the Internet. The latter is not a must but it is a very useful feature. This can be achieved by using a mobile internet

key or an internet connection if it is already present in the building. The only prerequisite for the PC is that it should run java and should support Graphical User Interface (GUI).

The external weather data is obtained by Davis Vantage Pro 6152 weather station which is a professional wireless weather station. The connection between the console of this weather station and the PC is provided through a USB connection. Figure 2 in chapter 3 shows a photograph of this weather station. Special drivers are provided by the manufacturer of this weather station which turns the USB connection into a virtual serial communication port. Furthermore, the manufacture published the communication protocol used by the weather station. The software application uses this protocol to communicate with the weather station and to download the data through this virtual serial port.

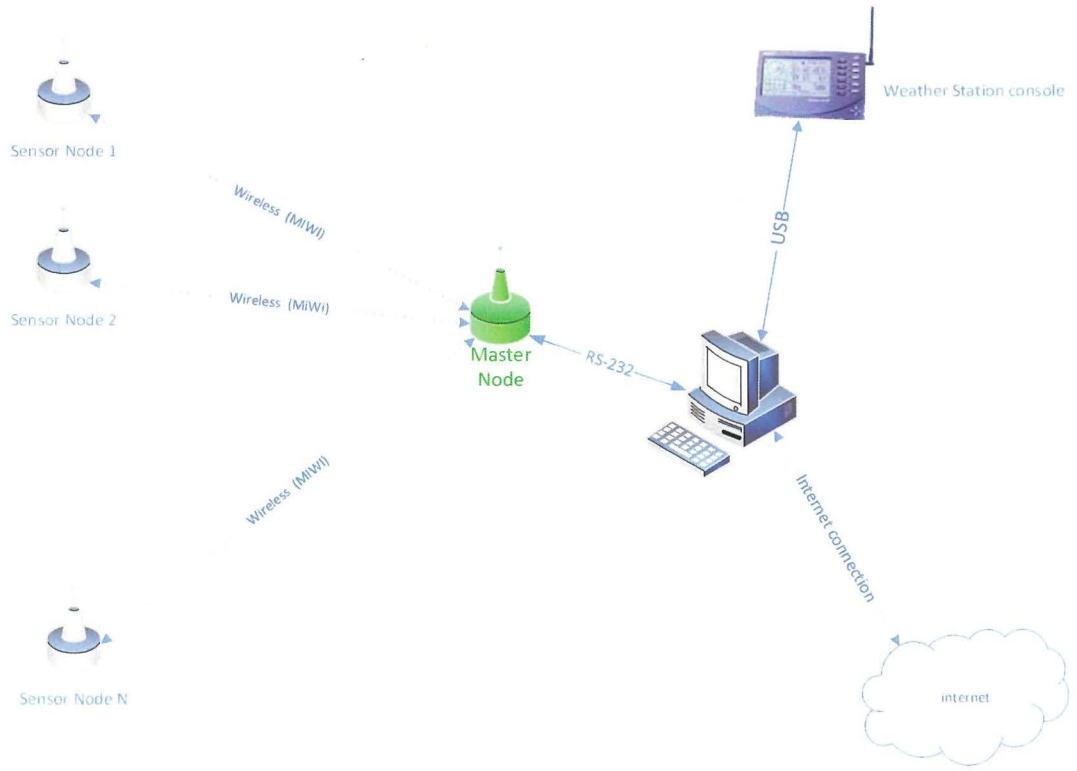

Figure 6.1 An overview of the proposed system

The system contains one master node and a number of sensor nodes. The number of sensor nodes varies according to the size of the building. All the sensor nodes

communicate directly with the master node through a wireless communication using a MiWi stack. The MiWi stack is a propriety protocol from Microchip which is based on IEEE standard 802.15.4. One can use MiWi protocol for free with the condition of using it on Microchip devices. The MiWi protocol supports star topology as well as mesh topology. A MiWi network can support up to 8000 nodes which is more than enough for a typical dwelling. Moreover, MiWi supports up to 64 hops which means that a message is relayed from one node to another until the message reaches its destination. This makes the system usable even if the building is very large [27]. The function of the master node is to act as a bridge between the MiWi network and the PC. Communication between the PC and the master node is achieved through a serial port. All the messages from the PC to the MiWi network are communicated through the serial port, to the master node and the master node relays the message to the intended sensor node. All the messages intended to the master node are forwarded to the PC through the serial port.

The function of the sensor node is to collect the data and transmit it back to the PC. Another indispensable function of the sensor node is the temperature control in a given room. Each sensor node has eight temperature sensors, a humidity sensor, an energy meter, three fan controls and finally a temperature control which uses the PI control algorithm. Further details on the sensor node and on the master node are given in the hardware section 6.5.1 and 6.5.5.

The software part consists of three programs and is written in Java. One program is used for the sensor node configuration and calibration. Another program is used for the data analysis and the data exportation and the last one is used as a data logger and control. Further details of these programs are given later on in this chapter.

6.5 Hardware

The sensor nodes and the master nodes were designed and built as part of this research project to enable the implementation of the proposed protocols and for

further analysis in the future. This section which is divided into five parts, is going to give more details on the node design and on the embedded software. Four sections describe the sensor node while another one describes the master node.

6.5.1 Sensor Node - the Hardware

This section is going to describe the hardware of the sensor node without going in too much technicalities. Figure 6.2 shows a block diagram of the sensor node. It also shows the connectivity among the various components in the sensor node. The various blocks of this block diagram are discussed further in this section.

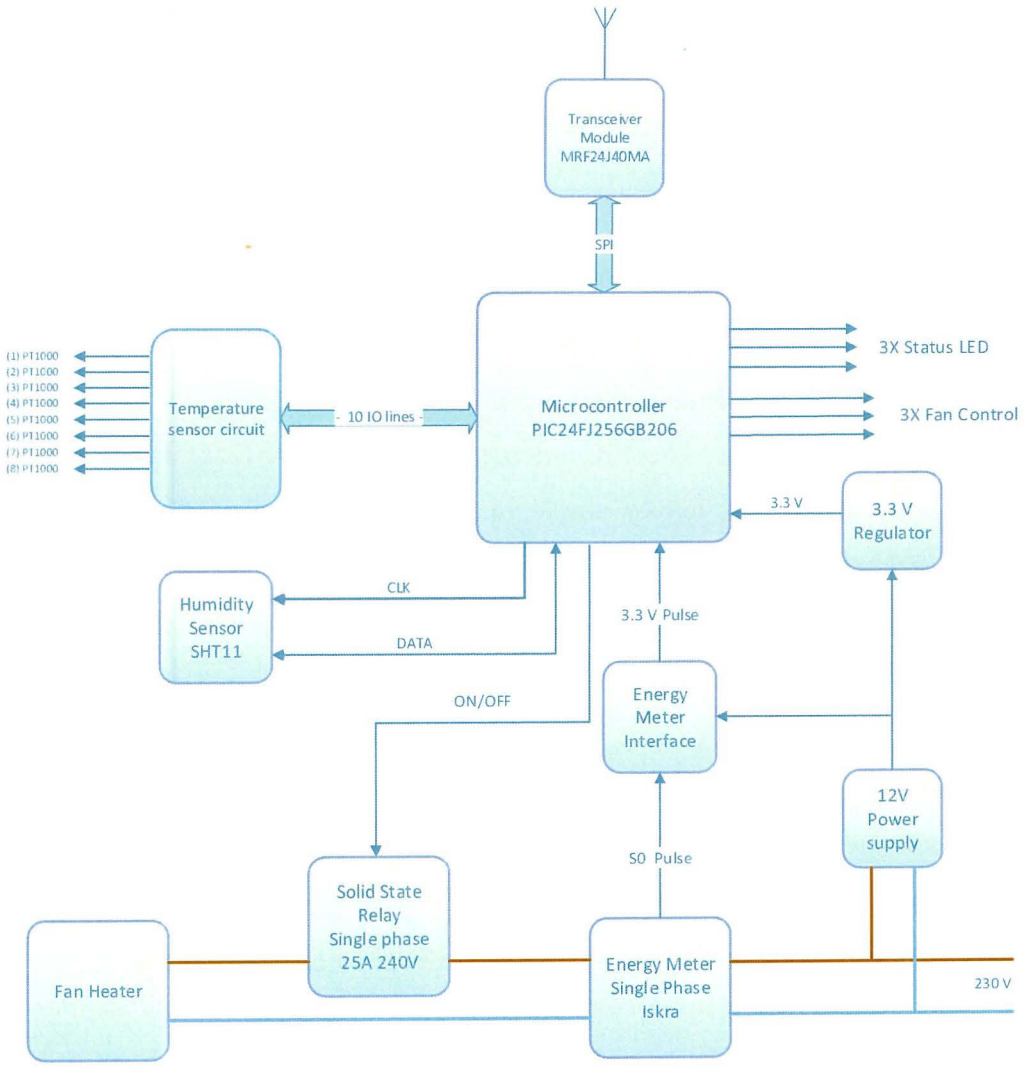

Figure 6.2 The block diagram of the sensor node

The first important decision that had to be taken before starting the hardware design was to choose a wireless technology for the data transmission. As stated in the previous section, the technology chosen is MiWi. From the design point of view, MiWi has a number of advantages, mainly the availability of tools, libraries and demo boards which facilitate the development. Moreover, Microchip offers their clients a set of complete RF transceiver models which are 2.4GHz IEEE 802.15.4 compliant and are compatible with MiWi and Zigbee stacks. Furthermore, these modules are already certificated to be used in Europe and other countries around the world. This eliminates any complications which are related to the transceiver design and reduces the development time. For these reasons transceiver module MRF24J40MA was selected. This module can support up to 250 kbps data transfer which is more than enough for the requirements of this project.

As a minimum requirement, the microcontroller should be a Microchip microcontroller. It has to support at least one Serial Peripheral Interface (SPI), which is needed by MRF24J40MA module and it has to support twenty five input output single pin ports. Furthermore, the microcontroller should have enough resources to support the MiWi stack. The PIC microcontroller PIC24FJ256GB206 provides all these requirements and leaves ample resources for the needed development and further enhancements in the future. For this reason, the PIC microcontroller PIC24FJ256GB206 was selected. The full details of this microchip can be found on the Microchip website [28].

The humidity sensor used in the sensor node is SHT11 which is supplied by Sensirion. This sensor measures the relative humidity with an accuracy of ±3% and the temperature with an accuracy of ±0.4 °C. The latter is used by the embedded routines to compensate for changes in temperature. The SHT11 sensor similarly to the PIC24FJ256GB206 microcontroller operates from 3.3V power supply and its interface consists of a single serial input clock and a bidirectional serial data. The real challenge with the SHT11 is the communication protocol. This protocol is

propriety and it has to be coded in the embedded software. Further details on the SHT11 can be found on the Sensirion website [29].

The sensor node incorporates three LEDs. The purpose of these LEDs is just informative. The red LED indicates that the heater is on, the amber LED indicates that a command was received and is being processed, while the green LED indicates that an energy pulse is received. The Green and the amber LED are also used for node identification purposes. In the latter case, a command is received from the PC.

As already indicated, the fan control is not used in the research project but it is here implemented for future use. The hardware implementation of the three fan controls is very simple and straightforward. The three fan control outputs are directly connected to three i/o port lines of the microcontroller. The maximum current sinking or current sourcing, and the output voltages are limited by the microcontroller specifications. In our case, the current limit is 18 mA, while the output voltage is limited to a maximum of 3.3V. Each fan control can have five possible states which are listed below:

1. High - the fan control line can source current
2. Low - the fan control line can sink current
3. High-impedance - the fan control line does not sink or source current
4. Variable speed using pulse width modulation
5. As in state 4, but the output is inverted

With regards to states 4 and 5, the output has a fixed frequency and a variable space mark ratio. In total, 16 different space mark ratios are possible. The state of the three fan controls, and the space mark ratios can be changed from the PC software. The embedded software implementation of the fan control is also straightforward. It is based on an interrupt service routine (ISR) of one of the internal timers. The ISR checks for changes in the configurations at predefined intervals and changes the output accordingly.

The electrical energy supplied to the heater is measured by means of Iskra ME 162 digital energy meter which is commercially available. This energy meter can handle up to 100A loads and has class 1 accuracy. It is also compliant with many international standards. This energy meter has an SO output which is opto-isolated and which produces a series of 30 ms pulses. Every 1000 SO pulse is equivalent to 1kWh. The SO output was used to interface the microcontroller with the energy meter. As a consequence, an interface circuit was built and incorporated in the sensor node.

The interface circuit consists of a monostable and a potential divider. The latter is directly connected to one of the IO pins on the microcontroller with an input change notification and which is configured on this IO pin. The monostable was required because the SO pulse raising and falling time was not fast enough and it caused false pulses. When a pulse from the energy meters is received an interrupt service routine is executed and two counters are updated. One of the counters is reset with every read command received from the PC, while the other one is never clear and therefore it keeps count of the total energy used by the heater. Furthermore, the SO required a 12V supply. As a consequence, a commercially available 1A 12V switch mode power supply was modified and fitted in the sensor's node box. Moreover, a 3.3V voltage regulator circuit was also added to the sensor node. This regulated 3.3V supply was needed by the rest of the sensor node's circuitry. Figure 6.2 shows also the solid state relay block and the temperature sensor circuit block. The descriptions of these two blocks are covered in more detail in the next two sections.

6.5.2 Temperature Measurements

As already stated in the requirements section, the temperature measurements should have an accuracy of ± 0.1 °C. This requirement brought a lot of challenges, mainly because the analogue to digital converter (ADC) of the selected microcontroller does not handle this resolution. The solution for this problem was found in the application note AN685 [29] from Microchip. This application note explained how one can measure resistance of a component by using an internal timer and an internal

comparator of a Microchip microcontroller. In our case, the setup is needed to measure the resistance of a PT1000 which is a platinum temperature resistance of 1000Ω. The principle of operation is based on the RC time response and figure 6.3 shows the circuit setup required to measure the PT1000 resistance.

The Reference resistor R_{rf} is used as a reference, therefore it should be stable and it should have a very low tolerance. In our case, the tolerance is of 0.1%. The discharge resistor R_{disch} is used to discharge the capacitor C, therefore it must have a low value in the range of 50 to 100Ω.

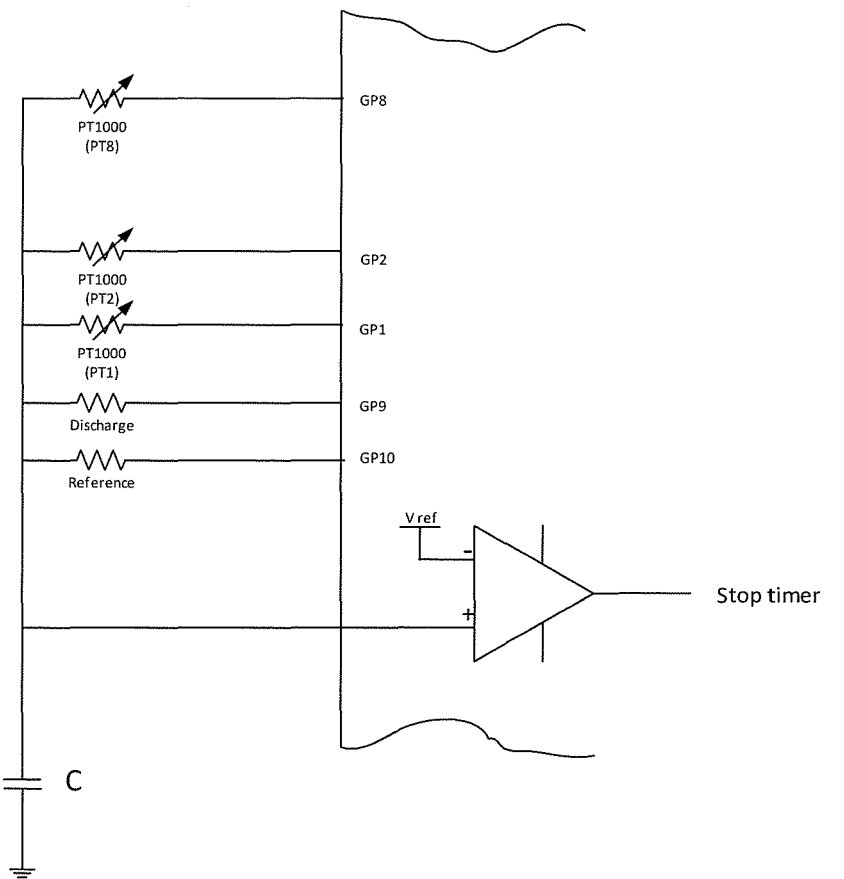

Figure 6.3 The circuit to measure temperature with accuracy of ±0.1 °C

In order to reduce the effects of errors especially due to induced noise from the surrounding environment, the reading process is repeated several times and an average is calculated. The resistance value was calculated using:

$$R_{PTX} = {(R_{ref} * T_{PTX})}/{T_{ref}}$$

where : R_{PTX} is the resistance value of the given PT1000

R_{ref} is the resistance value of the reference resistor

T_{ref} is the time measured so that the voltage across C reaches V_{ref} when C is charged through reference resistor

T_{PTX} is the time measured so that the voltage across C reaches V_{ref} when C is charged through a PT1000

The calculated resistance value is transmitted to the application on the PC. It is up to the application on the pc to calculate the temperature from this resistance.

Another challenge encountered was that of the temperature calibration which required a third order polynomial fit. This meant that for calibration, each temperature sensor requires four constants of the type double. This translates into 32 byte of storage per temperature sensor or 256 bytes per sensor node. Since these constants are closely associated with the temperature sensors on the sensor node, it was decided to store these constants on the flush of the microcontroller of each sensor node. It is up to the application on the PC to retrieve these constants and perform the calibration. As a consequence, a number of routines were developed and were included in the embedded software which allows an application to read and write these constants.

6.5.3 Temperature Control

The temperature control is achieved by using a 2 kW fan heater, a 25A solid state relay and a proportion and integral (PI) control algorithm which is coded in the embedded software. As expected, the main challenge here was to program the PI control and to find the proportional and the integral gains. The latter can be a problem because the sizes and the characteristics of the rooms are not known. There are methods which auto tune the PI control, but they are left for possible future work.

However, the system is designed in such a way that it allows the proportional gain, the integral gain and the sample rate to be changed on the fly. Furthermore, the system provides also a means of resetting the variables related to the PI controller. The temperature control is achieved by switching on and off the heater by means of the solid state relay. The switching on time is dependent on the output of the PI algorithm. Figure 6.4 depicts this in more detail.

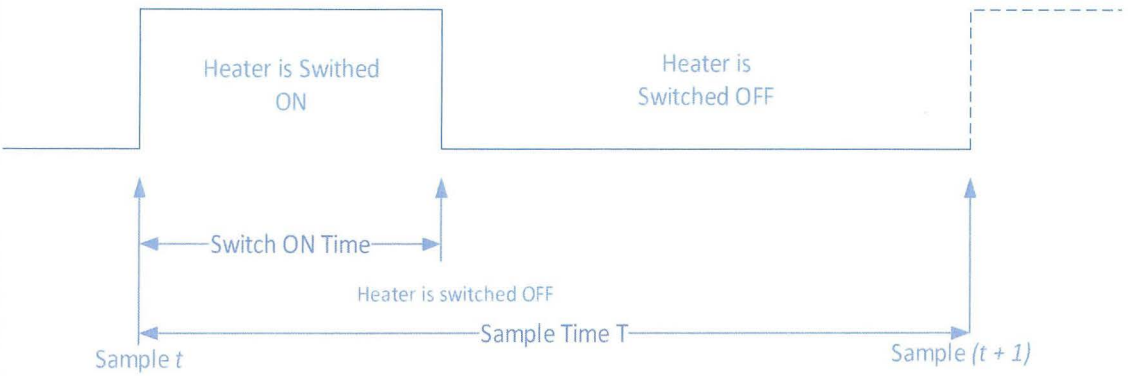

Figure 6.4 How the temperature control is performed

At sample *t* a new error is measured and a new PI output is calculated. Once the new PI output is known, first it is truncate to a range between 0 and 4000, and then the new switch on time is calculated using a proportional method, where the maximum possible value is set to 4000.

PI Control analysis:

The heat generated by the heater is partly accumulated as heat inside the room and partly lost outside the room.

Express in differential form at any instant the mathematical expression is given by;

$$P_{gen}dt = mcd + A\alpha dt \qquad (6.01)$$

Heat generated by the heater	Heat accumulated in the room	Heat lost to the outside

where;

P_{gen} is the heater power (W)

Θ is the time in (s)

A is the Average surface area through which the heat is lost (m^2)

α is the Average heat transfer constant ($Wm^{-2}K^{-1}$)

m is the Average mass used for heat storage (Kg)

c is the Average specific heat capacity ($K^{-1}Kg^{-1}$)

$$P_{gen} = \frac{mcd}{dt} + A\alpha \tag{6.02}$$

in Laplace the above can be written as;

$$P_{gen} = mcs + A\alpha$$

$$P_{gen} = (mcs + A\alpha)$$

The Laplace transfer function of a first order system, therefore

$$= P_{gen}\left(\frac{1}{mcs + A\alpha}\right)$$

$$= P_{gen}\left(\frac{1/mc}{S + A\alpha/mc}\right) \tag{6.03}$$

$(mc/A\alpha)$ is the time constant of the first order response. The time constant is the time taken for the temperature to reach 0.632 of its final value. mc is the heat capacity/Kelvin rise of the complete room. The close loop of the heat control is represented by the below block diagram.

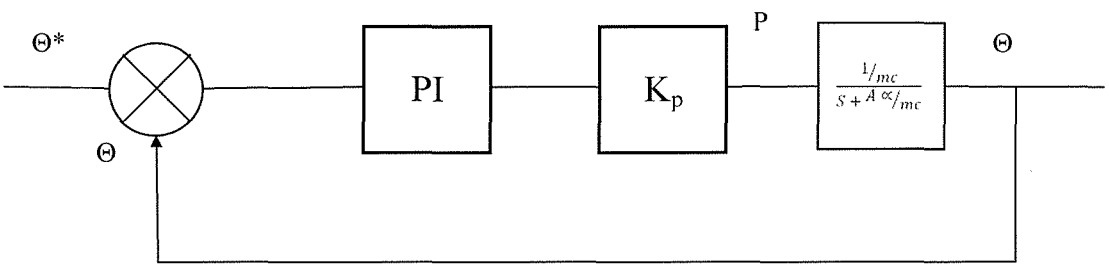

Figure 6.5 The close loop control for the temperature control

K is the constant of the heater. The heater used is 2KW and the output of the PI $\left(\frac{K(s+a)}{S}\right)$ varies for 0 to 4000. Therefore Kp is equal to 1/2. The close loop poles are determined by the characteristic equation.

$$1 + G(S)H(S) = 0$$

$$1 + \frac{K_c(S+a_c)}{S}(K_P)\left(\frac{1/mc}{S+ A\alpha/mc}\right) = 0 \qquad (6.04)$$

$$\left(S + A \propto/mc\right) + k_c(S + a_c)k_p \, 1/mc = 0$$

$$S^2 + \left(a \propto/mc\right)S + + \frac{k_p k_c}{mc}S + \frac{a_c k_c k_p}{mc} = 0$$

$$S^2 + \left(\frac{A \propto}{mc} + \frac{k_p k_c}{mc}\right)S + \frac{a_c k_c k_p}{mc} = 0$$

Comparing the above to the standard second order equation we have

$$S^2 + 2\zeta\omega_0 S + \omega_0^2$$

The discrete PI control equation used is given below :

$$O_{(t)} = O_{(t-1)} + Ki_{(t)} - Ki_{(t)}(1 - aT)i_{(t-i)}$$

Where: $O_{(t)}$ is the output at sample t

K is the proportional gain

a is the integral gain

$i_{(t)}$ is the error at sample t

T is the sample time

The above formula holds only if the sample time T is greater than the responding time. In practice T should be about 10 times greater than the responding time.

Temperature respond time in a building tends to be slow and typically it takes several minutes. This was confirmed by a run test conducted on the Test room. The details of the test room are found in chapter 2 and the results are displayed in Figure 6.6.

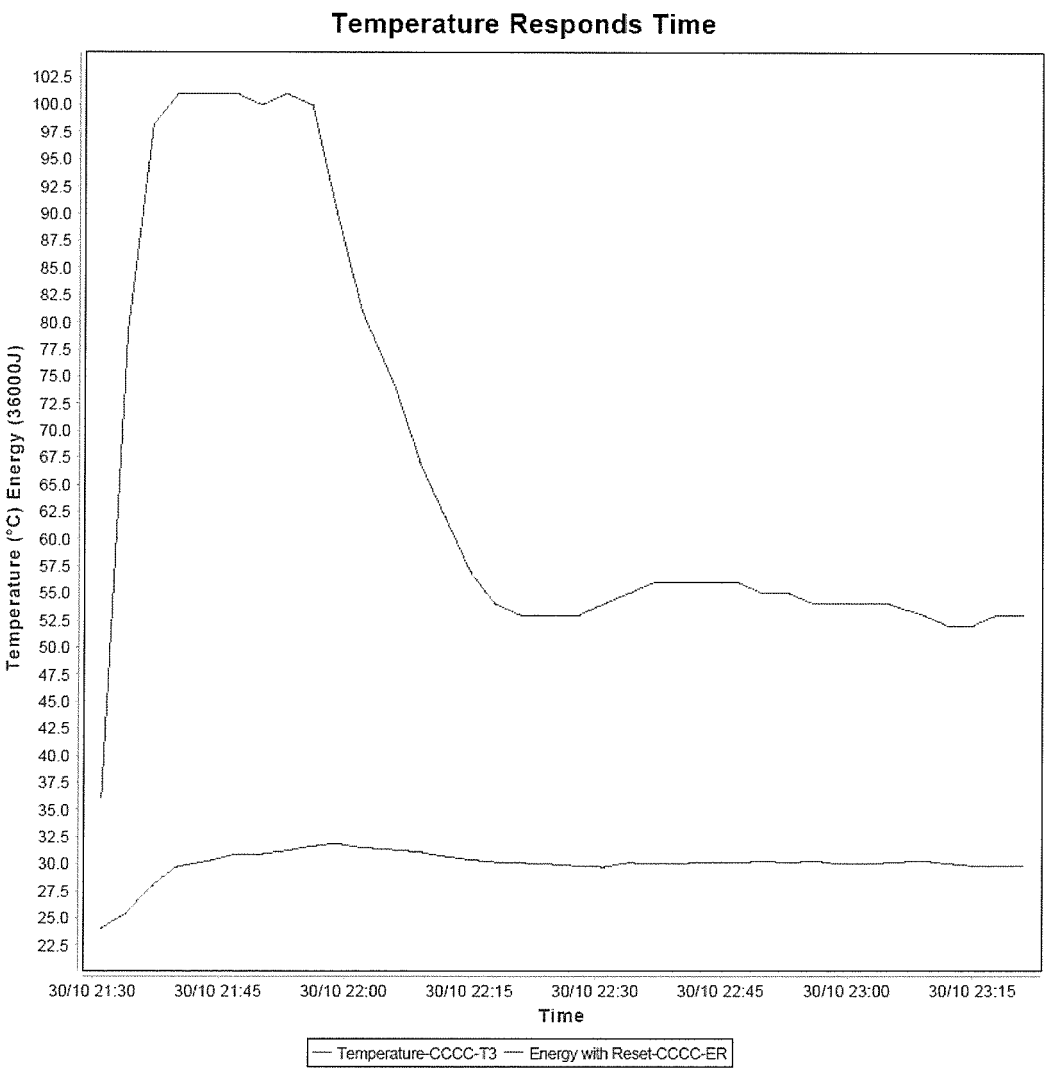

Figure 6.6 The internal temperature and the average energy supplied

Figure 6.6 shows a line graph of the internal temperature along with the average energy supplied every 2.5 minutes. The red line represents the internal temperature, while the blue line represents the average energy supplied to the heater. As can be seen in the first 30 minutes, the power of the heater was full. Similarly, if the internal temperature is observed during the first 30 minutes one will notice that the rate of temperature change is very slow. It should be noted that the testing room is smaller

than the average room in a typical dwelling, which means that the temperature respond time is expected to be slower for a 2 kW fan heater.

The temperature control setup was tested in the test room and the result is shown in Figure 6.7.

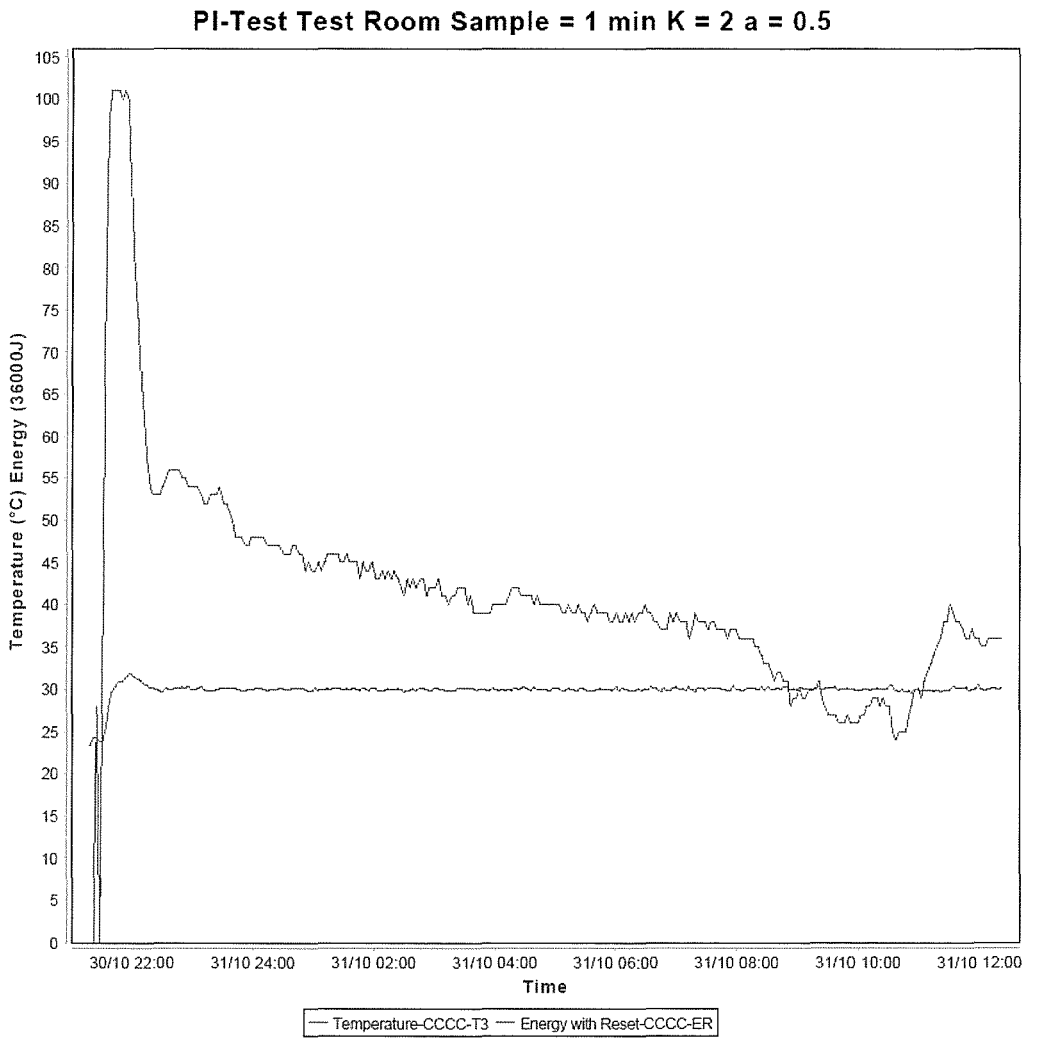

Figure 6.7 The result of the temperature control

The red line in the line graph represents the internal temperature while the blue line represents the energy supplied to the heater between two successive readings. The sample time was set for 1 minute, the temperature set point was set to 30°C, the proportional gain was set to 2 and the integral gain was set to 0.5. As can be seen,

the internal temperature is sufficiently stable. As expected, there was an overshot in the beginning of the graph but this is just 1.5°C.

6.5.4 Sensor Node - the Embedded Software

This section is intended to give a good overview of the embedded software implemented in the sensor node. The method chosen to perform this task is a Data Flow Diagram (DFD). Figure 6.8 shows a level 2 DFD diagram of the sensor node embedded software.

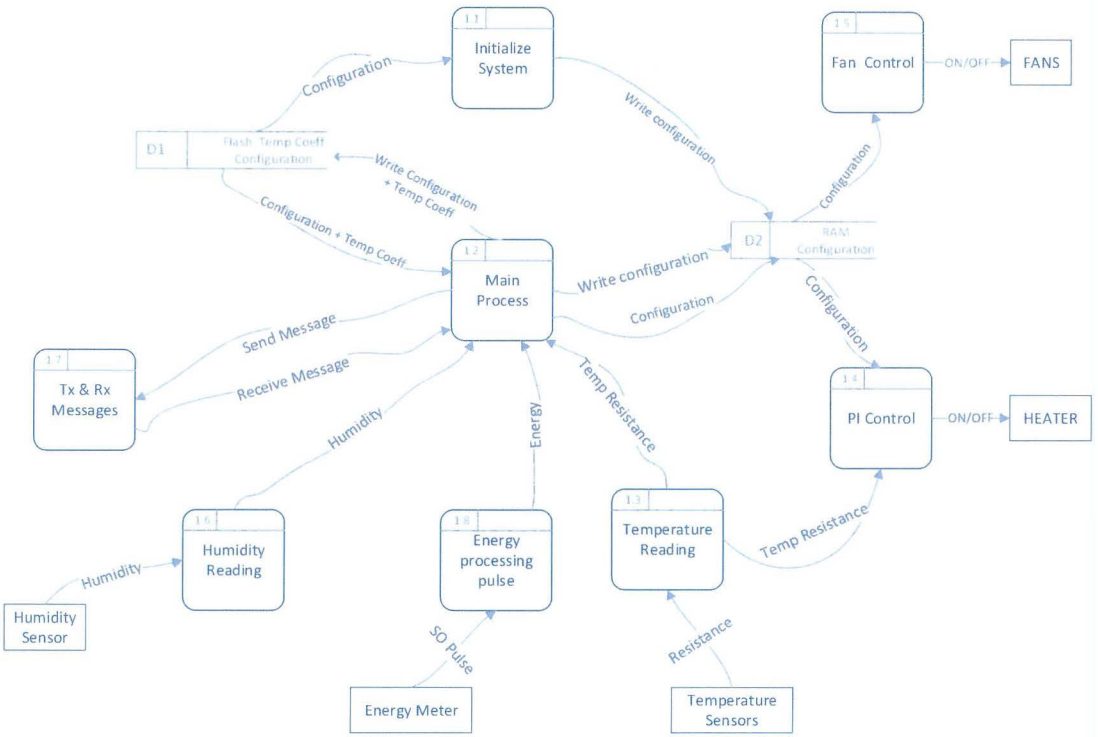

Figure 6.8 Level 2 DFD diagram of the sensor node embedded software

Before explaining in more detail the DFD diagram, the meaning of the symbols used is explained first. A square box with a rounded corner, for example 1.1, represents a process. A closed rectangular box, for example Fan, represents an external entity, while a rectangular box, with one end open, represents a storage. An example of such symbol is D1. The data flow is represented by arrows.

D1: Represents the temperature calibration data, and the default configurations stored permanently on the flash. This allows the configuration of the sensor nodes to be

complete before they are used on site. The settable parameters of each sensor node are listed below:

1. enable or disable the temperature control
2. the temperature set point in the form of resistance value
3. the sample time used by the PI algorithm
4. the proportional gain of the PI
5. the integral gain of the PI
6. which temperature sensor to use for the temperature control
7. enable or disable humidity sensor
8. enable or disable the individual temperature sensors
9. enable or disable energy data collection
10. sets the state of the individual fan control
11. sets the speed of the fan control

D2: Represents the temporally configuration of the sensor node which is stored in RAM and which is a volatile memory. This configuration is intended to be changed on the fly and can be accessed by various processes. The settable parameters are similar to those listed above for D1.

1.1: This process is only executed once and it is the first process to be executed by the sensor node when the node is turned on. This process initializes the node, retrieves the configuration data from D1 and makes it available to other processes by placing it in D2.

1.2: This is the main process where the communication with the application on the PC takes place. It is responsible for receiving commands from an application on the PC, executing those commands and returning a message if necessary. Broadly speaking, these commands are divided into three categories, those that read and write to D1, those that read and write to D2 and finally those that read data from the sensors.

1.3: This process is responsible to read the resistance of the PT1000 when requested. The request contains the sensors which the process has to read and the number of times the sensors are read.

1.4: This process is responsible for the temperature control. This process is executed continuously by one of the microcontroller internal timer. It is also responsible to switch on and off the solid state relay. On each predetermined time interval, which is equal to the sample time, the process first checks D2 for any changes in the configuration and then it requests a temperature reading to process 1.3, which is responsible for the temperature resistance reading. Once the temperature resistance is known a new switching time is calculated and executed.

1.5: This process is responsible for the control of the three fans and it is executed continuously by one of the microcontroller's internal timers. At predetermined time intervals, this process checks for any changes in the configuration stored in D2 and executes the changes if necessary.

1.6: This process is responsible for retrieving the data from the SHT11 and performs the necessary corrections to the retrieved data. This process is executed whenever it is requested.

1.7: This process receives any messages sent by the applications on the PC and transmits back any message when required. The main process continuously polls this process for any messages received from the applications on the PC.

1.8 This process is activated whenever an S0 pulse is received from the energy meter. Every time an S0 pulses, two counters are incremented.

Figure 6.9 shows the complete unit of the sensor node

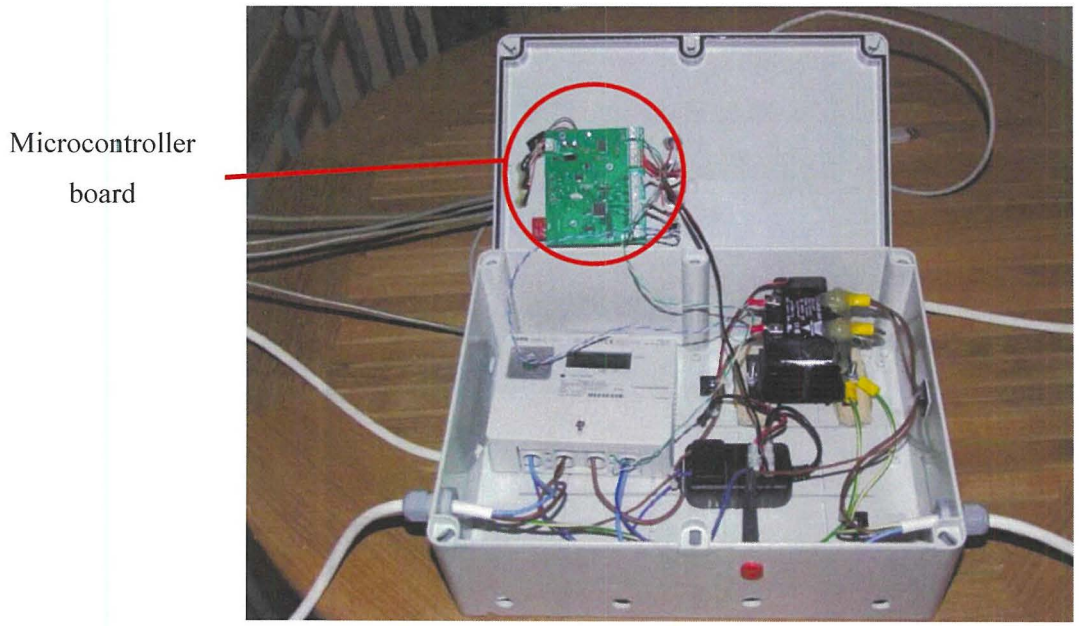

Figure 6.9 The complete sensor node

6.5.5 Master Node Hardware and Embedded Software

Figure 6.10 shows a block diagram of the master node. As expected, the master node is simpler than the sensor node. Even the embedded software is simpler. This section describes in further details the hardware and embedded software.

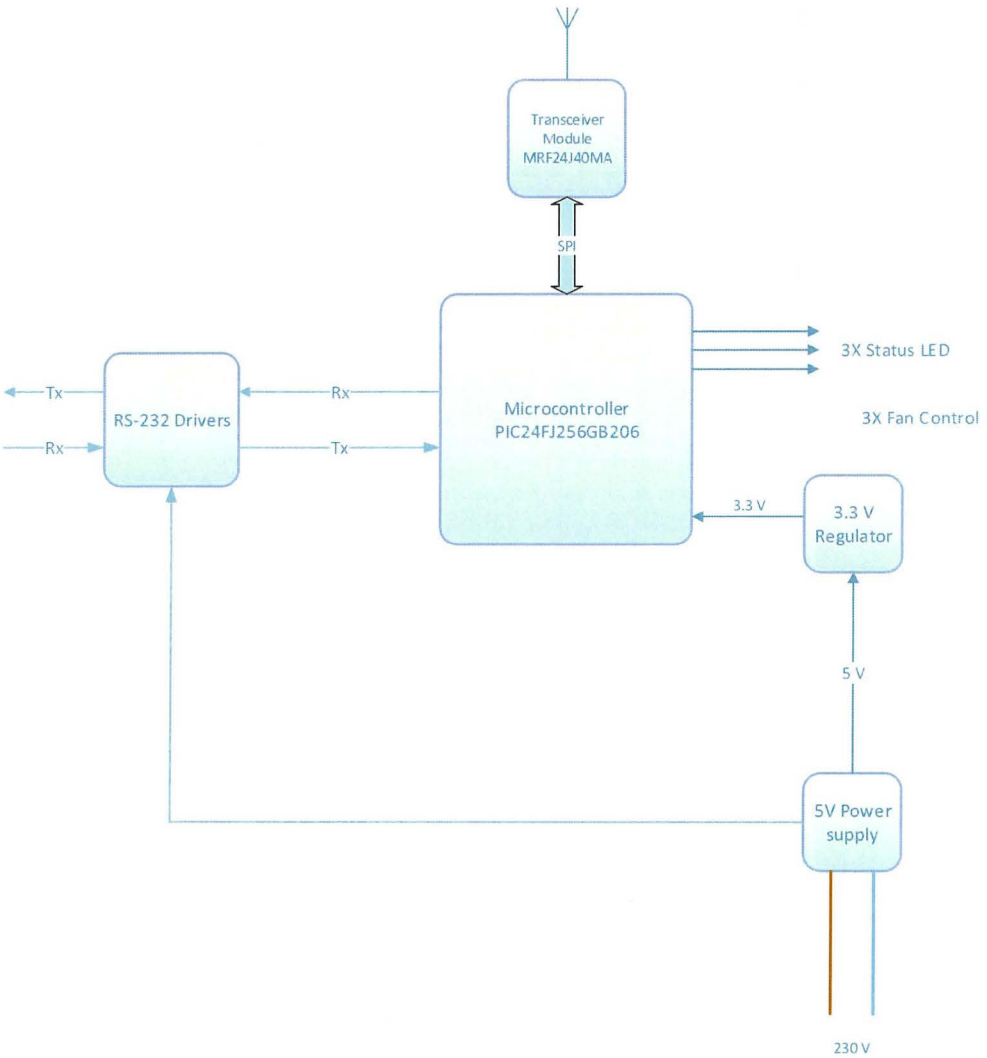

Figure 6.10 The block diagram of the master node

Similarly, as in the case of the sensor node, the master node is built around the microcontroller PIC24FJ256GB206 and the transceiver module MRF24J40MA. These two components were discussed in detail in section 6.5.1. Three status LEDs are also used for information purposes only although their meaning is different than that of a sensor node. The status LEDs are here used to indicate data flows. As already indicated in the system overview, the communication between the master

node and the PC is carried out over an RS-232 line. With the use of an RS232 connection, it is possible to place the master node a few meters away from the PC. This permits the user to place the master node in an ideal place for the optimal wireless communication. The interface between the master node and the RS-232 line is provided by the RS-232 block. The RS-232 interface is made from a single MAX232 IC and a few support capacitors. This IC requires 5V DC supply and thus a 5V regulator circuit was incorporated in the design. As explained in section 6.5.1, the transceiver module and the microcontroller operate from a 3.3V supply. As a consequence, a 3.3V regulator circuit was also added to the master node.

Similarly to the hardware, the embedded software is not complicated. As mentioned in the previous sections, the function of the master node is that of a bridge. Figure 6.11 shows a flow chart for the operation of the master node.

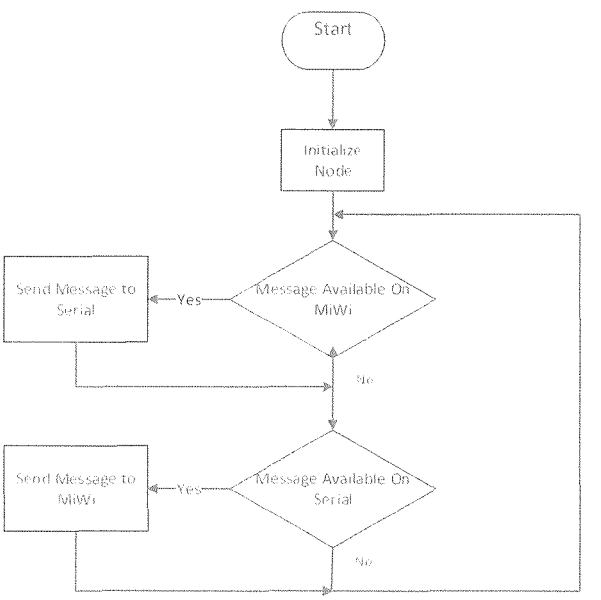

Figure 6.11 Flow Chart of software on a master node

6.6 Software

6.6.1 Introduction

In this section, the application software installed on the PC is discussed. The software is made from three applications namely, the calibration and configuration, the data logging and the reporting. Each individual application is discussed in detail in the next sections. The discussion focuses mainly on the features of the application and how they fit with the goals and priorities as listed in section 6.2.

6.6.2 Calibration and Configuration application

This application is intended to facilitate the calibration of the temperature sensors and the configuration of the sensor nodes, if needed, before they are dispatched on site. Before going in more detail, the temperature calibration process is explained first.

As already stated, each temperature sensor requires a third order polynomial fit to calibration. This means that five calibration points are needed. They must be equally spread along the desired temperature calibration range. These calibration points must be acquired by using a temperature calibration bath. Each calibration point is made from two values, one value which holds the actual temperature, while the other value holds the resistance of the PT1000 as read by the sensor node. Once the calibration points are known, a third order polynomial fit is performed and the coefficients are determined. It is also common practice to calibrate a number of sensors together.

The calibration and configuration application is intended to facilitate this process. Figure 6.12 shows the GUI for the calibration process. The user loads to the utility a CSV text file containing a list of temperature sensors to calibrate, along with their respective sensor node address. The blue box in figure 6.12 shows where this file is loaded. The CSV file should have the following format:

node address, list of sensors in binary

Example: EEEE,0001001

The previous example states that the calibration is performed on the Temperature sensor 1 and 4 of the sensor node whose address is EEEE. The least significant bit indicates sensor 1, while the most significant bit indicates sensor 8. Bit 1 indicates that the sensor is selected for calibration, while bit 0 indicates that the sensor is not selected for calibration.

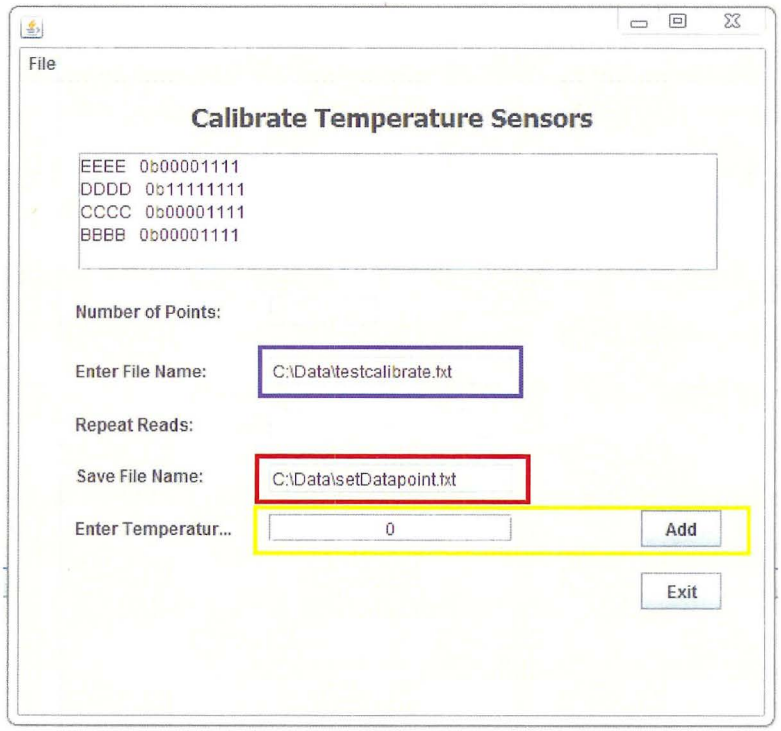

Figure 6.12 Application to calibrate the temperature sensor

This application writes the calibration point to a CSV text file whose path is given by the user. The red box in figure 6.12 indicates where the file name along with the path is entered. Each line contains a single calibration point and has the following format :

Node's address, PTx, where x is sensor number, Temperature, Sensor resistance

Example: CCCC,PT1,30,1047.2

The above example defines that, the calibration point belongs to temperature sensor 1 of the node with address CCCC and the calibration points are 30°C and 1047.2Ω.

The input text box and the add button, indicated by a yellow box in figure 6.12, are used by the user to generate the calibration data points. When the temperature of the hot bath reaches and stabilizes to the desired calibration temperature, the user enters this temperature and clicks the add button.
At this point, the application sends a temperature reading request to all nodes and sensors. A thread which is started in the background waits for the replies. When a message is received, the thread records the resistance value in the format explained above. This procedure is repeated for every desired calibration temperature under consideration. The end product of this process is a text file in CSV format containing all the calibration points. A third party application like MathLab should be used to perform a third order polynomial fit on the calibration points. This should yield 4 coefficients per temperature sensor.

The calibration and configuration application provides a utility which allows the user to load permanently the calibration data to the sensor node. Figure 6.13 shows the GUI window of this utility. The calibration data is loaded into the utility from a CSV text file which must have the following format:

Node address, sensor number, coefficient A, coefficient B, coefficient C, coefficient D

Example: BBBB,1,2.7093e-08,-8.5972e-05,0.3551,-295.23

This example states that sensor 1 of the node whose address is BBBB has the following calibration coefficients A = 2.7093e-08, B = -8.5972e-05, C = 0.3551 and D = -295.23.

This utility provides the users the facility of examining the calibration data in a more friendly way. The user can select a node address, and can load the associated calibration data into an organized table, as shown in figure 6.13.

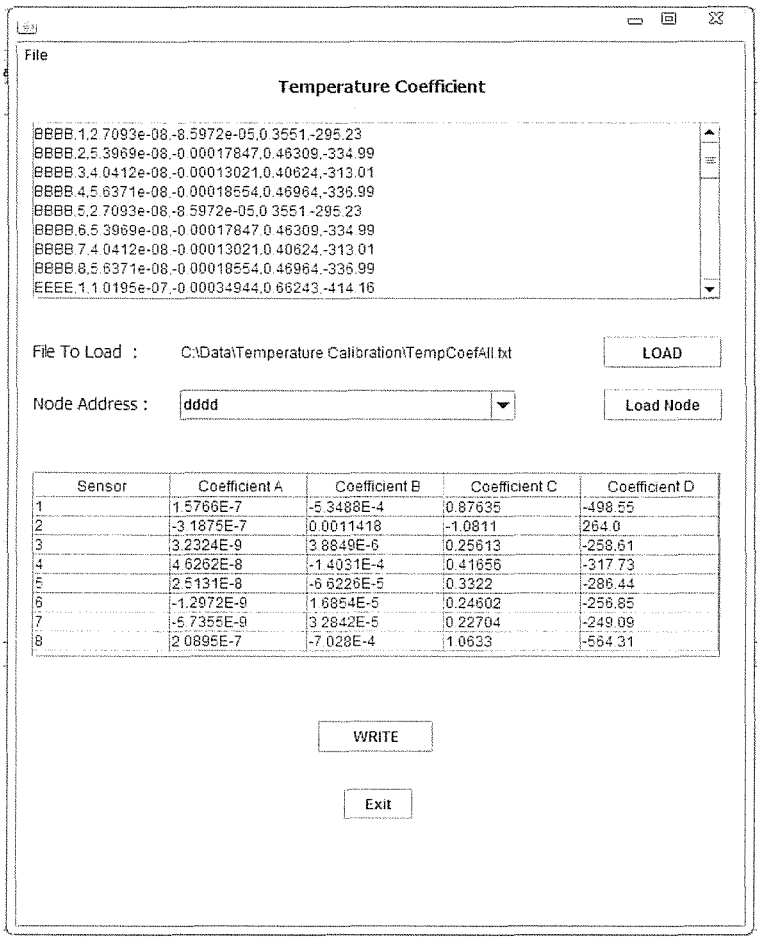

Figure 6.13 Application to write the calibration data

As indicated previously, the sensor nodes can be configured with some default configurations which are loaded automatically when the node is turned on. The calibration and configuration application provides a utility which allows the user to change these parameters. This utility is expected to be used more frequently than the previous ones, so an effort was made to make the utility more user-friendly. This utility requires that the temperature calibration data is already present in the sensor node before the default configuration is updating. This is important because the utility uses the calibration data to calculate the exact sensor resistance for the given temperature set point. The resistance value is used by the PI algorithm to control the temperature.

This utility is built on a dynamic list of records. Each record holds the default configuration of a single sensor node. The list of the available configuration is given in detail in D1 of section 6.5.4.

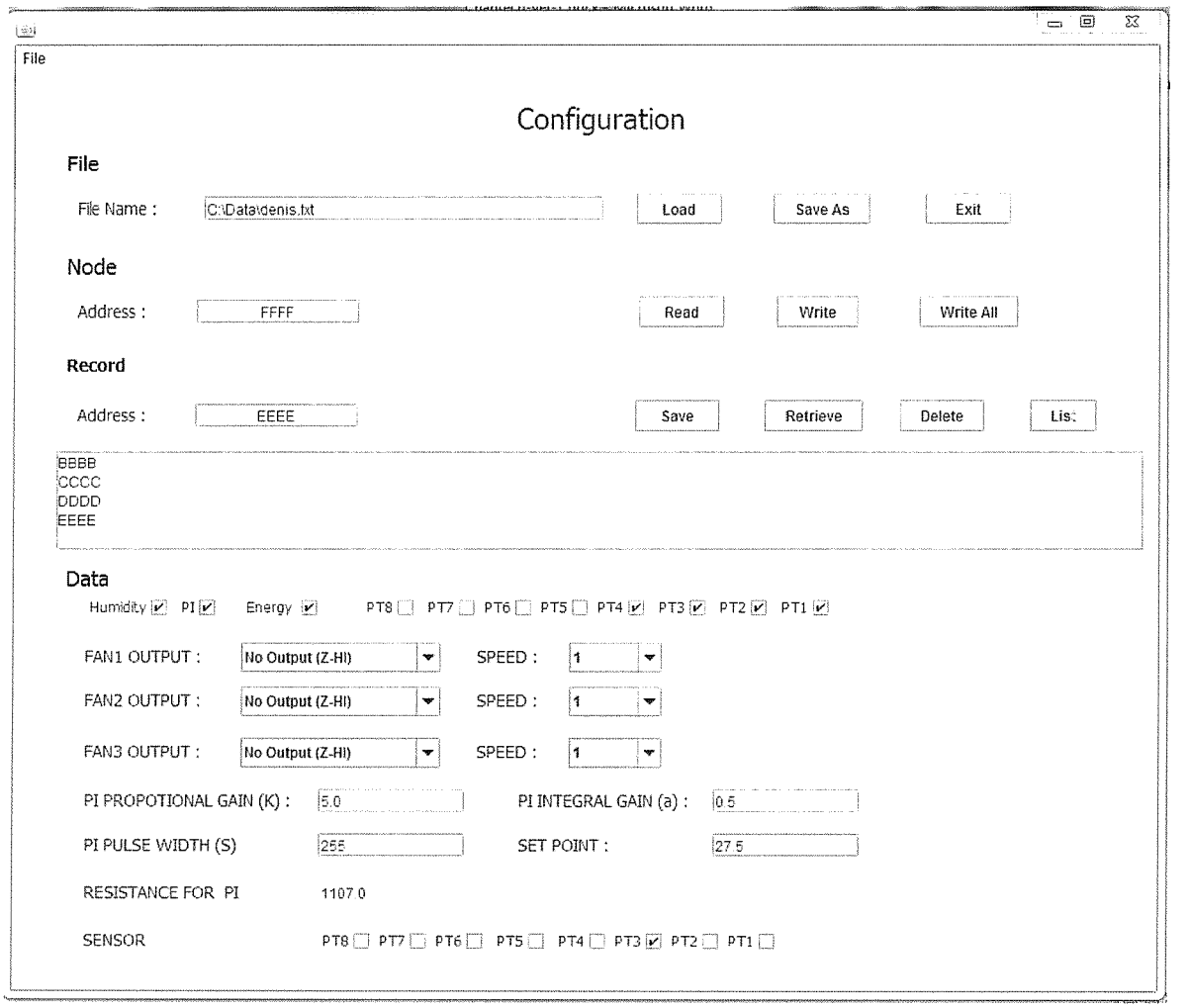

Figure 6.14 Utility to configure sensor nodes

Figure 6.14 shows the GUI window of this utility. As can be seen, the window is divided into four groups, namely: File, Node, Record and Data. Each group is discussed further in this section.

File: This part is used by the user to load records to the list from a file and to save the records in the list to a file. This file, similar to the previous utilities, is a text file in CSV format. Each line holds a single record and has the following format:

node address, $byte_1$, $byte_2$, $byte_3$,.....,$byte_{13}$, $byte_{14}$, $byte_{15}$

Each record is made from a node address and 15 bytes saved as text in hex format. The meaning of each byte is given in appendix A.

Example : BBBB,07,0F,00,00,00,00,32,00,32,1E,04,04,FB,2B,3E

Node: This part is used to write the default configurations from the list to the sensor nodes. One can just write a default configuration to a single sensor node or write the entire default configuration list to the respective sensor nodes. One can also read a configuration from a sensor node and load it into the list, then one can manipulate the configuration or save it to a file. It should be noted that bytes 14 and 15 of the configuration data holds a resistance value which is equivalent to the temperature set point. This value is automatically calculated before it is written to a sensor node.

Record: This part is used to manipulate the records in the list and it is closely tied with the data section in the same GUI window. This part permits the user to save a record to the list, to delete a record from the list and finally it allow the user to display and edit a record from the list. The record is displayed in the Data section of the GUI window.

Data: This section in the GUI window is used to view, edit and finally create a new record. As can be seen in figure 6.14, most of the configurations are carried out by dropdown lists or by ticking the check boxes. Where the text fields are used, checks are carried out. All this makes the utility less prone to human errors. If the Retrieve button in the Record section is clicked, the record whose address is listed in the address field is loaded into the Data section. Then, the user can edit its configuration and save it back by clicking the Save button in the Record section. Alternatively, the user can save the record into a new record by changing the address in the address text field and then clicks the Save button.

6.6.3 Data Logging software

The data logging software is designed to interact with the sensor nodes, controls them and uploads data from them. It is in this software that the temporal and conditional actions are required. It is also in this software where the automation is likely to take place. As a consequence, priority was given to these requirements. The usage of this software is expected to be more frequent than the other utilities, hence the software should be user friendly as much as possible.

It is very difficult to forecast what automation will be needed in the future or which software will have this utility to interact with. The solution for this is to make the application an extension of Java. By doing so, future developers can build applications with Java which uses this application directly in their programs. This has many advantages some of which are listed below:

1. Conditional action, which is one of the requirements, is easily implemented by using the Java control mechanism.
2. Temporal action, which is also one of the requirements, can be easily implemented by using the built in libraries and access the system time.
3. All libraries which are used in Java can be used in conjunction with this application to attain the desired result. An example of this, is the jfreechart library which is used here to draw the line graph.
4. Other applications which are coded in Java can be easily combined with this application to create more enhanced applications.

This list can be longer but it comes out with a cost. The design of the application should be well thought and fragmented into a number of reusable blocks. Even the interface of these blocks should be carefully designed. But before continuing with the application design it is better to discuss the functionality and other features of the application first.

When the Data Logging application is started, it checks which sensor nodes are reachable and for each reachable sensor node the application downloads the sensor

node's calibration data along with the default configuration. With this data, a node object is created for each reachable sensor node. For the sake of clarity, a class named node is created with all the necessary features and functions. A node object refers to a variable of the type node class. Each node object is uniquely associated with one sensor node but all the node objects save data to one file. Each node object communicates directly with its associated sensor node and controls it. It also polls the sensor node to acquire the data and performs the necessary calculations to derive the temperature values. Even the corrections to the temperature using polynomial coefficient takes place in this object. Any data acquired by the node object is saved to a text file in CSV format. The details of the CSV are found in appendix B. The node object provides a GUI interface which allows the user to interact with the sensor node and to display the last retrieved data. Figure 6.15 shows this GUI.

As can be seen, the GUI interface of the node object is divided into two sections namely Node and Configuration. The node section displays the last acquired data, while the configuration section is used to interact with the sensor node. The user can upload the configuration from the sensor node, manipulates it and downloads it back to the sensor node. It should be noted that most of the configuration is performed using a dropdown list and tick boxes. Where the user has to enter data in the text fields certain checks are carried out. At any time, the user can check the communication with the sensor node by clicking the "**A Life**" button. Moreover, the user can identify the sensor node associated with the given node object by clicking the "**Identified**" button. This causes the sensor node to start flashing two LEDs.

Figure 6.15 GUI interface for a Node object

The object node holds in a queue a certain amount of the most recent data acquired. The size of the queue is configurable and the user has the option to display in line graph the content of this queue at any time. The user can achieve this operation by clicking the "**Graph**" button. Figure 6.6 shows one such graph.

Similarly to the node class, another class named "**weatherJFrame**" was developed. This time only one object of the type "weatherJFrame" is created because there is only one weather station in the system. Similarly, the "weatherJFrame" class contains all the necessary features and functions to acquire data from the weather station and display it. This class provides also a GUI interface which allows the user to interact with the weather station and to display the last data acquired. Figure 6.16 shows such GUI interface.

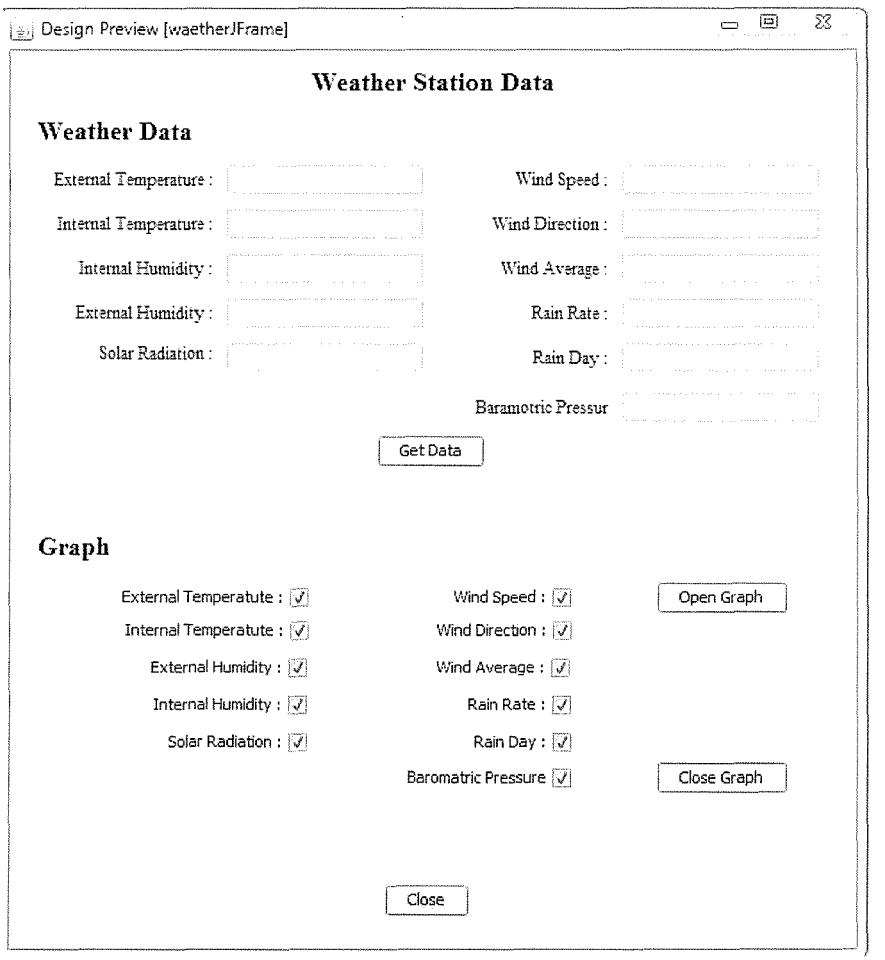

Figure 6.16 GUI interface for a "weatherJFrame" object

As can be seen, the GUI interface is divided into two parts, namely, the Weather Data and the Graph. As expected in the Weather Data section, the most recent acquired is displayed. At any time the user can click the **Get Data** button and acquire the most recent data from the weather station.

The "weatherJFrame" class has a queue which holds a number of the most recent acquired data. The size of this queue is determined during the creation of the object. As expected, the "**Graph**" section is used to display the data in this queue in line graph format. The user can determine which data to display in the line graph by ticking the corresponding box and by clicking the "**Open Graph**" button.

For the reasons previously explained, the design of this application, gave priority to the reusability of the main components used. Hence, the main components were

designed to make one particular task only. Furthermore, the interfaces to these components were designed to facilitate the interaction with these components. It is very difficult to appreciate the reusability aspect of this application with just words As a consequence a simple example is given. In this example a reachable sensor node. with address AAAA is assumed.

```
1.  byte [] arrayAAAA = util.readRom(0xAAAA, 7000);
2.  commThread master = new commThread();
    master.init();
    master.start();
3.  WriteFileThread dataBase = new WriteFileThread();
    dataBase.init("C:\\Path\\ToAfile.txt", 1);
    dataBase.start();
4.  Node nodeAAAA = new
    Node(master.inputQueue,dataBase.inputQueue,
                    100,0xAAAA,arrayAAAA)

5.  while(true){
        nodeAAAA.readDataCommand(); // execute every 1 minute

        packet tmp = master.outputQueue.poll(); //execute every 10s
        if(tmp != null){
            nodeAAAA.putPacket(tmp);
        }
    }
```

The above 12 lines of codes are enough to create an application which retrieves data from a single sensor node and saves it to a text file in CSV format. It should be noted that some Java statements are omitted for the sake of simplicity. This part of the program is explained further later in this section. While doing so an explanation of some classes is also given.

1: The first line of the codes retrieves the default configuration along with the temperature calibration data from the sensor node and saves it into an array of byte. This statement should be repeated for every sensor node in the system. The "**util**" class is a static class which provides a set of utilities which include "**util.readRom()**" and "**util.writeRom()**" which read and write configuration and calibration data respectively.

2: The next three lines of the codes start a thread in the background which provides a communication channel to the master node. The class "**commThread**" has two concurrent queues, one to dispatch messages and the other one to receive messages. Since the queues are concurrent, the multi node objects can access this thread without a problem of interfering with one another. Only one object of this class type is possible in an application.

3: The next three lines of the codes start also a thread in the background. The class "**writeFileThread**" has a single concurrent queue on which several node objects place string messages. In turn, this class opens a text file for writing and saves the strings on the queue one to each line. It is up to the node objects to form the string. Since the queue is concurrent, several node objects can access the "writeFileThread" object without causing interference. It is possible to have more than one object of the type "writeFileThread" in an application but it makes more sense to have only one.

4: This line of code creates a single node object using class "**node**". At this point, a window similar to figure 6.16 pops up and the system is ready for use. The creation of a node object requires a number of arguments which deserve some explanation. The first argument must contain a concurrent queue. This is used to place the messages which are intended for the master node. The second argument is also a concurrent queue but this is intended for strings which are saved to a text file. The third argument states that the number of the latest data records to be saved in the object. These records are intended to be displayed in a line graph. The fourth

argument is the node address while the fifth argument is a byte array containing the default configurations and the temperature calibration data.

5: This is the control part. Here some of the Java statements deserve some explanation. The *nodeAAAA.readDataCommand();* statement instructs the object node to poll for data. The *packet tmp = master.outputQueue.poll();* statement checks the head of the queue for any messages received. The messages are objects of the type **packet**. The *nodeAAAA.putPacket(tmp);* statement passes a message to a node object of the type **packet**. It is important to mention that the *tmp.sourceAdd* holds the source address. Conditional actions or temporal actions can also be implemented in this control part. Example of a conditional action is:

```
double x = nodeAAAA.getT1()
if( x <= 10){
        System.out.println("it is too cold");
}
```

In the example above, if the temperature sensor 1 is equal or smaller than 10°C a message is displayed.

The control part given in 5 is very basic and simple. A much more elaborated control is possible here, but this is left for the imagination of the application developers. In the case of the weather station, things are simpler. The "**weatherJFrame**" class requires only the "writeFileThread" object and a buffer size for the latest data. Similarly to the node class, the "weatherJFrame class" provides methods to access data from the "weatherJFrame" object. More than one "weatherJframe" objects is possible, provided that the comports do not interfere with each other.

Figure 6.17 shows the main window of the application developed for the proposed system. The application starts by requesting the user to provide: the filename where the data will be saved, the set point temperature and the time when the temperature control is turned on and off. Once the start button is clicked, the application scans the

predefined lists of the sensor nodes. For all those reachable sensor nodes, the application creates a node object. Furthermore, the application creates a "weatherJFrame" object. Once the initialization process is completed the application starts polling the sensor nodes and the weather station for data every 2.5 minutes.

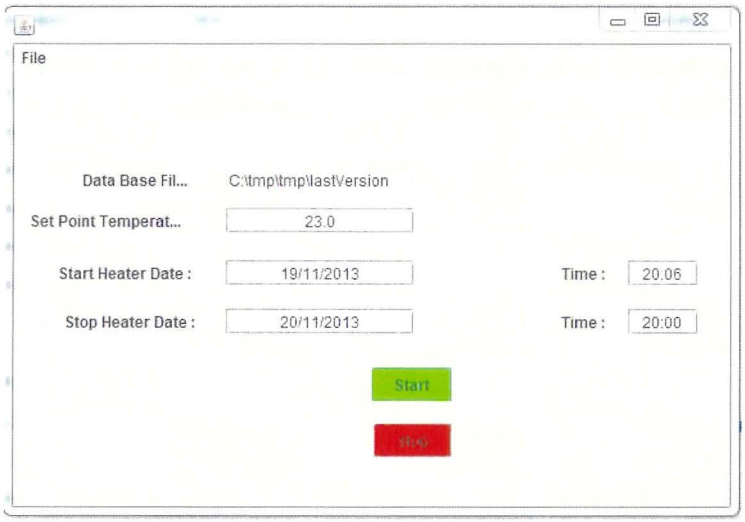

Figure 6.17 GUI interface for the data logger

6.5.4 Reporting Software

The intention of the reporting software is to facilitate the data exportation and to help the user to analyse the data acquired. The Reporting software is made up of three utilities, namely the Database report, the Data file report and the Graphs. The database is intended to export the data to tables, the file is intended to export the data to the CSV files, while the utility graph is intended to analyse the data in graph line format.

Nowadays, databases are very powerful tools which are widely used in the information systems. Furthermore, a number of databases are supplied for free. A common method to export data into a database is to use a CSV file. For this reason, a tool which exports the data into a CSV file suitable for databases was developed. Figure 6.18 shows the main window of this utility. The utility requests the user to supply the path for the input and output data files. The user is also requested to select which type of data to export. One can select the weather station data, the sensor

nodes data, the transmitted message and the received message. The last two types of data are intended for the system diagnoses and are useful only for the developers or the installers.

Sometimes, the date format may cause problems. As a consequence, the utility provides the user with the facility of changing the date format. Another function which may be useful is the facility to add a unique positive integer at the start of each line. This can be used as the primary key.

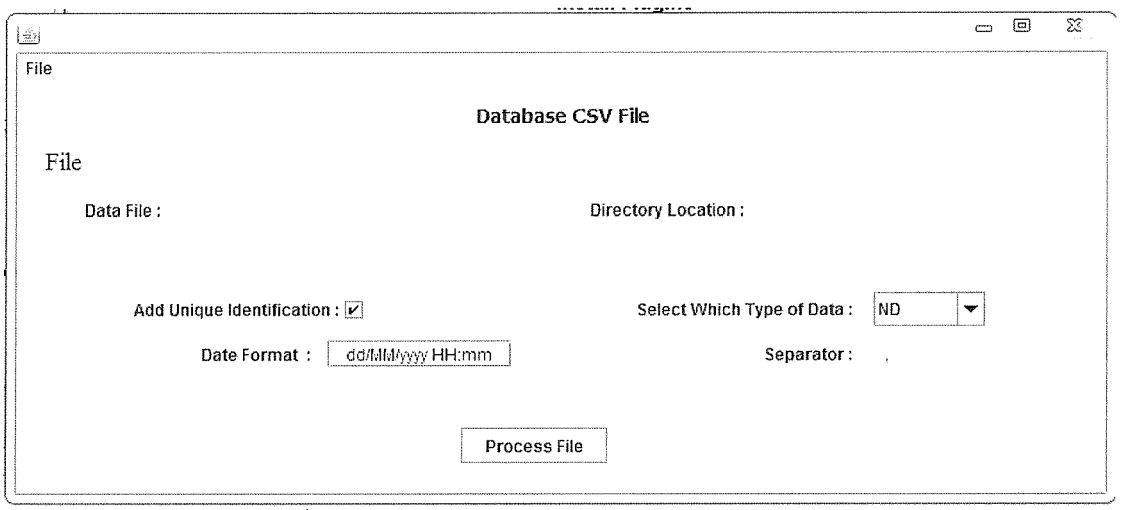

Figure 6.18 GUI interface for a Database report

The Data file report is intended to export the data of a particular sensor to a CSV file format.

Figure 6.19 shows the main GUI window of the Data File report utility.

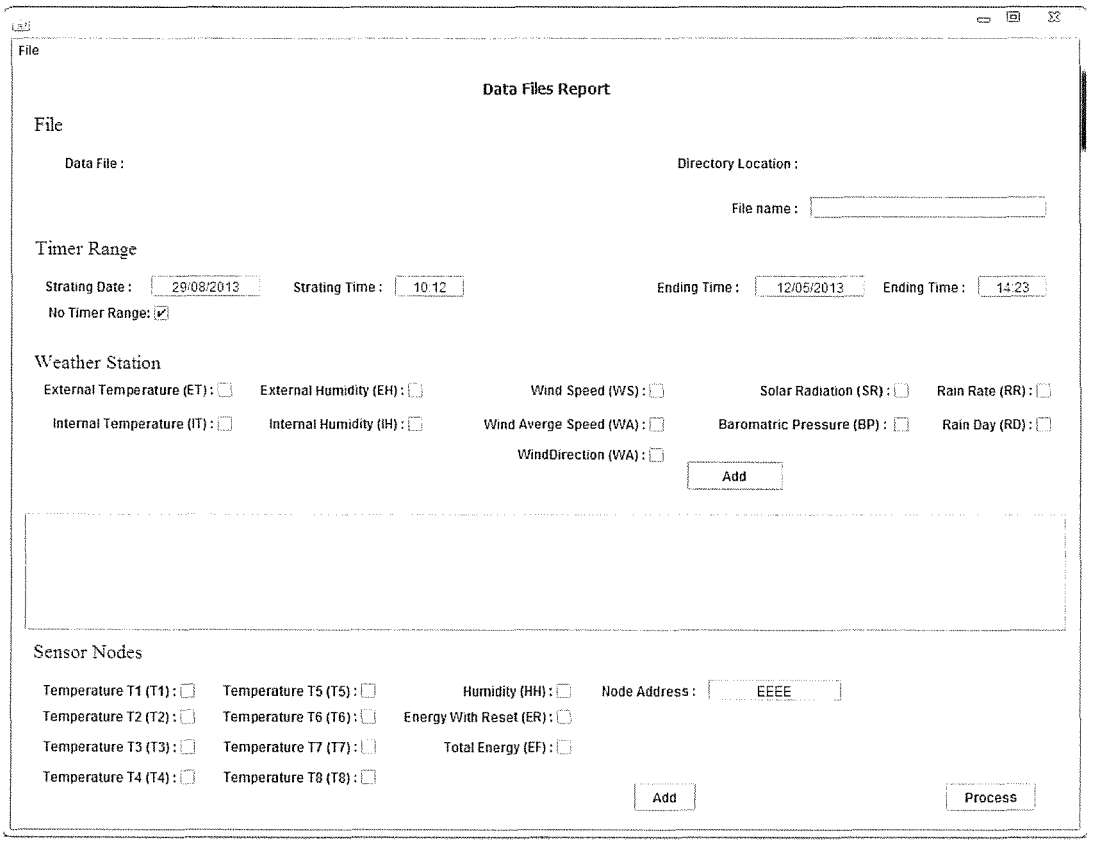

Figure 6.19 GUI interface for a Data File report

The user is requested to supply the path along with the file name of the source file and the output file. The user can specify the entire range or partial range by supplying the start time and the end time. At this point, the user can select the required sensors from the relevant sensor nodes or else from the weather station. The selection of multiple sensors is possible. In such case, multiple files are created. The file name format is made from the output file name given previously by the user, from the sensor node address or weather station and from the sensor. This is done for easy identification.

The Graphs report is intended only for data analysis. The user can display the data into a line graph format. Figure 6.20 shows the main GUI window for the Graph report utility. The user is requested to enter the source data file along with its path. Furthermore, the user is also asked to specify the pdf file name, where the displayed graph is saved. But the latter is optional.

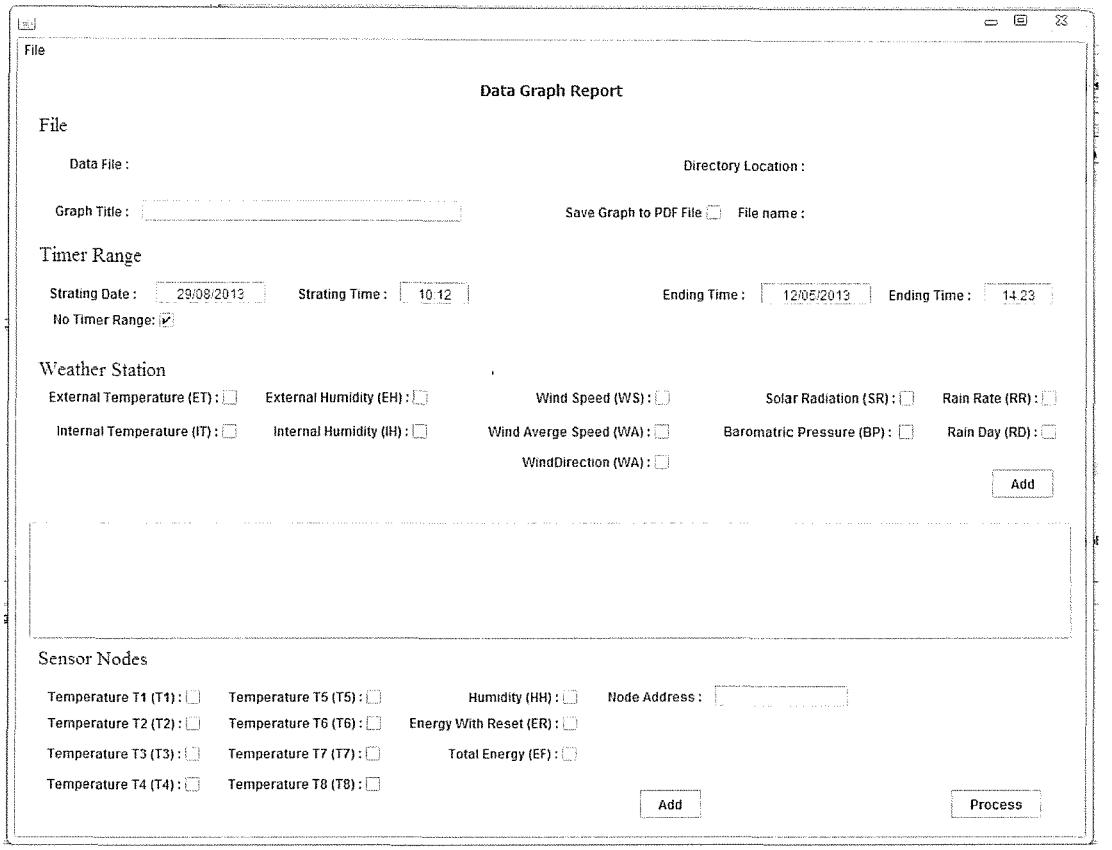

Figure 6.20 GUI interface for a Graphs utility

The user can display the whole range of the data or partial range of the data by supplying the start time and finish time.

At this point, the user can select any combination of sensors as needed by specifying the address of the sensor node and the sensor. Only the first ten are displayed. This is done to avoid too much cluttering in the line graphs. Figure 6.21 shows the output of a line graph in pdf format produced by this utility. In this case the following sensors were selected:

1. Weather station solar radiation
2. Weather Station External Temperature
3. Sensor node address 0xCCCC and Temperature sensor 1
4. Sensor node address 0xCCCC and Relative Humidity
5. Sensor node address 0xCCCC and Energy with Reset

where the Energy with Reset means the energy used by the heater between two successive readings.

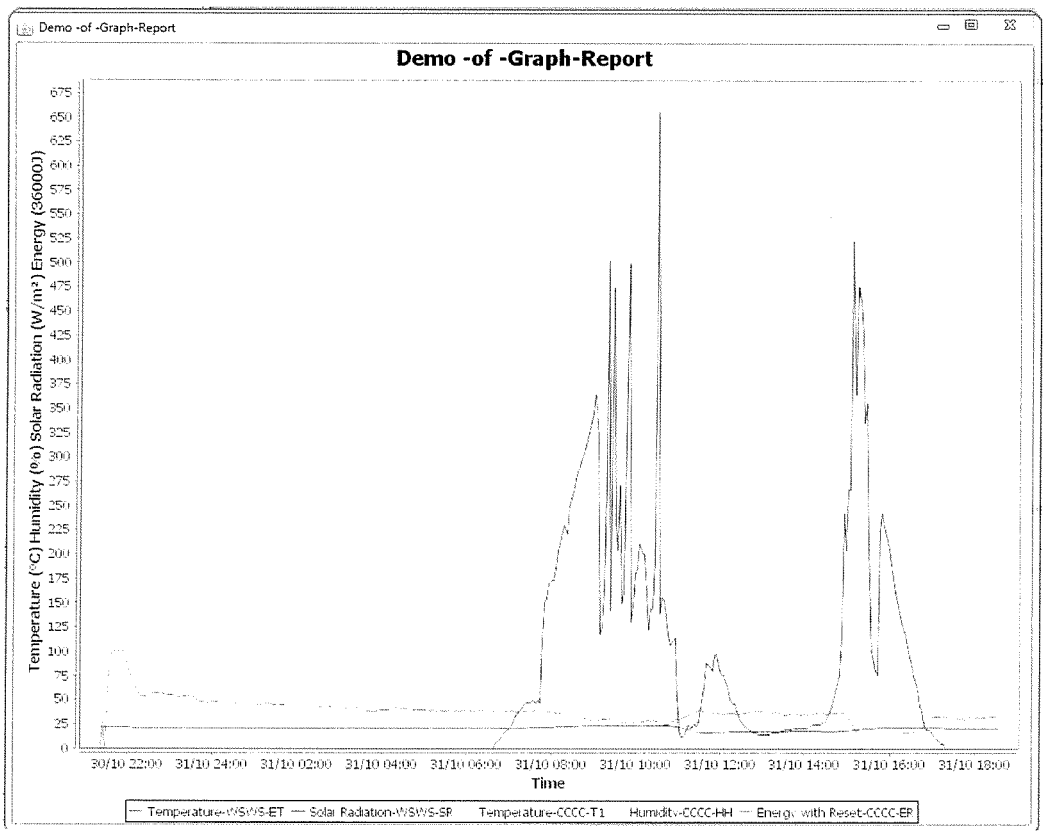

Figure 6.21 A line graph displayed by the Graphs Utility

6.7 Discussion

This chapter started by defining the system goals and their priorities along with the requirements. Since the proposed system is described in detail, now it is possible to discuss how well the proposed system met the original goal. Each goal in section 6.2 is discussed in this section.

With regards to the first goal, the system provides all that is necessary to implement the proposed protocols. It also provides the additional sensors which may be needed to implement the other established protocol. This satisfies the sixth goal. All the utilities provide the GUI interface to the user and include some data input checks. Moreover, the utilities are also provided to export the data in different forms. This satisfies the eighth goal. The system software was designed with reusability in mind.

This does not only satisfy the seventh goal but indirectly satisfies the third and the fifth goals as explained in section 6.3. The reusability design facilitates automation and future developments. Communications among the nodes are performed through a wireless channel. Furthermore, the wireless technology used supports thousands of nodes. This satisfies the fourth goal as well as the second one, since the user has to plug in the node to a power outlet and place the sensors to the right place only. Furthermore, the developed utilities reduce time to process the data. For example, it only takes few seconds to produce the line graph of figure 6.21. Producing the same line graph using raw data from three different systems usually takes about 30 minutes. The designed hardware and software offer a very powerful setup to reach the achieved and future requirement for the testing of various protocols to determine the building efficiency.

7 Energy Performance protocols

7.1 Introduction

This chapter addresses in detail the three proposed energy performance protocols which are based on the three potential methods discussed in chapter 5. Each energy performance protocol was separately tested against a benchmark data which was obtained in an experiment. The details of this experiment are given later in this section. This chapter gives also the details of how the required energy is calculated for the given Effective U-Value.

7.2 Temperature sensor inside a wall

Methods two, three, and four were required to monitor the temperature inside one of the walls. This was performed by placing a temperature sensor about 2 cm inside one of the walls. With this sensor one can determine when the temperature inside the wall is approaching the saturation temperature. Instead of placing this sensor inside the wall, it is possible to place the same sensor touching the wall. The readings are different but the trends are the same. Figure 7.1 shows the data from an experiment which was carried out to proof this point. The temperature inside the wall is shown by the light pink curve and is denoted by B while the temperature touching the wall is shown by the green curve and denoted by A. In the experiment the internal temperature was held constant to 32 ^{o}C.

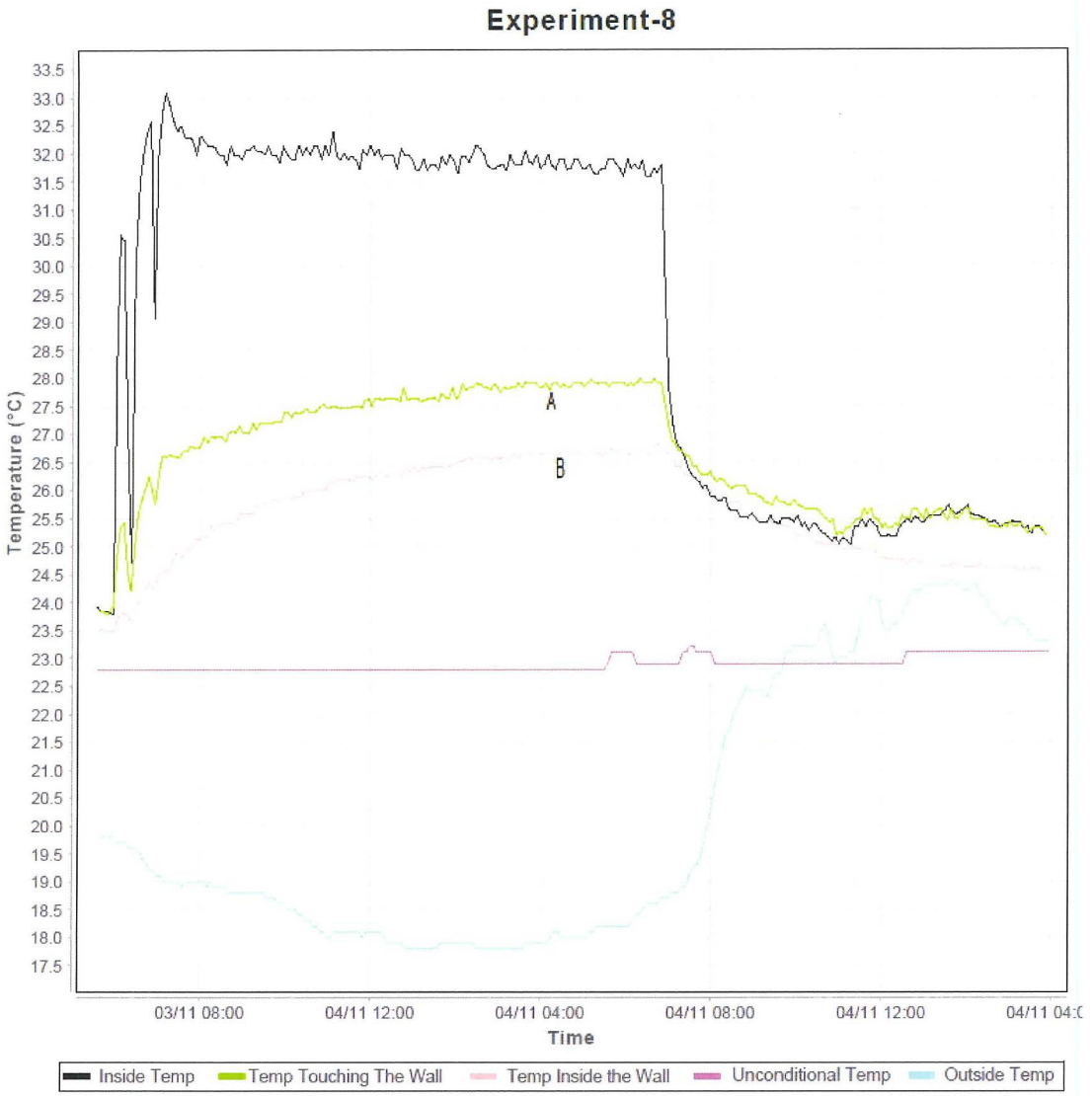

Figure 7.1 The temperatures from experiment 8

7.3 Energy Performance Protocol one

This energy performance protocol is based on method two which is described in section 5.5. The room must have all its doors and windows closed. It should be unoccupied and free from any possible internal heat gains. Any opening for ventilation purposes must be left open. These openings will ensure that the measured Effective U-Value incorporates the ventilation losses.

For this energy performance protocol, five temperature sensors were needed. The following list gives the location where the temperature sensors were placed:

1. Temperature sensor 1 was placed at about 20 cm below the ceiling.
2. Temperature sensor 2 was placed at about 20 cm above the floor.
3. Temperature sensor 3 was placed equidistant from temperature sensor 1 and temperature sensor 2
4. A temperature sensor 4 was placed touching the wall, (ideally it should be placed in the same height of sensor 3).
5. A temperature sensor 5 was placed in the outside environment. It was properly protected with a solar radiation shield.

Sensor 4, was placed touching a wall which had the highest thermal mass. For example, if a room has walls built from a 23 cm hollow concrete bricks and from 15 cm hollow concrete bricks, then the temperature sensor should be placed touching a wall built from 23 cm hollow concrete bricks. Furthermore, the boundary wall must be avoided where possible. The temperatures from the sensors were recorded every 10 minute intervals. The temperature monitoring was started about two hours before heating was switched on.

Method two stipulates that the room is heated up to a pre-define temperature. The set point temperature was about 7°C above the average external temperature. The time window for heating was started just before sunset and lasted till sunrise of the next day. The time window for heating was long enough so that it allowed the temperature inside the building components to saturate. This was achieved by monitoring the temperature sensor touching the wall. Figure 7.2 shows a typical time window for heating for energy performance protocol one.

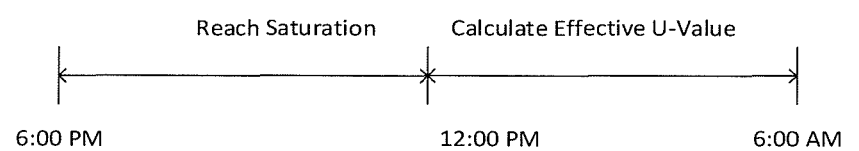

Figure 7.2 A typical time window for heating for the energy performance protocol one.

A fan heater was used for heating and its energy supplied was measured and recorded at intervals of at least 10 minutes each.

The calculation of the effective U-Value is exactly the same as describe in section 5.5 of the method two. Therefore they were not repeated here. The only slight difference is that the average internal temperature is calculated using temperature sensors 1, 2 and 3. This gave more accurate temperature inside the room.

7.4 Energy Performance Protocol two

Energy performance protocol two is based on method three which details are found in section 5.6. There were no changes in the room conditions, measuring requirements or heating requirements from the previous energy performance protocol. Therefore, they are not repeated here and one can refer to section 7.3 for the complete details. The only difference is the time window for heating and the calculation method of the Effective U-Value.

7.4.1 Time window for Heating

The time window for heat should ideally start just before sunset and it should continue for the next 36 hours. Figure 7.3 shows a typical heating window for the energy performance protocol two. The first 12 hours of heating are used to saturate the thermal mass of the room. The remaining 24 hours are used to determine the Effective U-Value. The time period to be used for the calculation of the Effective U-Value should start just before sunrise. With this approach, the effect of the daily solar gain is captured in the Effective U-Value.

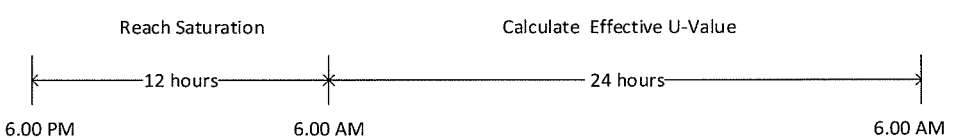

Figure 7.3 A typical time window for heating for the energy performance protocol two

The calculation details of how the Effective U-Value was measured is found in section 5.6 with the difference that the internal temperature was calculated on the data from temperature sensors 1, 2 and 3. It should be noted, that the 12 hours allocated for the temperature to stabilize in the thermal mass are likely to be more than enough. Therefore, one can reduce this period and save energy. This is achieved by monitoring the sensor touching the wall.

The Effective U-Value is expected to contain some elements of the solar gain in the building. If the solar gain in the building in question is relatively high, then one has to consider the solar radiation during the measurements of the effective U-Value. If the solar radiation is normal, no action is required, but if it is too low or too high then an action is required. An easy solution for this problem is to repeat the measurements, if the solar radiation levels are extreme. Another solution to this problem is to multiply the calculated Effective U-Value to a factor. The latter solution was not investigated and therefore is left for future work.

7.5 Energy Performance Protocol three

This energy performance protocol is the only protocol in this work which specifically takes into account the solar radiation. In essence, this strategy is similar to the energy performance protocol two, but the calculation of the Effective U-Value and the calculation of the energy requirements are adjusted for the solar gain. This protocol is based on method four which measures the effective U-Value, the details of which are described in section 5.7.

All the measuring requirements and conditions of energy protocol one were needed here. Therefore, they were not repeated and one can refer to section 7.3 for more details. In addition to the temperature sensors, a pyranometer sensor was placed outside the building. Furthermore, the measurements of the internal temperatures, the external temperature and the solar irradiance were monitored at least for five days before the time window for heating is started. There were no changes in the heating

requirements or in the time window for heating. The complete details are found in section 7.5.1.

7.5.1 Time window for heating.

Figure 7.5 shows a typical time window for heating for energy performance protocol three.

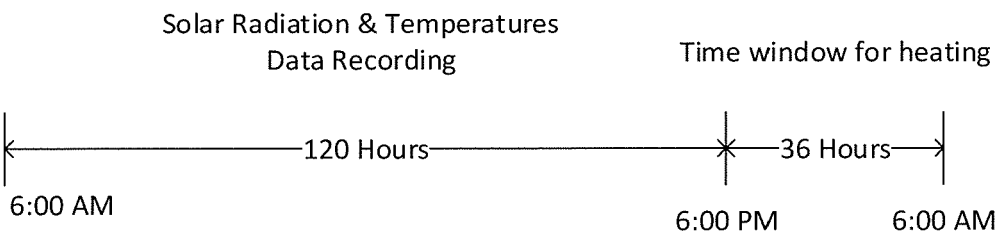

Figure 7.4 A typical time window for heating for the energy performance protocol three

The temperature and solar irradiance data recording was done for a number of complete days starting just before sunrise. Similar to the previous protocol, the first 12 hours were used to saturate the thermal mass of the room, while the remaining 24 hours were used to determine the Effective U-Value. The calculation of the Effective U-Value is the most complex one out of the three energy performance protocols considered. The procedure will give two values, the effective U-Value and the $K_{avg.}$ which is a relation between the accumulative solar irradiance and the increase in the internal temperature.

7.6 Multi-roomed building

A scenario of a single roomed building was always assumed up till now. As already mentioned, all the three energy performance protocols discussed here are built on either method two or three or four. As explained in chapter 5, these methods permit concurrent measurements of adjacent rooms. This can be done if the following rules are observed:

1. The start and the end time of the heating window should be common to all rooms.
2. The selected internal temperature set point should be equal to all rooms.

If the above rules are observed there will be no heat transmission between the adjacent rooms. This scenario is depicted in figure 7.7. Since the set point temperature in both rooms is the same, then the temperature difference between the two rooms is expected to be minimal. In steady-state conditions, the heat transmission between the two rooms is proportional to the temperature difference, therefore, the heat transmission between the two rooms is also expected to be minimal.

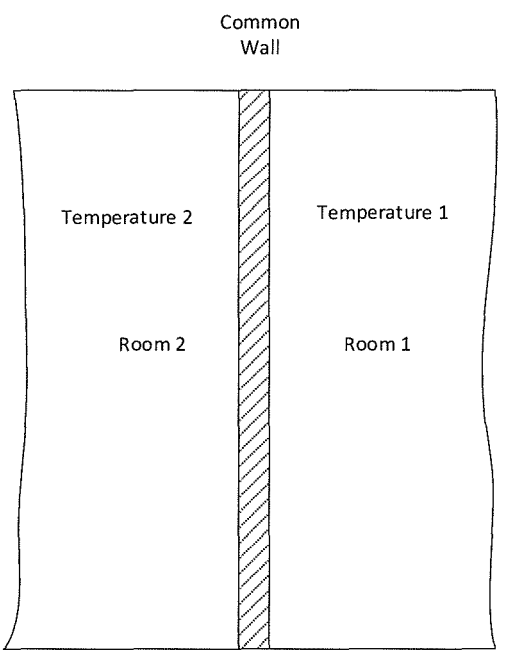

Figure 7.5 Two adjacent rooms

In a situation where the construction of the wall is uniform and made from homogeneous material, both heat sources in the rooms contribute equally to heat energy stored into the thermal mass of the wall.

7.7 Test Methodology – Effective U-Value

The method chosen to validate and to compare the protocol was the Empirical validation. In empirical validation, the protocol output is compared with the data from real building energy usage. Unfortunately, this data was not available. Therefore, it was necessary to generate the real data first by means of an experiment. The experiment was carried out for 21 days of heating. It was started at 23:00 of the 9th October 2012 and stopped at 00:27 of th 31st October 2012. In this experiment, the internal temperature was kept constant to 32 ^{o}C. The external temperature, the internal temperature, the solar irradiance and the electrical energy supplied to the fan heaters were all monitored and recorded. Figure 7.6 shows some of the data attained from this experiment in line graph format.

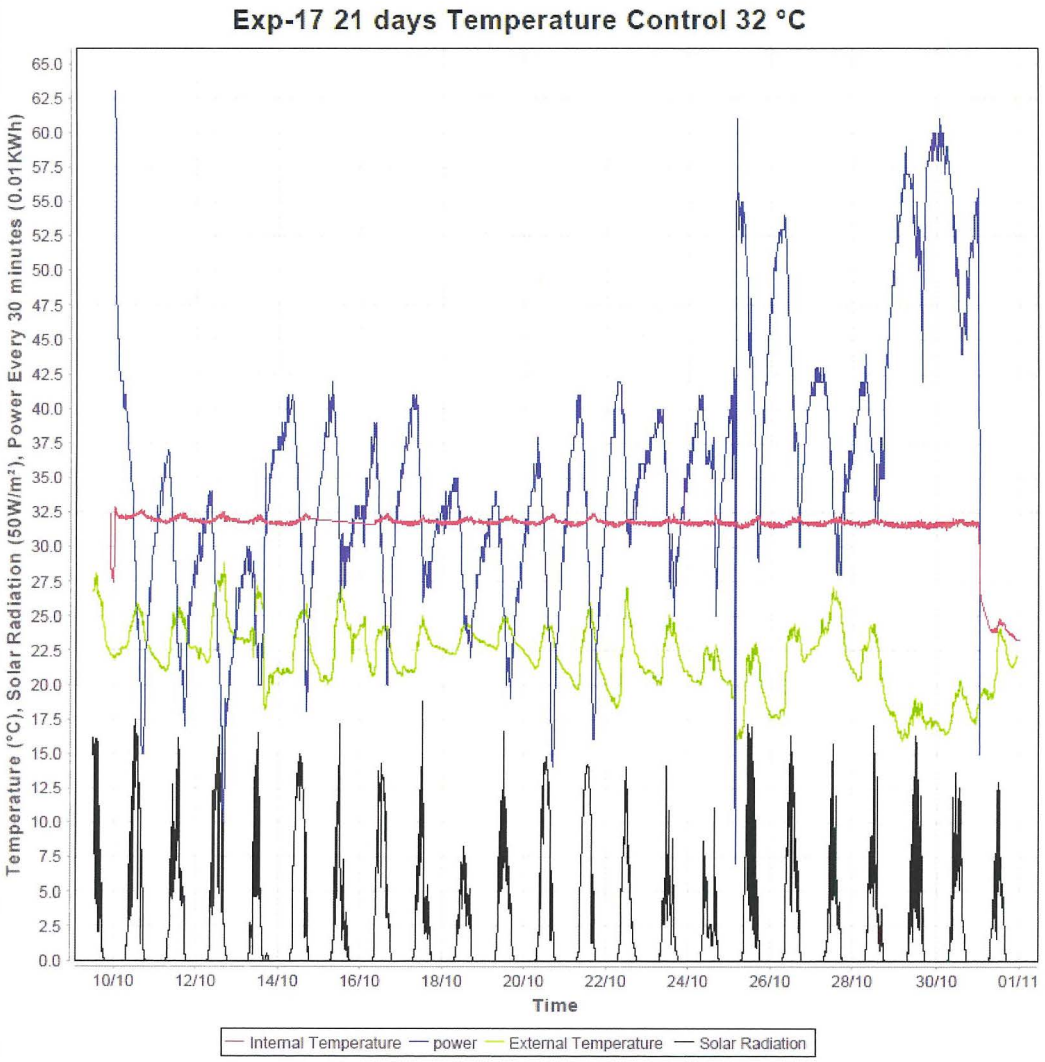

Figure 7.6 The Temperatures, power and solar irradiance for experiment number 9

The red and green curves represent the internal and the external temperature respectively. The blue curve represents the power supplied to the heater, while the black curve represents the external solar irradiance.

The data of the first day had to be eliminated because during the first day a considerable amount of energy was consumed by the thermal storage of the test room. Therefore, the electrical energy supplied does not reflect the actual heat transmission loss. So in total, there were 20 days of data. The daily energy usage during these days were added together to give a total of 337.6 kWh. This value was used later as a benchmark. The next task was to calculate the energy usage for the 20

days using the Effective U-Values derived from the three energy performance protocol discussed above. The next three sections describe how this was accomplished.

7.7.1 Calculation of the energy usage using Effective U-Value of protocol one

The total heat energy usage for a given number of days using the Effective U-Value derived from the energy protocol one is calculated by:

$$E_{Total} = \frac{24}{1000} * U_{Effective} * \sum_{n=1}^{n}(Tint^n - Text^n) \quad (7.01)$$

where;
n is the day number
E_{Total} is the total heat Energy used for n number of days in (KWh)
$U_{Effective}$ is the calculated Effective U-value in (W/^{o}C)
$Tint^n$ is the average internal temperature for day number n in (^{o}C)
$Text^n$ is the average external temperature for day number n in (^{o}C)

7.7.2 Calculation of the energy usage using Effective U-Value of protocol two

The total heat energy usage for the energy performance protocol two is exactly the same as the previous protocol, therefore, formula 7.01 can be also used here.

7.7.3 Calculation of the energy usage using Effective U-Value of protocol three

The procedure for the calculation of the total heat energy usage for the energy performance protocol three is more complex because the procedure has to compensate for the solar gain. The energy performance protocol three identifies the Effective U-Value along with the proportional relation between the accumulative solar irradiance and the average internal temperature increase K_{avg}. The procedure of how the K_{avg} was calculated was given in section 5.7.2. Both the Effective U-Value and the K_{avg} should be known before calculating the heat energy usage over a number of days.

This is calculated by:

$$E_{Total} = \frac{24}{1000} * U_{Effective} * \sum_{n=1}^{n} (Tint^n - (K_{avg} * Sacc^n + Text^n)) \qquad (7.02)$$

where;

n is the day number

E_{Total} is the total heat Energy used for n number of days in (KWh)

$U_{Effective}$ is the calculated Effective U-Value in (W/^{o}C)

K_{avg} is the average proportional relation between the average internal temperature increase and the accumulative solar radiation in (^{o}Cm^2/J)

$Sacc$ is the accumulative solar energy for day number n in (J/m^2)

$Tint^n$ is the average internal temperature for day number n in (^{o}C)

$Text^n$ is the average external temperature for day number n in (^{o}C)

8 Results

8.1 Introduction

In this chapter the three proposed energy performance protocols are evaluated on their deviation from the benchmark data which is retrieved from a long term experiment. The performance of each protocol is also evaluated into three different scenarios. The chapter concludes by comparing the protocols together and by stating the advantages and disadvantages of each protocol.

8.2 Results – Effective U-Value

With regards to the experiment described in section 7.7, once the heat energy stored in the thermal mass reached saturation point, it remained unchanged for the rest of the experiment. This means that any day from the 11th October 2012 to the 30th October 2012 can be used to calculate the Effective U-Value using any one of the 3 energy performance protocols mentioned in chapter 7. In fact, for each day, 3 Effective U-Values were calculated, one Effective U-Value for each of the three protocols discussed in chapter 7. With regards to the energy performance protocol, the K_{avg} was calculated over 6 days. This calculation started on the 5th October 2011 and was terminated on the 10th October 2011. Although the data used was gathered a year ago, K_{avg} is valid because there were no physical changes to the testing room or to the surrounding shade. The calculation is 6.454X10^{-8} ^{o}C.m^2/J and its calculation is based on section 5.7.2.

The Effective U-Values obtained are given in table 8.1 along with their associated error in % form. The error is calculated by the following formula:

$$Error = 100 * \frac{E_{Total} - E_{Actual}}{E_{Actual}} \ (\%) \qquad (8.01)$$

Where,

E_{Actual} is the actual total energy used from the 11th to the 30th October 2012, both days included. E_{Total} is the total energy as calculated for the given Effective U-Value, using the calculation method as described in sections 7.7.1, 7.7.2 and 7.7.3.

Date	Effective U-Value Protocol One (W/°C)	Protocol One Error (%)	Effective U-Value Protocol Two (W/°C)	Protocol Two Error (%)	Effective U-Value Protocol Three (W/°C)	Protocol Three Error (%)	Daily Energy (kWh)
11/10/2012	64.58	-8.66	63.8	-9.76	70.23	-7.6	13.33
12/10/2012	62.60	-11.46	67.0	-5.21	76.87	1.1	11.81
13/10/2012	65.06	-7.98	66.35	-6.14	69.93	-8	15.31
14/10/2012	69.73	-1.37	68.65	-2.89	77.1	1.4	15.71
15/10/2012	65.38	-7.52	82.9	17.26	89.44	17.6	15.84
16/10/2012	78.12	10.49	66.57	-5.83	73.51	-3.3	15.65
17/10/2012	70.24	-0.65	72.43	2.46	77.58	2.04	15.61
18/10/2012	70.35	-0.49	68.21	-3.52	71.93	-5.4	13.91
19/10/2012	70.10	-0.85	65.29	-7.26	70.64	-7.1	13.66
20/10/2012	66.87	-5.42	60.97	-13.77	67.82	-11	14.19
21/10/2012	63.85	-9.69	62.54	-11.53	69.35	-8.8	15.28
22/10/2012	59.92	-15.24	73.81	4.4	79	3.89	17.43
23/10/2012	68.72	-2.8	69.03	-2.36	72.3	-4.9	16.46
24/10/2012	66.65	-5.72	66.09	-6.52	68.33	-10	17.84
25/10/2012	59.72	-15.53	73.47	3.92	78.71	3.52	21.62
26/10/2012	72	1.83	89.05	25.96	98.13	29.1	20.07
27/10/2012	98.81	34.1	83.53	18.15	93.56	23.1	16.68
28/10/2012	75.31	6.53	75.52	6.83	79.26	4.25	21.38
29/10/2012	73.1	3.37	78.61	11.19	82.25	8.18	26.93
Average	69.32	-1.95	71.26	0.79	77.15	≈1.4	
Effective U-Value Calculated over 19 days						71.38 W/°C	

Table 8.1 The Calculated Effective U-Value with the associated error

The content of Table 8.1 is best explained by means of an example. Let's take the row which is dated on the 17th October 2012.

The Column named Effective U-Value Protocol One:
Shows the calculated Effective U-Value using Protocol One by means of the measurements taken between the 17th October at 12:00 AM and the 17th October at 6:00 AM.

The Column named Protocol One error:
Shows the error of the Effective U-Value Protocol One, using the error formula (8.01) given in this section.

The Column named Effective U-Value Protocol Two:
Shows the calculated Effective U-Value using Protocol Two by means of the measurements taken between the 17th October at 6:00 AM and the 18th October at 6:00 AM.

The Column named Protocol Two error:
Shows the error of the Effective U-Value Protocol Two using the error formula (8.01) given in this section.

The Column named Effective U-Value Protocol Three:
Shows the calculated Effective U-Value using Protocol Three by means of the measurements taken between the 17th October at 6:00 AM and the 18th October at 6:00 AM. In this case K_{avg} has a value of $6.454X10^{-8}$ $^{o}C.m^2/J$.

The Column named Protocol Three error:
Shows the error of the Effective U-Value Protocol Three using the error formula (8.01) given in this section. In this case K_{avg} has a value of $6.454X10^{-8}$ $^{o}C.m^2/J$.

The Column named Daily Energy:
Shows the energy used on the 17th October 2012.

The last row shows the Effective U-Value calculated over 19 days.

The row before the last is the average Effective U-Value with its associated errors. As can be seen, the Effective U-Values calculated on the 15th, 26th and 27th October had an error which is above than ±16% and hence they deserve some investigation. These three days are highlighted in yellow in table 8.1 for easy identification.

Before explaining the cause of these errors, it is more important to explain the ideas behind the adopted method. Basically, these methods measure the steady state Effective U-Value, while the environment is a dynamic one. As expected, this will produce errors in the results. In the protocol these errors were minimized by performing the necessary measurements during the time when the external temperature variations are relatively small, as explained in section 4.5.3. In the protocols two and three the dynamic effect is averaged out over a 24 hour period. It is good to recall that normally the external temperature variation follows a sinusoidal like path with a time period equal to 24 hours. Further information on this can be found in section 4.5.2. Figure 8.1 shows the typical external temperature variation in a day. The one shown in figure 8.1 belongs to the 23rd October 2012.

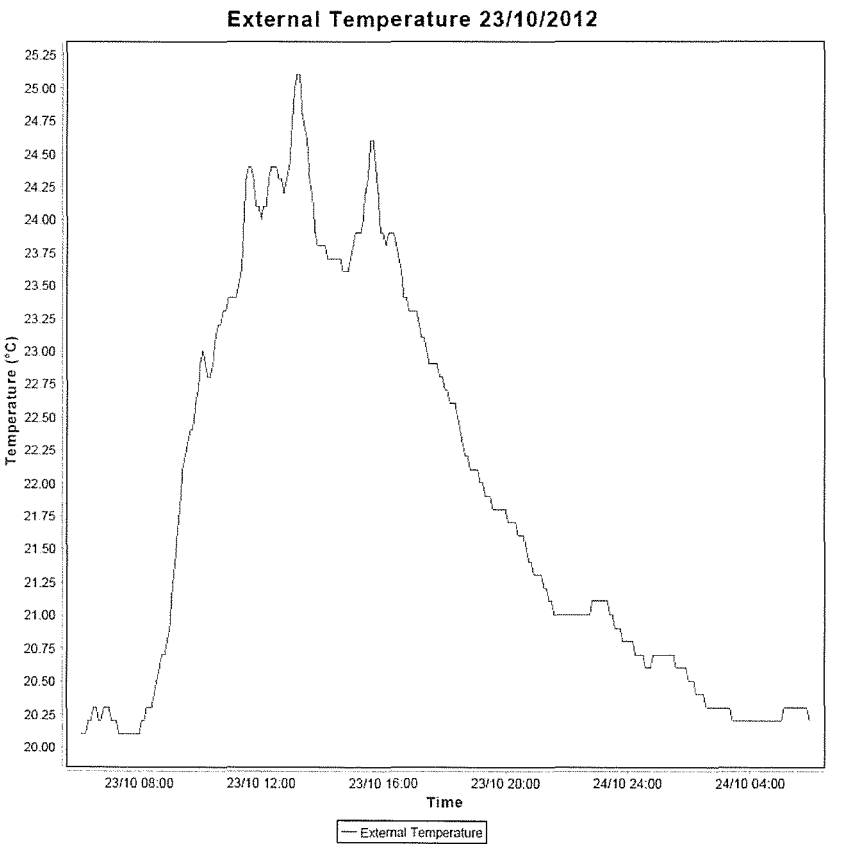

Figure 8.1 The external temperature for the 23rd October 2012

The thermal mass of the building delays the effect of the external temperature variations on the internal heat energy requirements. So when the external temperature increases in the morning, the internal heat energy required does not change immediately. With an increase in the external temperature, the difference in temperature between the inside and outside of the building decreases. This is because the internal temperature is kept constant and is higher than the outside temperature. So in this scenario there is a decrease in the temperature difference while the internal energy requirements remained relatively unchanged. If the Effective U-Value is calculated in the morning, the U-Value result is expected to be greater than the actual one.

On the other hand, if the Effective U-Value is calculated in the evening the Effective U-Value result is expected to be below the actual one. This is because, with a decrease in the external temperature, the temperature difference between the inside and outside of the building increases. Due to the thermal mass of the building, the internal heat energy requirements do not change right away and remain relatively unchanged. Furthermore, the heat energy requirements are substantially lower than what was required in the morning. This is because the internal heating requirements start to reflect the increase in the external temperature. Besides this, there will also be some solar gain which reduces further the heat requirements. Calculating the Effective U-Value in this scenario will result into a low value which does not reflect the actual one.

If the Effective U-Value is calculated over a period of 24 hours and the outside temperature variations are normal ones, then the errors should cancel each other. For example, in the case of figure 8.1 where the temperature variations are normal, the error is less than 5 %.

A similar phenomenon occurs when the daily average temperature difference, between two successive days, is greater than 3°C. If the difference is positive, then the calculated Effective U-Value is expected to be greater than the actual one while if

the difference is negative the calculated Effective U-Value is expected to be smaller than the actual one.

Figure 8.2 shows the external temperature for the 15th October 2012. As can be seen, the temperature variations are not normal ones. The temperature started to increase after midnight when it was expected to go down. Due to this abnormality the dynamic effect was not averaged out properly and caused an increase in the calculated Effective U-Value. This resulted into an overall error of 17% in the required energy.

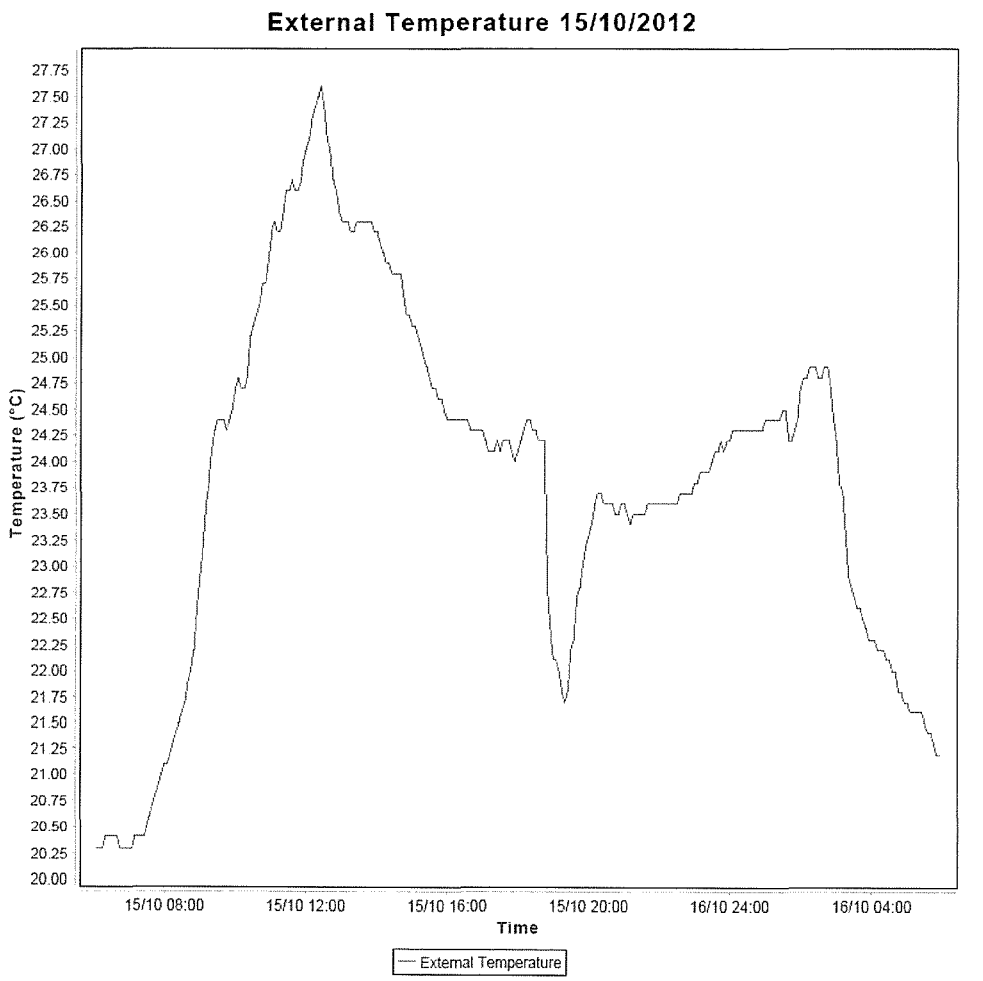

Figure 8.2 The external temperature for the 15th October 2012

Similar to the previous date, the external temperature variation for the 26th October 2012 was also abnormal. In fact, the external temperature started to increase after midnight when it was expected to decrease. Figure 8.3 shows the external temperature variation for the 26th October 2012. Once more, due to this abnormality in the external temperature variation, the dynamic effects were not averaged out properly. Furthermore, there was also an increase in the daily average external temperature. The latter as previously explained will also increase the calculated Effective U-Value.

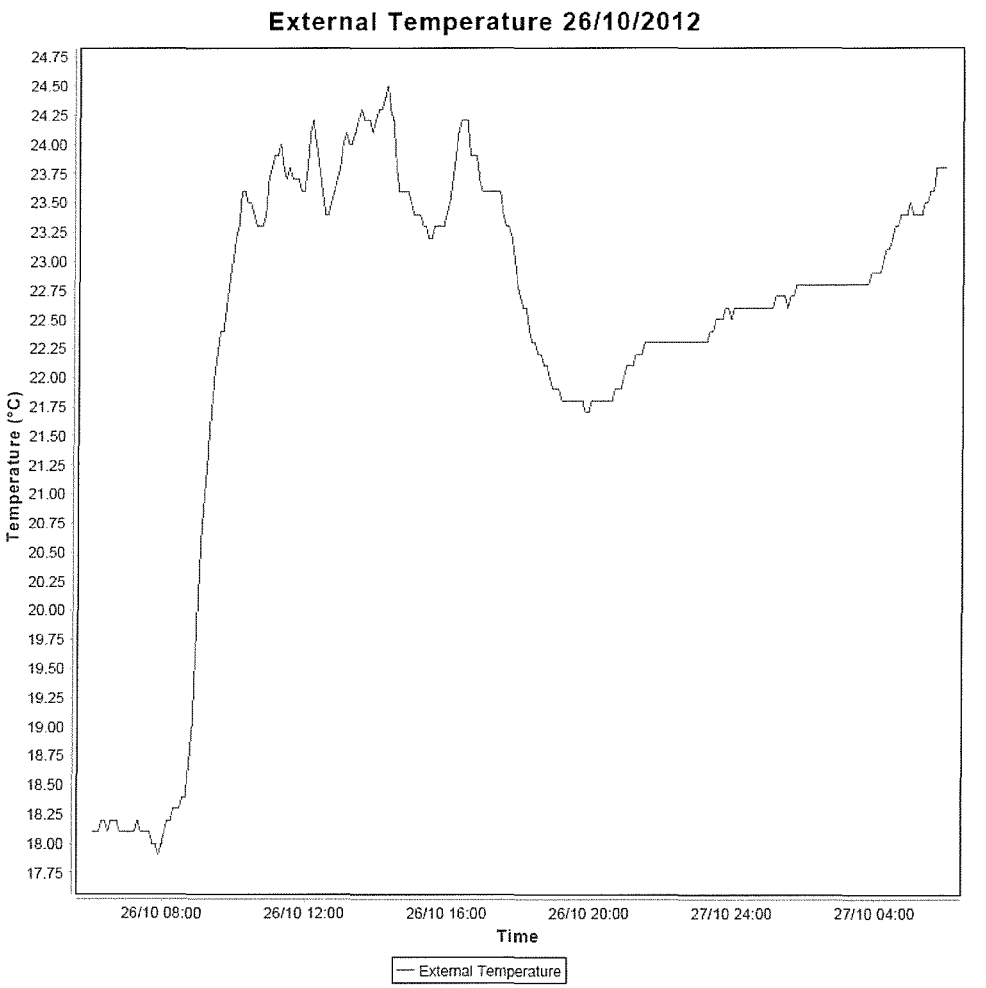

Figure 8.3 The external temperature for the 26th October 2012

The calculated Effective U-Value resulted in a 29% error when it was used to calculate the energy used. The largest error occurred on the 27th October 2012 using

the energy performance protocol one. Figure 8.3 shows the external temperature for the 26th October 2012 which includes also the first 6 hours of the 27th October 2012. In the energy performance protocol one, these 6 hours are also used to measure the Effective U-Value. Similarly, as in the previous case, the abnormal increase in temperature after midnight resulted into a large Effective U-Value. This over estimated the Effective U-Value and resulted in an over estimated error of 34% in heat energy requirements.

With regards to the errors associated with the energy performance protocol two and three on the 27th October 2012, it should be noted that there was a change to winter time on the 28th October at 2:00 which happened to be in the time window for heating of the 27th of October. This resulted in shifting back the temperature by one hour. The effect of such action was likely to cause an increase in the average external temperature. Correcting the data was not an option because the original data was overwritten. Furthermore, the shift back of time resulted in an increase in the average power used. This suggests that the increase in the Effective U-Value was at least partially attributed to the shift in time. There was also a significant change in temperature. For these reasons, the effective U-Values measured during the 27th October were not considered for some of the analysis.

8.2.1 Protocol Rule Update

Two important observations came out from the above analysis. The first one is that the measurements have to be discarded if the external temperature variations are not typical; that is the external temperature does not follow a sinusoidal like path. Figure 8.1 shows such external temperature variations. The second observation is that the measurements should be discarded if there is a change in the average temperature which is greater than 3 ^{o}C from the previous day. If these observations are followed, the accuracy of the measurements is expected to improve. As a consequence, these observations are added to all strategies as a rule. From now on these rules are referred to as **rule one.** As an alternative to this rule, one can perform average over multiple U-Values. This is discussed in the next section.

8.2.2 Multi measurements of Effective U-Value

An alternative solution for rule one discussed above is to conduct multi Effective U-Value measurements and then compute the average Effective U-Value. This not only reduces the errors but also improves the accuracy of the Effective U-Value. Figure 8.4 shows the accuracy attained for the given average Effective U-Value for protocol one. The average Effective U-Value for a given day is calculated from the given day and from the number of previous days. For example the average Effective U-Value for three days on the 15th October is calculated from day 13th, 14th and the 15th October.

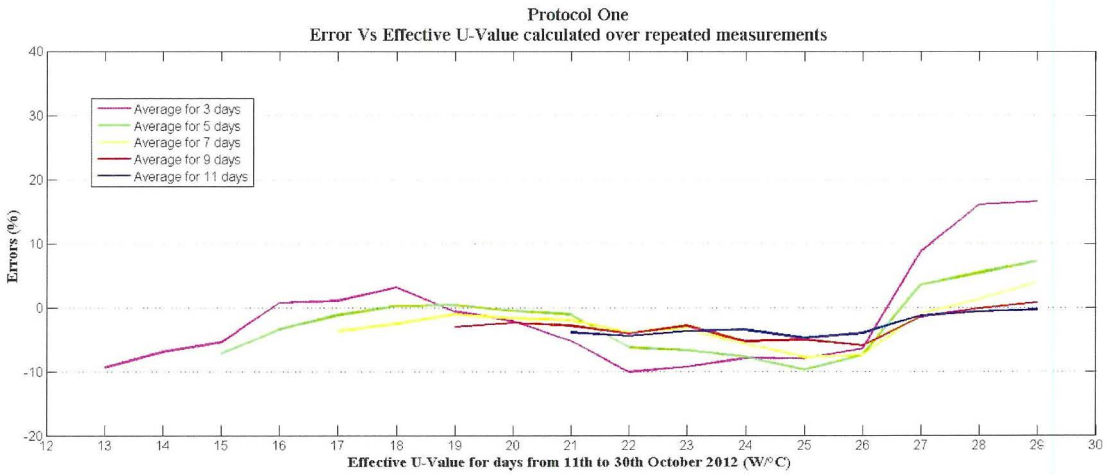

Figure 8.4 Comparing errors for different averages of Effective U-Values for protocol one

As can be seen, the overall error as well as the maximum error are both decreased with the increase of number of days on which the averages are calculated. The same results were obtained for protocol two and protocol three. Figure 8.5 and 8.6 shows the accuracy obtained for protocol two and protocol three respectively.

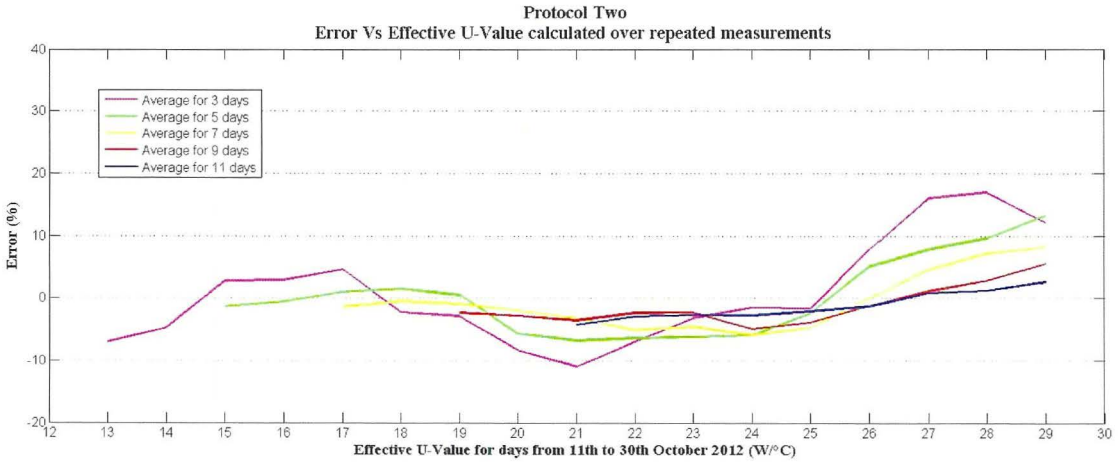

Figure 8.5 Comparing errors for different averages of Effective U-Values for protocol two

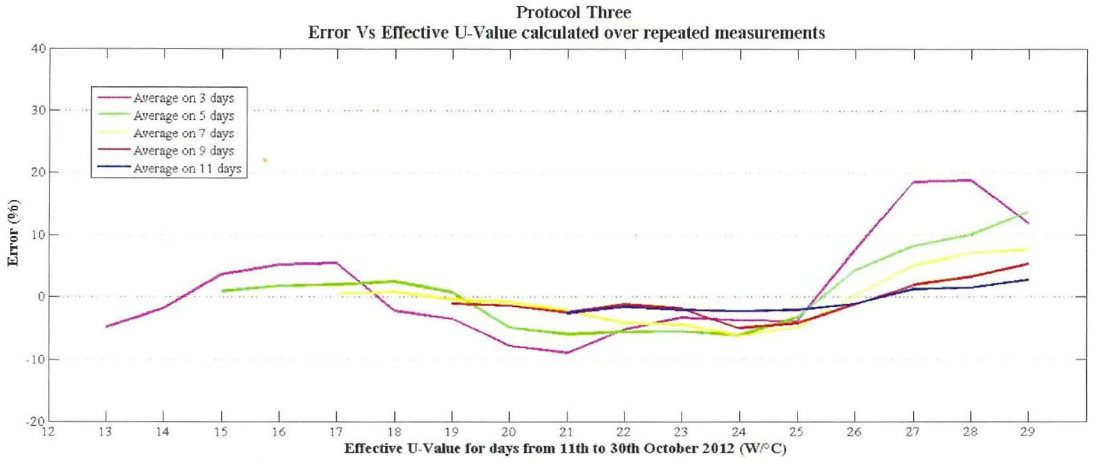

Figure 8.6 Comparing errors for different averages of Effective U-Values for protocol three

In both protocols, and similarly to protocol one, the overall error and the maximum error are both decreased with the number of days measured.

From the above analysis two things were concluded. The first one is that the accuracy of the protocol can be improved by repeating the measurements, Secondly peak errors due to unusual external temperature behavior can be averaged out if at least three measurements of the Effective U-Value are performed. For an example of two consecutive relatively high Effective U-Values see table 8.1 were smoothed out

to an acceptable level. The main disadvantage of this approach is the consumption of the required energy. As a consequence, the rule one approach, is preferred. On the other hand, this approach requires the intervention of a knowledgeable person who has to decide whether the measurement is a valid one or not. The latter can be avoided if an expert system is built which is able to distinguish between a valid external temperature profile or not. A likely candidate for such a system is an artificial neural network. Artificial neural networks, by their nature, are very well suited for pattern recognition. This option is not investigated in this research and is left for future work.

8.3 Comparing the three energy performance protocols

It is possible to compare the results obtained using three energy estimation protocols. Figure 8.7 shows a graph which compares the errors among the measured Effective U-Values from the 11th to the 29th October 2012. All the measured Effective U-Values are considered and rule one is not applied.

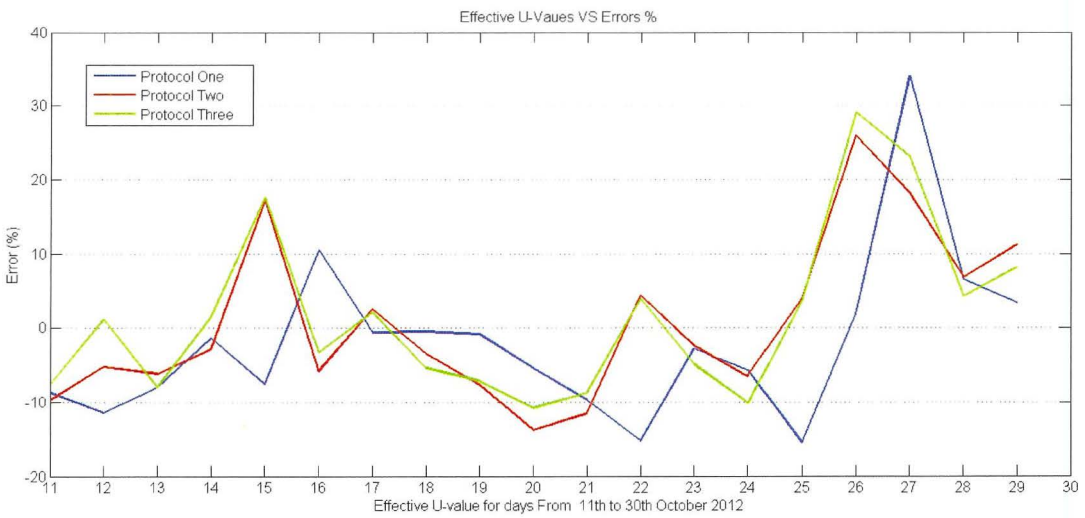

Figure 8.7 Comparing errors from the different Effective U-Values

The same data was considered but rule one was applied. Therefore, the Effective U-Values calculated on the 15th, 26th and 27th October were not considered in the

analysis. Figure 8.8 shows a curve graph which compares the errors among the measured Effective U-Values from the 11th to the 29th October 2012. As can be seen, the maximum error dropped to a maximum of 15% and the overall error was improved.

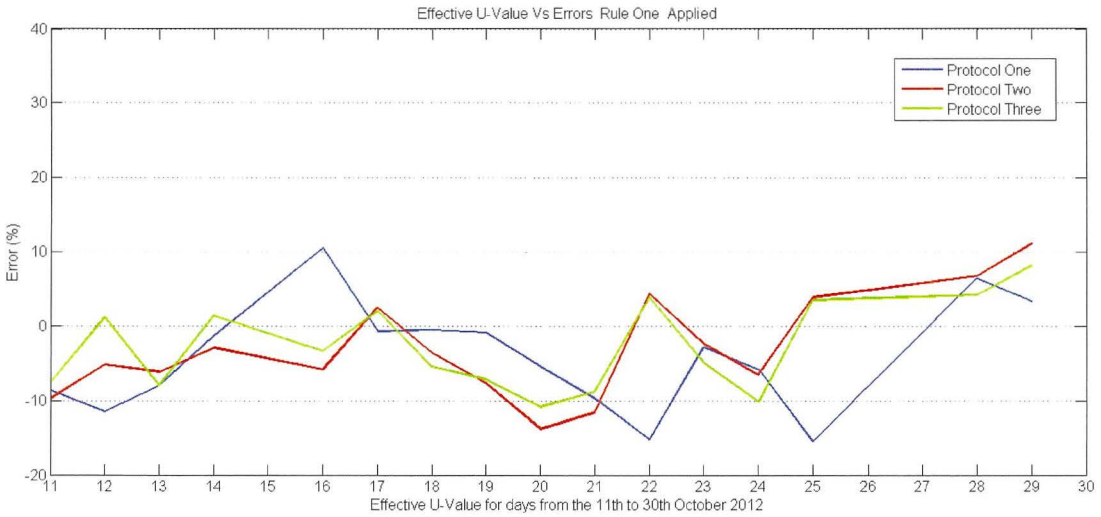

Figure 8.8 Comparing errors from different Effective U-Values with rule one applied

Once more, the same data was considered, but this time the Effective U-Value was of an average of two Effective U-Values measured over two consecutive days. Rule one was also applied here, therefore, the Effective U-Values calculated on the 15th, 26th and 27th October 2012 were not considered in the analysis. Figure 8.9 shows a graph which compares the errors of the Effective U-Values measured on an average of two consecutive days from the 11th to the 29th October 2012. As can be seen, the maximum error dropped below the 15% and the overall error improved. This suggests that if the accuracy measurements need to be improved, then one has to repeat the measurement and take the average.

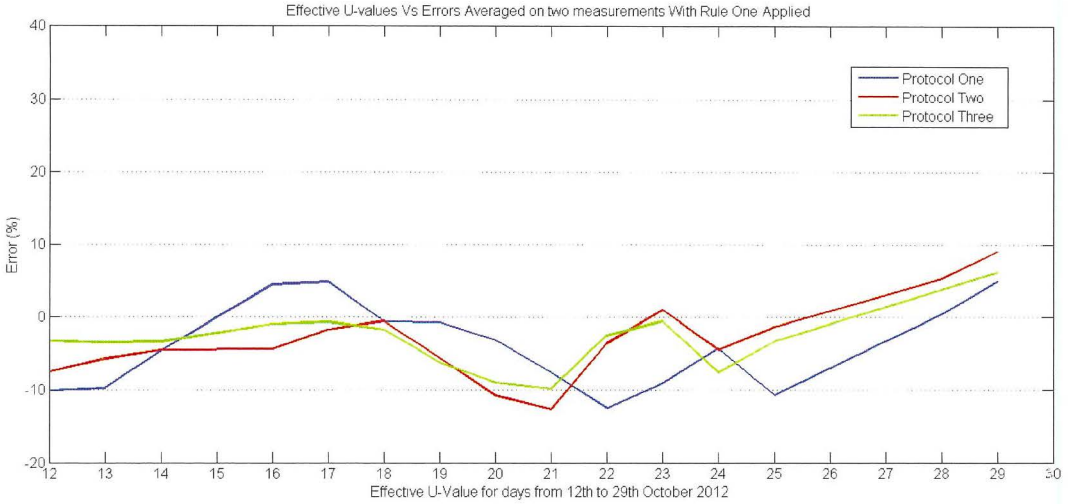

Figure 8.9 Comparing errors from different Effective U-Values computed on two days of measurements with rule one applied

These three energy performance protocols were also compared through their Root Mean Squared Error (RMSE). The RMSE captures both the negative and positive errors so it is a good method to compare the performance of each protocol used. Table 8.2 shows the calculated RMSE for the three protocols for the three different scenarios discussed here.

	Protocol one	Protocol two	Protocol three
RMSE Scenario 1	11	10.7	11.1
RMSE Scenario 2	8.2	7.3	6.4
RMSE Scenario 3	6.9	6.2	5

Table 8.2 Comparing the RMSE among the different protocols and scenarios

In Scenario 1, no restrictions were applied and all the Effective U-Values were considered.

In Scenario 2 and 3, the restriction of rule one were applied, therefore the 15th, 26th and 27th October 2012 are not considered in the analysis.

In Scenario 3, the Effective U-Value is calculated on an average of 2 measurements.

In Scenario 1, where no restrictions were applied, the average RMS error was about 11% and the maximum error was of 34%. In the case of Scenario 2, the average RMS error was about 7.3% and the maximum error was about 15%. In the case of Scenario 3, the average RMS error was about 6.0% and the maximum error was of 12%.

From literature a validation exercise is conducted to find the performance of other energy prediction methods. Most of the related literature refers to the artificial neural networks as the best performed method, with the best results reaching a 4% error. T.Olofsson and S Andersson [17] achieved a deviation of 4% between the predicted and the actual energy used, with a correlation of 90-95% when they applied the neural network method to six different residential buildings. The number of observations which were carried out varied from 12 to 36 days. The artificial neural networks were trained from these observations and from other training data which was artificially generated from a simulator which simulated buildings with same blue-print data. In total there were 29 tests which were carried out in six different buildings and performed in different months of the year. This paper by T.Olofsson and S Andersson [17] presented two tables of results. One table specified the deviation between the predicted and the measured energy used for space heating, while the other one represented the deviation between the predicted and the measured energy used for the total demand. The total energy demand includes energy for domestic hot water preparation and the electrical appliances. For obvious reasons the interesting results for this research are the results for the space heating only. Table 8.3 shows these results in percentage error.

	House 2	House 3	House 4	House 6	House 8	House 10
January	3%	2%	-1%	-8%	0%	
February	-6%					
March		2%	-9%		-4%	-6%
April		4%	-2%		-2%	15
May		19%	22%	31%	11%	27%
June						
July						
August						
September	30%	12%	17%	3%	7%	5%
October					1%	2%
November		-5%		-6%		
December						

Table 8.3 Percentage error between the predicted and actual energy use [17]

The worst 9 errors for the space heating were 31%, 30%, 27%, 22%, 19%, 17%, 15%, 12% and 11%, that is, almost one third of the measurements. The average deviation between the predicted and the measured energy used is 8.86%. It is not clear how the claimed 4% deviation from the actual energy use was calculated, therefore, the content of the table 8.3 for space heating was used for comparison.

Comparing the results of table 8.3 directly with the results of table 8.1 which were obtained in this research is not possible because the testing grounds are very different, but one can observe many similarities. Both of the results occasionally have significant errors. Some of the errors are very small and the average deviation error is more or less the same, that is, about 8%. All this suggests that up to now the performance of the proposed protocols is in line with other energy use prediction methods. On the other hand, further testing is required to confirm this performance but this is left for future work.

Considering that the proposed protocols are steady state and the measurements are performed on one day without any assistance of a simulator, a minimum accuracy of

about 15% is assumed as good. If rule one is enforced, then all the three protocols can have a minimum accuracy of 15% or better. As a consequence, all the protocols can be safely used. The next section will discuss the advantages and disadvantages of each of these protocols.

8.3.1 Advantages and Disadvantages

Protocol one has the largest errors of the three protocols. It has an average error of 8% and a maximum of 15% when rule one is applied. On the other hand, this protocol requires a time window for heating of about 12 hours, which is about 60% less than that of the other two protocols. It also requires less time than the other two protocols because the procedure takes only about 13 hours to complete. Repeating two consecutive measurements can improve the average error to 7%.

Protocol two has less error than the first protocol but it has a greater error than the third one. It has an average error of 7% and a maximum error of 12% with rule one applied. On the other hand, this protocol requires a time window for heating of about 36 hours which is about 200% more than the first protocol, but is the same as the third protocol. The whole procedure takes around 37 hours to complete. This is a shorter period than that taken by the third protocol but it is longer than the first one. Repeating the measurements for two consecutive times will improve the average error to about 6%.

Protocol three has the least errors of the three protocols. It has an average error of 6% and a maximum error of 11% when rule one is applied. On the other hand, this protocol requires a time window for heating of about 36 hours which is about 200% more than the first protocol but is the same as the second one. The whole procedure takes around 77 hours to complete which is significantly a longer period than that of the second one. Repeating the measurements for two consecutive times will improve the average error to about 5%. The details of the best protocol are given in the conclusion of the next chapter.

9. Conclusion and Future Work

9.1 Conclusion

9.1.1 Hardware and software

As a part of this research project a complete system made from hardware and software was developed. The design of this system was made in such a way that it facilitates the implementation of the three proposed protocols developed in this research. In fact, the processing of the data to get the required information used to take more than half an hour when discrete and separate system were used. With the developed system the same information is obtained in a few seconds.

The design of the system is modular, with each module having the appropriate interface features. This will facilitate future improvements, automation and adaptation for other energy performance protocols or building analysis.

The system integrates together, a wireless weather station, a PC and a number of wireless sensor nodes. The PC serves as the repository for the data, provides the remote control of the system through the Internet, if needed, and provides the necessary processing power for data analysis, if required. The weather station provides the system with the required external sensors. It provides the system with the external temperature, humidity, solar irradiance, wind direction, wind speed and rain rate. Each sensor node is equipped with a humidity sensor, eight temperature sensors, a three fan speed control, a temperature controller and an energy meter. As can be seen, the system provides more than what is required for the proposed system. In fact, it provides all the necessary controls and sensors required by STEM & PSTAR protocol.

The software consists of three programs written in Java. One is used to configure and calibrate the sensor nodes, another one is used to process the collected data and the last one serves to control the sensor nodes. The latter is made from a number of modules which permit full control of the system from a Java program.

As can be seen, the system design minimizes the human intervention in the implementation of the three proposed protocols. Furthermore, with the extra sensors included in the system and the additional features implemented, the system is a useful tool for other researchers.

9.1.2 Effective U-Value

As a result of this research project, three energy performance estimation protocols for buildings were developed. The accuracy of these protocols were validated with real data acquired by an experiment. In this experiment, the test room was heated up for a given internal set point for 21 days. The accuracy obtained is given in table 9.1 below.

Protocol number	Average error (%)	Maximum error (%)
one	7.9	34
two	8.7	25
three	8.4	29

Table 9.1 Accuracy of the protocols without rule one

If rule one of section 8.2.1 is applied the accuracy improves, as can be seen in table 9.2.

Protocol number	Average error (%)	Maximum error (%)
one	6.6	15
two	6.4	14
three	5.6	10

Table 9.2 Accuracy of the protocols with rule one applied

The average error was decreased to an average of 4.7% if the measurements were conducted over two days. Protocol one requires a time window of 12 hours for heating, while protocol two and three require a time window of 36 hours for heating. Protocol one requires 13 hours to complete, protocol two requires 37 hours to complete and protocol three requires 156 hours to complete. Protocol three takes

into account the solar irradiance. Further analysis showed that the maximum and average error are lowered when the measurements are repeated and an average Effective U-Value is calculated.

9.2 Future Work

This research project, showed that the three proposed protocols performed well for the short time prediction. The next step is to check the performance of these protocols for a longer prediction preferable for one year. Thus this could be one possible future project which can also lead to the analysis of the performance of these protocols in different buildings with different characteristics. A useful investigation for the proposed protocols is to identify the minimum internal set point temperature to use when carrying out any of the proposed protocols. Another interesting future work, in relation to the proposed protocols, is to implement an expert system which can identify atypical external temperature profile.

With regards to the Effective thermal capacitance, there are two priorities for future work. One is to investigate the possibility to extrapolate the average temperature inside the building components. The other one is to investigate the utilization of the thermal capacity for the accumulated heat stored in a steady-state heat condition. Then, based on this investigation, the calculation procedure of the method for the measurement of the effective thermal capacitance is adjusted to reflect the findings.

Another possibility for future work is to investigate the possibility to determining the rate of air exchange in the building by monitoring the external and internal relative humidity. This was briefly discussed at the end of section 4.4.4.

Appendix A:

Sensor node configuration format and meaning

$byte_1$: $b_7, b_6, b_5, b_4, b_3, b_2, b_1, b_0$ Bit value of 1 enable while bit value of 0 disable

b_0: enable/disable humidity sensor

b_1: enable/disable electrical energy meter

b_2: enable/disable temperature control

$byte_2$: $b_7, b_6, b_5, b_4, b_3, b_2, b_1, b_0$ Bit value of 1 enable while bit value of 0 disable

b_0: enable/disable temperature sensor 1

b_1: enable/disable temperature sensor 2

b_2: enable/disable temperature sensor 3

b_3: enable/disable temperature sensor 4

b_4: enable/disable temperature sensor 5

b_5: enable/disable temperature sensor 6

b_6: enable/disable temperature sensor 7

b_7: enable/disable temperature sensor 8

$byte_3$: b_7, b_6, b_5, b_4 b_3, b_2, b_1, b_0 Fan control - 1

b_3, b_2, b_1, b_0 PWM space mark ratio

b_7, b_6, b_5, b_4	Fan Control	For a value of 0 Fan output is high impedance
		For a value of 1 Fan output is 3.3V
		For a value of 2 Fan output is 0V
		For a Value of 3 Fan output is PWM
		For a Value of 4 Fan output is PWM-inversed

$byte_4$: Fan control - 2 configuration as $byte_3$

$byte_5$: Fan control - 3 configuration as $byte_3$

$byte_6$: Most Significant Byte - Proportional gain (Temperature control)

$byte_7$: Least Significant Byte - Proportional gain (Temperature control)

The actual value is obtained by dividing the proportional gain 10

$byte_8$: Most Significant Byte - Integral gain (Temperature control)

$byte_9$: Least Significant Byte - Integral gain (Temperature control)

The actual value is obtained by dividing the Integral gain 100

$byte_{10}$: PI sampling time

$byte_{11}$: Temperature sensor to use for the temperature control

For a value of 1 temperature sensor 1 is used

For a value of 2 temperature sensor 2 is used

For a value of 4 temperature sensor 3 is used

For a value of 8 temperature sensor 4 is used

For a value of 16 temperature sensor 5 is used

For a value of 32 temperature sensor 6 is used

For a value of 64 temperature sensor 7 is used

For a value of 128 temperature sensor 8 is used

$byte_{12}$: Most Significant Byte - set point temperature (Temperature control)

$byte_{13}$: Least Significant Byte - set point temperature (Temperature control)

The actual value is obtained by dividing the set point value by 10 and add 100

$byte_{14}$: Most Significant Byte - set point resistance (Temperature control)

$byte_{15}$: Least Significant Byte - set point resistance (Temperature control)

The actual value is obtained by dividing the set point value by 10. This value is generated by the application.

Appendix B:

Data logging record format

There are four types of records: Sensor node record, Weather station record, Transmit data record and Received data record. The last two are used for diagnosis purposes only.

Sensor node record:

A Sensor node record contains ND in the first field of the record. The format of the record is as follows

ND, node address, date & time, sensor, data

ND, ZZZZ, DD/MM/YYYY HH:mm ,XX, data

EX ND,CCCC,25/12/2013 18:04,T4,16.4

ZZZZ: This is a 4 digit hex decimal number.

DD/MM/YYYY HH:mm :

DD is the day of the month

MM is the month

YYYY is the year

HH is the hour of the day in 24 hour format

XX is the sensor type where T1 means temperature 1

T2 means temperature 2

T3 means temperature 3

T4 means temperature 4

T5 means temperature 5

T6 means temperature 6

T7 means temperature 7

T8 means temperature 8

HH means internal Humidity

ER means Energy used since last read

EF means Total energy used

Weather Station record:

A Weather Station record contains WS in the first field and WSWS in the second field of the record. The format of the record is as follows

WS, WSWS, date & time, sensor, data

WS, WSWS, DD/MM/YYYY HH:mm ,XX, data

EX WS,WSWS,25/12/2013 18:04,ET,16.4

DD/MM/YYYY HH:mm :

DD is the day of the month

MM is the month

YYYY is the year

HH is the hour of the day in 24 hour format

XX is the sensor type where IT means internal temperature

ET means external temperature

IH means internal humidity

EH means external humidity

SR means solar irradiance

RR means rain rate

RD means rain day

WS means wind speed

WD means wind direction

WA means wind average

BP means barometric pressure

Transmit data record:

A Transmit data record contains NT in the first field of the record. The format of the record is as follows:

NT, node address, date & time, sensor, data

NT, ZZZZ, DD/MM/YYYY HH:mm ,Packet Transmitted : , data

NT,CCCC,25/12/2013 18:13, Packat Transmitted : ,FFFF,CCCC, 64 ,0 ,0 ,10 ,00, 00

ZZZZ: This is a 4 digit hex decimal number.

DD/MM/YYYY HH:mm :

DD is the day of the month

MM is the month

YYYY is the year

HH is the hour of the day in 24 hour format

Receive data record:

A Receive data record contains NR in the first field of the record. The format of the record is as follows:

NR, node address, date & time, sensor, data

NR, ZZZZ, DD/MM/YYYY HH:mm ,Packet Received : , data

NR,CCCC,25/12/2013 18:13, Packat Received: ,CCCC,FFFF, 64 ,4E ,0 ,1B ,0F, 29

ZZZZ: This is a 4 digit hex decimal number.

DD/MM/YYYY HH:mm :

DD is the day of the month

MM is the month

YYYY is the year

HH is the hour of the day in 24 hour format

Appendix C:

Method for measuring $C_{Effective}$

The following section describes a method which measures the effective thermal capacitance $C_{Effective}$ of the building. This section starts by going through the experiments on which this method is based and then covers the details of the method. Figure C.1 shows the data of experiment number 2. The blue curve and the light pink curve represent the internal and external temperatures respectively. The red curve represents the temperature inside the wall, while the green curve indicates the average power supplied to the heater. The black curve represents the solar irradiance.

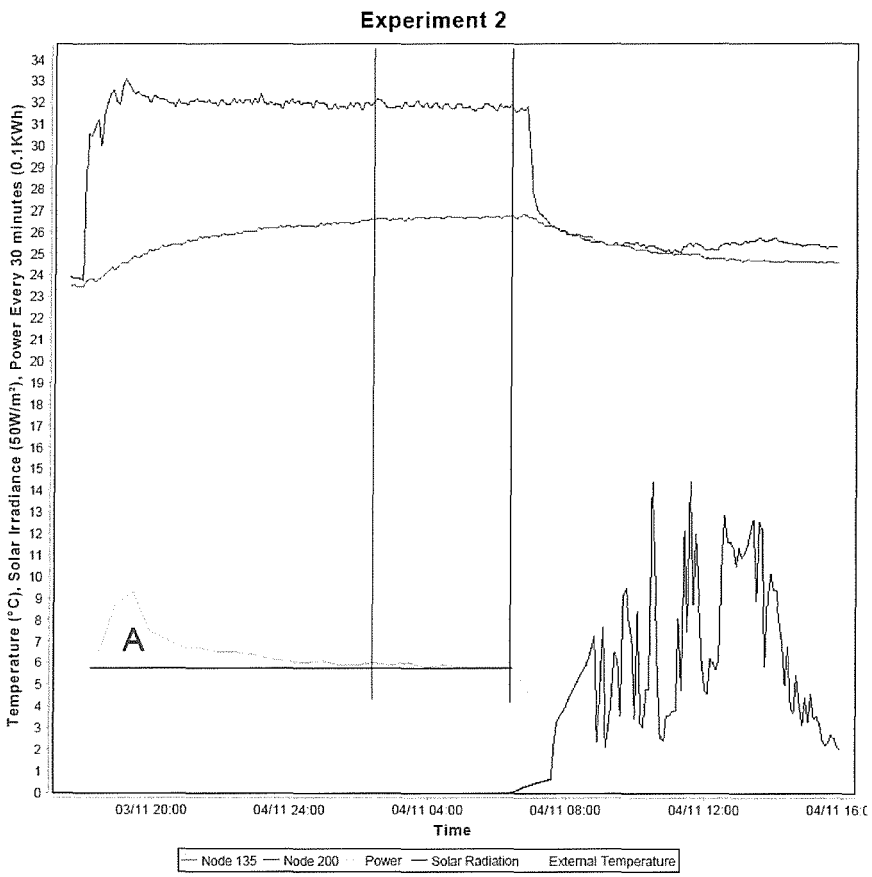

Figure C.1 The temperature power and solar irradiance for experiment number 2

By observing the temperature growth inside the wall, one will notice that the temperature increase inside the wall is following an exponential like path. Even the

electrical energy supplied to the heater is following an exponential like path, although this time it is decaying. Another important observation is that both the temperature inside the wall and the electrical power supplied reach a saturation point at around the same time. This is a clear indication that the initial higher supplied heat energy is stored in the thermal mass. The heat energy stored in the thermal mass is equivalent to the area enclosed by the green line and the red straight line denoted by letter A in figure C.1. Once the heat energy stored in the thermal mass is known, the thermal capacitance can be found by:

$$Thermal\ capacitance = \frac{Energy\ stored\ in\ the\ thermal\ mass}{Change\ in\ temperature\ inside\ the\ wall} \qquad (C.01)$$

C.1 The test Procedure adapted to measure $C_{Effective}$

The procedure for this method is given below:

1. A temperature sensor was placed at 20mm inside one of the internal walls.
2. The temperature inside the building was held constant and about 7°C higher than the outside temperature. A fan heater was used to control the internal temperature. The temperature inside the wall was monitored for at least one hour before the room was heated.
3. The electrical energy supplied to the heater was monitored.
4. It was ensured that the temperature inside the wall reached a stable state just before midnight.
5. The temperature was held constant for a further 6 hours.
6. The thermal mass was calculated as described in section C.2.

All sensors were monitored and recorded at pre-determined intervals.

C.2 The Calculation procedure to calculate $C_{Effective}$

The calculation procedure for this method is as follows:

Identify a time window after midnight in which the temperature inside the wall and the electrical power supplied to the fan heater reaches a stable point. Then, for this time window, the average temperature inside the wall $T_{Avg\ Stable}$ and the average electrical power supplied to the fan heater P_{Avg} are calculated. The time window in this case is indicated by two blue horizontal lines in figure C.1.

The heat energy stored in the thermal capacitance is calculated by the following formula:

$$Q = T * \sum_{n=1}^{n=k} (P_n - P_{Avg}) \quad (J) \qquad (C.02)$$

where:

Q is the energy stored in the thermal mass in joules.

T is the sample time in seconds.

n is the sample number, where 1 indicates the first sample after the starting of the time window for heating and k is the last sample before the stability point is reached.

P_n is the electrical power supplied to the fan heater for the given sample in Watts.

P_{Avg} is the average electrical power supplied to the fan heater in Watts calculated for the identified time window.

The thermal capacitance is calculated by the following formula:

$$Thermal\ Capacitance = \frac{Q}{T_{Avg\ Stable} - T_{Avg\ Initial}} \ (J/^{o}C) \qquad (C.03)$$

In the case of experiment number 2, the measured thermal capacitance is 1.909 MJ/°C.

It is impossible to determine the actual thermal capacitance of the testing room for the reasons mentioned in section 2. However, the calculations of the thermal capacitance of the testing room were carried out and gave 4.7059 MJ/°C. The following assumptions were made:

1. An average of 900 J/kg °C specific heat capacitance was assumed.

2. An average of 2400 kg/m^3 specific density for the roof was assumed, while 2000kg/m^3 specific density for the walls was assumed.

3. The maximum roof thickness considered was 10 cm, as stipulated by the ISO 13790 standard.

4. The maximum floor thickness considered was 10 cm as stipulated by the ISO 13790 standard, 5cm for the slab and 5 cm for the limestone (torba). The specific density for the limestone was assumed 1300kg/m^3.

5. The maximum wall thickness considered 8 cm for 23 cm hollow concrete bricks, and 5 cm for 15 cm hollow concrete bricks.

The measured thermal capacitance was expected to be less than the actual one. This is because the temperature inside the wall is assumed to be homogenous, but in fact this is not the case. On the other hand, such a big difference was not expected. Therefore, further investigation was carried out.

The measurement was repeated twice more times and the results were 2.075 MJ/°C and 1.838 MJ/°C. As can be seen the results are in the range of the previous one, this suggests that there something wrong with the method or in the assumption. The test room was heated up again and this time 7 temperature sensors were used. One sensor was placed inside the roof, other one was placed inside the floor and the remaining five temperature sensors were placed at different location inside the walls. The changes in temperatures ranges from 2.25°C to 2.75°C.

But the main culprit for this difference between the measured thermal mass and the calculated one is the assumption that the temperature was homogenous. This was not the case in fact the temperature varies according to the depth and time. The temperature inside a slab at depth x and at time t after a step increase in temperature at one side of the slab is given by

$$T(x,t) = T_0 + (T_1 - T_0) * \left(1 - \frac{x}{L}\right) - (T_1 - T_0) * u(x,t)$$

$$u(x,t) = \frac{2}{\pi}\sum_{n=1}^{\infty}\frac{1}{n} * \sin\left(\frac{n\pi x}{L}\right) e^{-n^2\pi^2 at/L^2} \quad [26]$$

where;

T_0 is the temperature surrounding the slab before the change in temperature (°C)

T_1 is the temperature after the step change in temperature (°C)

L is the slab thickness (m)

a is the thermal diffusivity of the material (m^2/s)

x is the depth inside the slab (m)

t is the time (s)

The above formula assumes homogenous material and no surface resistance. If the material is not homogenous and the surface resistance has to be included, then the calculations had to be more complex. It should be noted, that as time passes the temperature becomes directly proportional with the depth and becomes time independent. Unfortunately, this could not be used here, because a typical dwelling in Malta has a long time constant. This suggests that the temperature inside the wall becomes linear with depth after significant hours of heating. In which case, the readings are likely to become influenced by the external temperature variations as shown by experiment 7. This experiment was carried out when there was a significant change in the external temperature. Figure C.2 shows the data from this experiment.

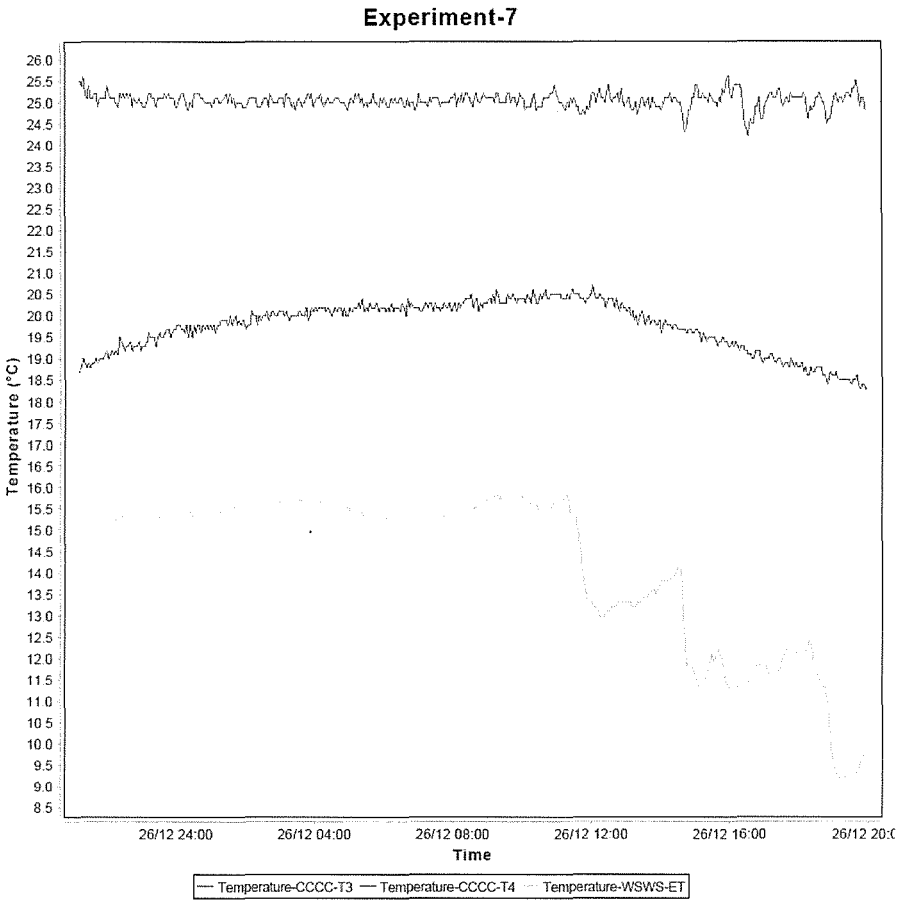

Figure C.2 The temperatures of experiment 7

The red and green curves represent the internal and external temperatures respectively. The blue curves represent the temperature inside the wall in one of the boundary walls. In this experiment, the internal temperature was kept constant to 25°C. As can be seen, the temperature inside the wall was affected heavily by the external environment. Determining the average temperature inside the building components cannot be achieved by a single point of measurement. On the other hand, extrapolating the average temperature inside the building components, using a single or multi point measurement, is possible, but needs further investigation.

Another reason for such a discrepancy is that the utilization of the thermal mass for heat accumulation decreases with depth. Figure C.3 shows that only a small part of the thermal mass is utilized beyond 5cm depth. This is likely to be the reason why the

effective thermal capacity measured here is less than half of the calculated one. Further investigations are needed to confirm this.

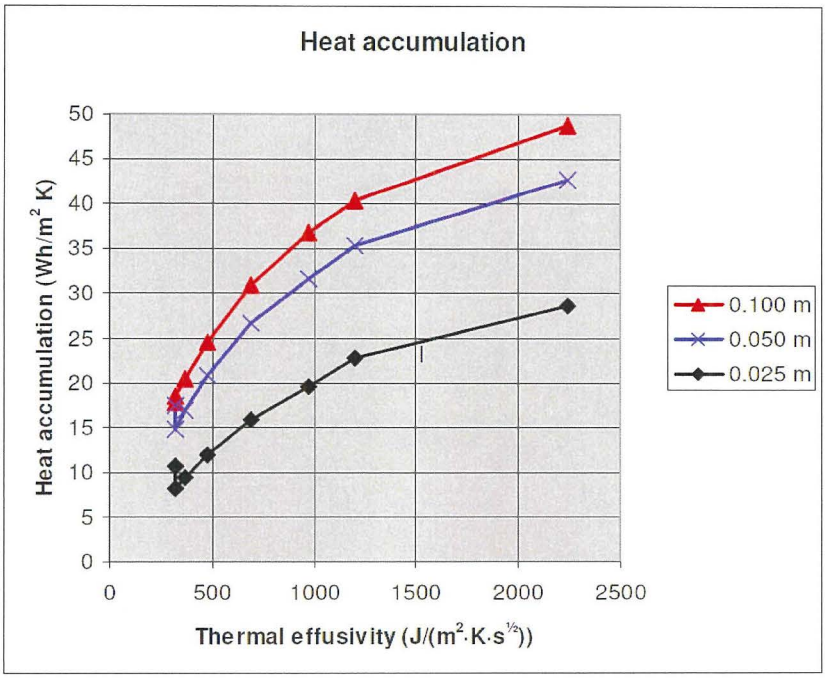

Figure C.3 The heat accumulated in relation to the depth, taken from "Heat capacity in relation to the Danish building regulations" by Lars Oslen [6]

The above is an example where the standard calculation significantly deviates from the real value. This shows the importance of a system which is able to measure the energy efficiency of a building instead of using the computation approach.

Since the main objective of this research is to determine the effective U-Value of a residential building, further investigation regarding the effective thermal capacitance is left for future work. With the effective U-Value only, the efficiency of a building can be measured.

References

[1] ASHRAE Handbook Fundamentals 2005 F30.3

[2] http://energy.gov/energysaver/articles/blower-door-tests

[3] Tracer gas :M.H.Sherman,1990: Trace case Techniques for measuring ventilation in a single Zone Building and environment Vol 25 No4 pp365-374

[4] http://www.engineeringtoolbox.com/heat-loss-buildings-d_113.html

[5] ASHRAE Handbook Fundamentals 2005 F23.2

[6] Heat capacity in relation to the Danish building regulations by Lars Olsen Danish Technological Institute, Department of Building Technology.

[7] A. Rabl, 1988, Parameter Estimation in Building: Methods for Dynamic Analysis of Measure Energy use in February 1988, Vol. 110 Journal of Solar Energy Engineering.

[8] Energy Performance of Residential building by M.Santamouris 2005 page 8 ISDN 1-902916-49-2

[9] ASHRAE Handbook Fundamentals 2005 F32.4

[10] ASHRAE Handbook Fundamentals 2005 F32.25

[11] ASHRAE Handbook Fundamentals 2005 F32.31

[12] ASHRAE Handbook Fundamentals 2005 F32.26

[13] ASHRAE Handbook Fundamentals 2005 F32.1

[14] Mikael Lundin et al. Development and Validation of a method aimed at estimating building performance parameters. Energy and Building 36 (2004) 905-914

[15] A.E. Ruano et al. Prediction of building's temperature using neural networks models. Energy and Building 38 (2006) 682-694

[16] Abraham Yezioro et al. An applied artificial intelligence approach towards assessing building performance simulation tools. Energy and Building 40 (2008) 612-620

[17] T. Olofsson, S.Andersson. Long-term energy demand predictions based on short-term measured data. Energy and Building 33 (2001) 85-91

[18] Melek Yalcintas. Energy-savings predictions for building-equipment retrofits. Energy and Building 40 (2006) 2111-2120

[19] J.F Kreider J.S Haberl, Predicting hourly building energy use: the great energy predictor shoot-out overview and discussion of results, ASHRAE Trans 94(17/7) 1104-1118

[20] Energy Performance of Residential building by M.Santamouris 2005 page 11 ISDN 1-902916-49-2

[21] Subbarao K, 1988, PSTAR-Primary and secondary terms analysis and renormalization: A unified approach to building energy simulations and short monitoring. SERI/TR-254-3175 Golden Co Solar Energy Research Institute.

[22] Subbarao K et al 1988, Short Term Energy (STEM): application of the PSTAR method to a residence in Fredericksburg, Virginia SERI/TR3356 Golden Co Solar Energy Research Institute.

[23] Introduction to Building Physics by Carl-Eric Hagentoft 2003 ISBN 91-44-01896-7 page 153

[24] Introduction to Building Physics by Carl-Eric Hagentoft 2003 ISBN 91-44-01896-7 page 112

[24] Introduction to Building Physics by Carl-Eric Hagentoft 2003 ISBN 91-44-01896-7 page 13

[25] S. Hammarsten. A critical appraisal of energy-signature models. Applied Energy, Volume 26 Issue 2 (1987) pages 97-110

[26] Introduction to Building Physics by Carl-Eric Hagentoft 2003 ISBN 91-44-01896-7 page 208

[27]http://www.microchip.com/pagehandler/enus/technology/personalareanetworks/home.html

[28] http://www.microchip.com

[29] http://www.sensirion.com/en/home/